Noradrenergic Modulation in the Mouse Auditory Midbrain

Charles A. Williams

A dissertation

submitted in partial fulfillment of the

requirements for the degree of

Doctor of Philosophy

University of Washington

2019

Reading Committee:

David J. Perkel, Chair

Martha Bosma

William J. Moody

Program Authorized to Offer Degree:

Biology

University of Washington

Abstract

Noradrenergic Modulation in the Mouse Auditory Midbrain

Charles A. Williams

Chair of the Supervisory Committee:
David J. Perkel, Ph.D., Professor
Departments of Biology and Otolaryngology

The orchestration of diffuse actions is essential for the efficient functioning and behavior of animals. Information processing across the central nervous system is regulated and coordinated by small groups of neurons in the brain that express neurochemicals known as neuromodulators. The modulator norepinephrine is important for regulating arousal and attention. Norepinephrine modulates many sensory systems, including the central auditory system. Here we examined the modulatory effects of norepinephrine in the principal midbrain auditory nucleus, the inferior colliculus (IC). Using calcium imaging, we found that norepinephrine modulates the physiology of cells in the IC. We observed increases in intracellular calcium in cells across the inferior colliculus. This effect is mediated by all three adrenergic receptor subtypes. Noradrenergic effects were not

observed in excitatory neurons in the IC. We also examined cellular expression of adrenergic receptor-encoding mRNA using fluorescent *in situ* hybridization. We found expression of α_1, α_{2A}, and β_2 receptor-encoding mRNA throughout the IC. We observed similar levels of expression of α_1 and α_{2A} receptor-encoding mRNA across the IC, while β_2 receptor-encoding mRNA was expressed in a higher proportion of cells in the outer subregions of the IC. Co-expression of adrenergic receptor-encoding mRNA was greater than expected. Together, this research provides the first evidence for noradrenergic modulation of the inferior colliculus and furthers our understanding of the expression of adrenergic receptors in the auditory midbrain.

TABLE OF CONTENTS

List of Figures

Acknowledgements

I would like to thank my advisor, Prof. David Perkel, for providing mentorship and support throughout my time as a graduate student. I have no doubt that without the patient guidance you have given me throughout the years and research projects, I would not be where I am today.

I would like to thank the members of my supervisory committee, Prof. Bill Moody, Prof. Marti Bosma, and Prof. Andres Barria for their expertise and assistance throughout my time as a graduate student.

I would like to thank the members of the Perkel lab. In particular, Kim Miller and Agata Budzillo for their teaching, assistance, and companionship over the years.

I would like to thank my family for putting me in the position to succeed. My mother and father for their support over the many years, in and out of school, and for being my first scientific role models.

Finally, and most importantly, I would like to thank my wife, Nisa. You make my life better in every way.

For my wife

Chapter 1. Introduction

The orchestration of diffuse actions is essential for the efficient functioning and behavior of animals. In mammals, activity across the central nervous system gives rise to complex psychological processes such as mood, arousal, attention, and motivation. The cognitive state of an animal influences and directs its interaction with the world. This widespread function across the central nervous system is regulated and coordinated by small groups of neurons that express neurochemicals known as neuromodulators. To accomplish this, the neuromodulatory centers send far-reaching projections throughout the central nervous system[1]. While the regulatory functions of each central neuromodulatory system often overlap and interact[2], these systems can be defined based on which modulatory neurotransmitter they express and release onto downstream targets. Central nervous system neuromodulators include acetylcholine, the monoamines – dopamine, epinephrine, norepinephrine, serotonin, and histamine – and a variety of neuropeptides. Each of these neuromodulatory systems plays a role in controlling arousal, motivation, reward, and mood through actions throughout the brain.

1.1 Norepinephrine in the central nervous system

Noradrenergic cells in the mammalian brain are grouped into nuclei in the medulla and pons of the brainstem[3]. These noradrenergic nuclei were shown to project to multiple regions in the brain[4–6]. The A1 region projects to hypothalamus, nucleus of the solitary tract, and periambigual area and is involved in regulating autonomic and endocrine

systems[7]. The A5 region is also important for autonomic regulation and projects to the amygdala, hypothalamus, periaqueductal gray, parabrachial area, nucleus of the solitary tract, and thalamus[8]. Many noradrenergic regions (A5, A6, A7) project to the spinal cord as well, for the regulation of cardiovascular activity, pain sensation, and other autonomic functions[9]. The noradrenergic group A6, also called the locus coeruleus (LC), is unique in that its projections are spread widely throughout the forebrain in addition to lower areas and is the sole source of norepinephrine in the cerebral cortex[10,11] (Figure 1.1).

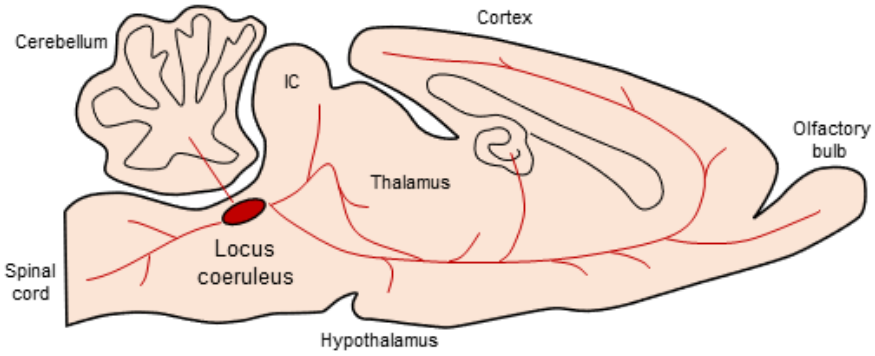

Figure 1.1: Noradrenergic projection pathways of the locus coeruleus of the mouse

Schematic diagram of the locus coeruleus and the major pathways of noradrenergic innervation in the brain of the mouse. Only some of the targets of noradrenergic projections are labeled. Adapted from Kandel et al. 2012[12] and Waterhouse and Navarra 2019[13].

The LC has been the principal focus of research on noradrenergic nuclei in the brain. The modulatory actions of the LC have been linked to arousal and the sleep-wake cycle[14,15], memory[16–18], sensory processing[13,19–21], and attention[22,23]. Many neuromodulatory neurons in the brain are spontaneously active, including the LC[24]. The tonic activity of LC neurons changes throughout the course of the day, entrained by the circadian system of the superchiasmatic nucleus. The activity of LC neurons is greatest during wakefulness, reducing with slow wave sleep and becomes almost completely silent during REM

sleep[14,25,26]. EEG-detected activity increases with higher rates of firing in the LC[27]. The LC's noradrenergic projections are unmyelinated[28] and consequently have slower conduction velocities than other, myelinated axons. Taken together, these early studies of LC structure and function suggested a role in brain-wide tuning of arousal and alertness, where increased release of norepinephrine during wakefulness increases cortical activity and promotes greater engagement and arousal with the environment.

Recordings of LC activity in behaving animals showed that patterns of LC firing were more complex than simple increases and decreases in tonic firing rates and emphasized a greater role in attention and reward-driven behavior. In behavioral tasks where an animal must detect and correctly respond to a stimulus that results in reward, LC neurons showed transient increases in firing following the presentation of the stimulus but preceding the behavioral response[23,29]. LC neurons also rapidly change their responses to match changes in salient stimuli, such as when stimulus-reward pairing is altered mid-experiment. The shifts in LC behavior occur before the animal shifts its response behavior to match the new environmental conditions. The transient responses to task-relevant stimuli does not occur when the animal was presented with task-irrelevant stimuli. These observations led to the adaptive gain hypothesis of LC and central norepinephrine. The transient increases in LC firing – phasic activity – is hypothesized to temporarily increase activity in the cortex to enhance the behavioral response to the current task. Tonic activity of the LC is thought to enhance disengagement from the current behavioral task and control overall levels of arousal. This was based on results that showed increased baseline tonic activity in the LC increased distractibility and lowered behavioral task

performance[23,30]. Tonic LC activity can inhibit or promote exploration of the behavioral environment to ensure that more lucrative opportunities are not missed[15]. LC activity and task performance results from

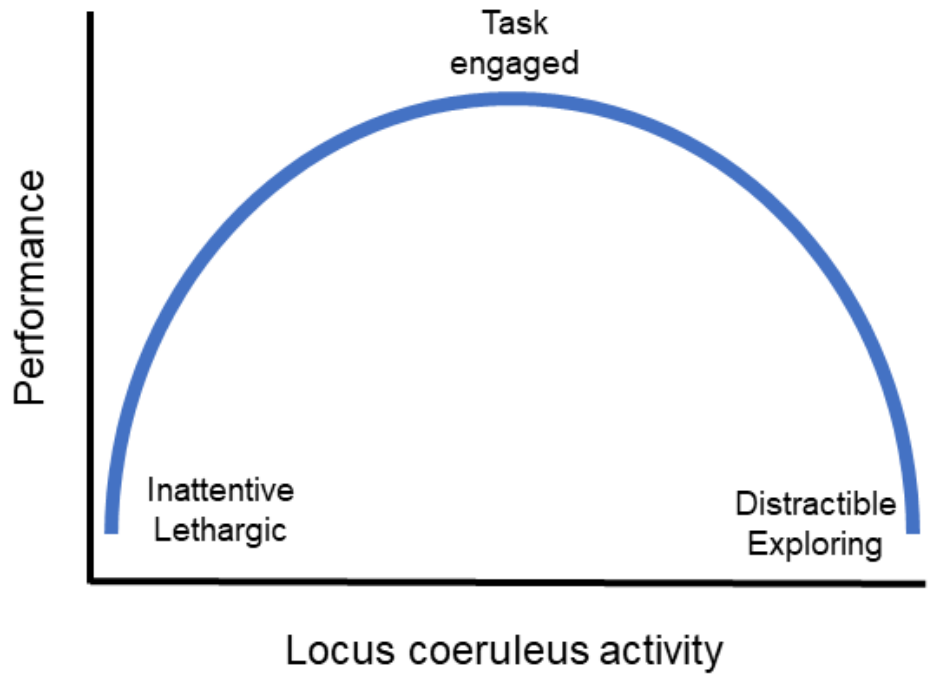

Figure 1.2: Yerkes-Dodson curve for locus coeruleus activity and task performance

Schematic showing the relationship between LC activity and task performance observed in behaving animals. Low levels of steady LC activity are associated with overall low levels of task engagement and attention. Moderate levels of LC activity are ideal for task performance, and phasic LC responses dominate. High levels of tonic activity in the LC results in hyper-arousal and poor task performance and higher levels of explorative behavior. Adapted from Aston-Jones and Cohen 2005[15].

the interplay between phasic spikes of firing that promote attention and responses and tonic baseline firing that promotes overall alertness but can override the phasic firing to find alternative behavioral responses when too high or result in lethargy when too low. These patterns in LC activity are similar to the Yerkes-Dodson law of performance and arousal that was developed in the early 1900s. Low levels of arousal leads to poor task

performance due to disengagement and low levels of energy. Performance is ideal when arousal levels are moderate but can become poor again with high levels of arousal. Higher levels of arousal lead to distractibility from the current task, resulting in poor performance but increased exploration for alternative behaviors to maximize efficiency (Figure 1.2).

The wider behavioral roles of noradrenergic release in the brain depend on neuromodulatory actions at the cellular level. Norepinephrine is synthesized by the enzyme dopamine β-hydroxylase (DBH) from the precursor dopamine, a neuromodulator itself[31]. Noradrenergic projections of the LC likely release norepinephrine by both traditional synaptic and extrasynaptic (volume) transmission methods[28,32]. Volume transmission is the release of norepinephrine widely into extracellular space, increasing the number of post-synaptic targets and time the neuromodulator can exert its influence. Noradrenergic modulation is accomplished through binding to 7-transmembrane g-protein coupled receptors (GPCRs)[33–35]. GPCRs affect intracellular function by activating or inhibiting second messenger pathways. Adrenergic receptors can be split into three groups, as defined by their effects on second messenger systems: α_1, α_2, and β. α_1 adrenergic receptors have three subtypes (α_{1A}, α_{1B}, and α_{1D}) that are coupled to the Gq/11 protein. Binding and activation of α_1 adrenergic receptors activates the phospholipase C and phosphatidyl inositol pathways, which in turn activates protein kinase C and the mobilization and release of intracellular stores of calcium, which then can cause numerous, long-lasting cellular changes[36,37]. α_2 adrenergic receptors have three subtypes (α_{2A}, α_{2B}, and α_{2C}) that are coupled to Gi proteins. Binding and activation of α_2 adrenergic receptors reduces the activity of adenylyl cyclase (AC), resulting in lowered levels of

intracellular cyclic adenosine monophosphate (cAMP)[37]. Finally, β adrenergic receptors have three subtypes (β_1, β_2, and β_3). These adrenergic receptors are coupled to the Gs protein and activation of this second messenger results in increased activity of AC and cAMP levels[37,38].

All three adrenergic receptor subtypes are expressed in numerous brain regions and can alter multiple neuronal properties, both intrinsic and synaptic. For example, β adrenergic receptors in hippocampal CA1 pyramidal neurons directly reduce the slow after-hyperpolarization that follows the generation of action potentials by inhibiting the calcium-induced potassium current. This effect requires the intracellular increase in cAMP that is the result of β adrenergic receptor activation[39–41]. α adrenergic receptor activity in the cortex increases spontaneous inhibitory post synaptic currents detected in GABAergic neurons[42], illustrating one of the many synaptic effects adrenergic receptors can have in the brain. Adrenergic receptors are also commonly expressed in astrocytes and other glia in the brain and can affect their function. Noradrenergic release in the cortex increases astrocyte activity and is thought to enhance the responsiveness of astrocytes to local cortical neuron activity[43]. The wide range of physiological modulation actions norepinephrine performs in the brain reflects the many functional and behavioral roles of noradrenergic modulation in the central nervous system.

Norepinephrine is critical for an animal's ability to attend to and make decisions about their environment. Focusing on and selecting relevant sensory information is an important factor of efficient attention and the decisions regarding an animal's environment.

Norepinephrine modulates the processing of multiple sensory modalities, including auditory, visual, gustatory, olfactory, and somatosensory systems[13]. In general, norepinephrine in central sensory processing areas increases neuronal responses to stimuli and alters excitatory and inhibitory synaptic activity to increase signal-to-noise ratios[19,44–47]. Noradrenergic neuromodulatory actions have been observed throughout the central auditory system, from the brainstem to the cortex, with the notable exception of the midbrain auditory nucleus, the inferior colliculus.

1.2 The ascending auditory system

The auditory system is responsible for the detection, transduction, processing, and conscious awareness of the differences in air pressure we interpret as sound[48,49] (Figure 1.3). Sound is transduced from oscillations in air pressure to electrical signals in the cochlea of the inner ear. Mechanosensory hair cells detect movements of the basilar membrane, which vibrates in tune with pressure that is transferred from sound to the fluid that fills the cochlea. The auditory nerve carries these signals to the cochlear nuclei of the brainstem, where it enters the central auditory system. Before connecting with the cochlear nuclei, the auditory nerve splits into ascending and descending pathways[50],

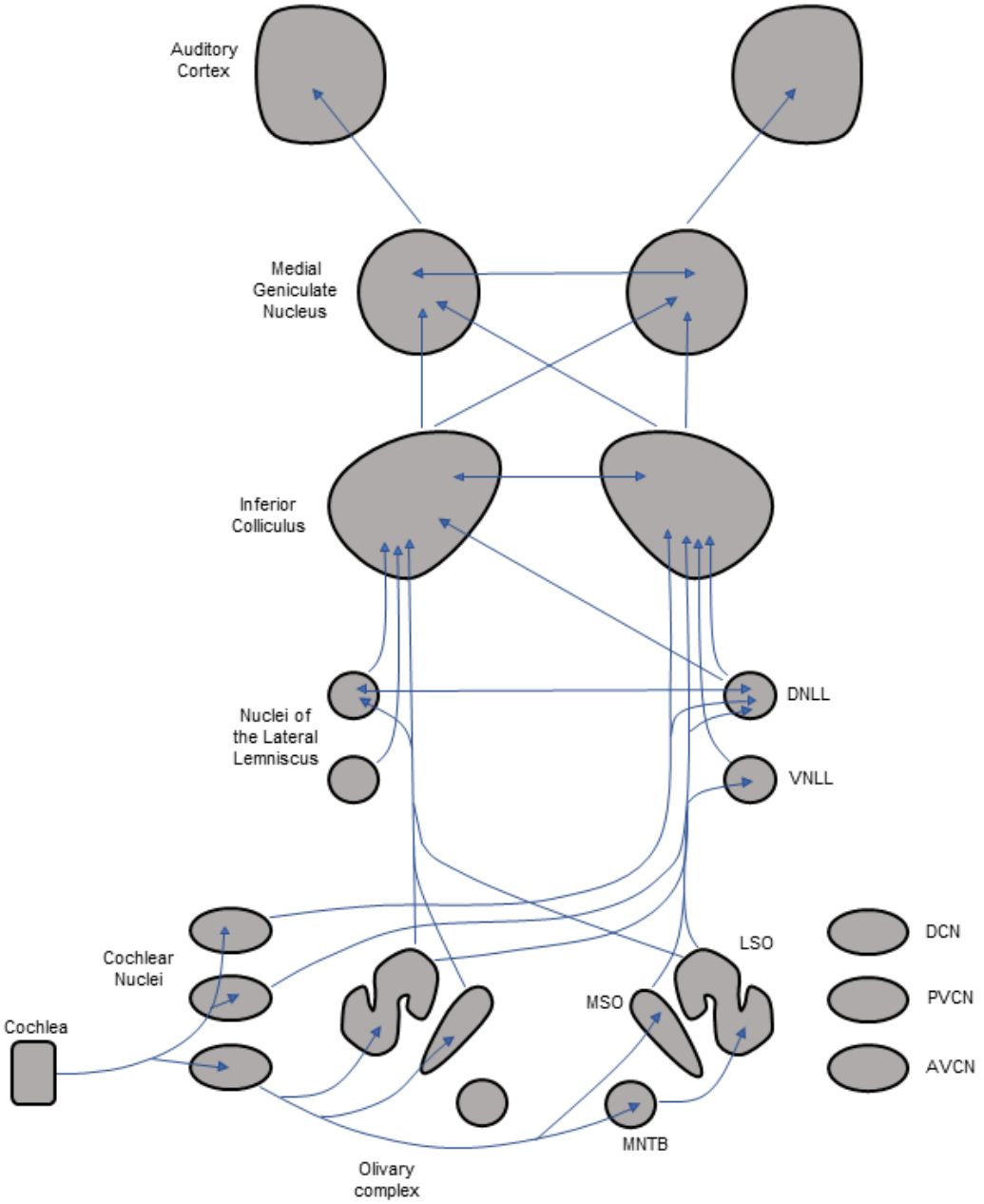

Figure 1.3: Ascending pathways of monoaural auditory stimuli

Diagram of the central auditory centers. Arrows represent the connections and pathways of auditory stimuli originating from a single cochlea. DCN: dorsal cochlear nucleus, PVCN: posteroventral cochlear nucleus, AVCN: anteroventral cochlear nucleus, LSO: lateral superior olivary nucleus, MSO: medial superior olivary nucleus, MNTB: medial nucleus of the trapezoid body, VNLL: ventral nucleus of the lateral lemniscus, DNLL: dorsal nucleus of the lateral lemniscus.

providing a small preview to the computational and functional specializations that exist in the areas of the central nervous system. The cochlear nuclei maintain the organization that is established in the cochlea[51]. The neuronal representations of auditory stimuli are spatially organized based on the frequency of those auditory stimuli, where cellular representations of similarly pitched stimuli are close to each other. This is known as tonotopic organization, an organizational pattern that continues through the ascending auditory pathways. The divergent pathways of auditory processing in the cochlear nuclei give rise to different neuronal representations of sound in the brainstem, despite the uniform source from the auditory nerve[52]. These differences are created by the differing populations of auditory nerve targets[53,54] and the introduction of lateral inhibitory circuits that emphasize certain features of the auditory stimulus[55]. The cochlear nuclei do not operate independently and are the targets of a variety of descending modulatory projections, including norepinephrine[56]. In the dorsal cochlear nucleus (DCN), norepinephrine quiets spontaneously firing inhibitory interneurons[57]. This in turn lowers background levels of inhibition in the DCN but enhances inhibitory glycinergic synaptic transmission via disinhibition. This effect of norepinephrine in the DCN is hypothesized to contribute to the filtering of auditory stimuli in the DCN.

The cochlear nuclei project to a multitude of targets, including the olivary complex and the inferior colliculus (IC). The olivary complex builds upon the computations of the cochlear nuclei and is best known for integrating the monoaural inputs from the bilateral cochlear nuclei into binaural signals that specialize in the spatial detection of sounds[58]. The lateral superior olive compares the intensity of auditory stimuli from each ear to

calculate location, while the medial superior olive compares the frequency and timing of binaurally represented auditory stimuli[59]. These processes also represent a change from the uniformly excitatory inputs of the auditory nerve to more complex representations of stimuli built on multiple excitatory and inhibitory pathways[60] that begins in the cochlear nuclei. The building of more detailed auditory processing from inputs of prior nuclei is a theme that continues throughout the ascending auditory system. The olivary complex is sensitive to noradrenergic modulation, with norepinephrine reducing excitatory glutamatergic synaptic transmission in the afferent connections between the ventral cochlear nucleus and the lateral superior olive[61]. This provides another example of noradrenergic modulation in the central auditory system.

The ascending projections of the olivary complex and cochlear nuclei make up a fiber bundle known as the lateral lemniscus. While some of these pathways project directly to the midbrain IC, some terminate in a series of three nuclei known as the nuclei of the lateral lemniscus (dorsal; DNLL, intermediate; INLL, and ventral; VNLL)[62–64] which then in turn send projections to the IC. The VNLL is a component of the monoaural information stream, receiving input primarily from the contralateral cochlear nucleus and ipsilateral olivary complex[62]. The DNLL receives binaural information from bilateral olivary complexes and contralateral cochlear nuclei and likely enhances the spatial detection of stimuli. Less studied in comparison to the cochlear nuclei and olivary complex, the nuclei of the lateral lemniscus are a center for the further refinement of ascending information.

Auditory information in the thalamus is represented in the medial geniculate nucleus (MGN or MGB). The MGN is composed of three subregions, the ventral, dorsal, and medial divisions of the MGN. The ventral portion of the MGN is the primary auditory region of the MGN[65,66], receiving ascending input from the central nucleus of the inferior colliculus (ICc) and descending inputs from the auditory cortex[67,68]. The ventral portion of the MGN is tonotopically organized, similar to its ascending inputs. Outputs of the ventral MGN primarily target the ipsilateral auditory cortex (A1). The dorsal and medial portions of the MGN are more eclectic in their inputs and outputs. The medial portion of the MGN receives inputs from the ICc and external cortex of the inferior colliculus (ICx)[67], a portion of the IC that is more multimodal than the ICc. The medial MGN also receives non-auditory input from a variety of sources, including the vestibular system[69] and somatosensory processing regions, directly and indirectly via the ICx. The medial MGN sends afferents to a wider region of targets compared to the ventral MGN, including the auditory cortex[70], the amygdala[71], and other non-auditory cortical regions[72]. The dorsal MGN receives input mainly from the dorsal cortex of the inferior colliculus (ICd)[67]. Activity in the dorsal MGN is implicated in auditory learning. Neurons in the dorsal MGN show stimulus specific adaptation (Antunes et al 2010) and can show increased responsiveness to auditory stimuli that are paired with an aversive stimulus[73]. The dorsal MGN projects to secondary auditory cortical regions that are near the primary auditory cortex[74]. Similar to other thalamic neurons, neurons in the MGN are sensitive to norepinephrine, responding to norepinephrine application with decreases or increases in their spontaneous firing rates[75,76].

The primary auditory cortex (A1) is the final destination of the primary stream of ascending auditory information. It is similar to other cortical regions, being composed of six distinct layers. Layers III and IV receive inputs from the ventral MGN and layers I and VI receive inputs from the medial MGN[77]. Of note here, layers V and VI are the sources of descending projections to the inferior colliculus[78,79]. The primary auditory cortex also project to numerous other regions. The primary auditory cortex is surrounded by non-primary auditory cortical regions, which receive inputs from the MGN as well as from the core of A1. The function of the auditory cortex, primary and nonprimary regions, is complex, integrating all of the components of stimuli extracted along the ascending pathway. While the superior olive is the first area in the ascending pathway that calculates the spatial origin of sounds, the auditory cortex is where that information is coalesced for higher cognitive functions. The auditory cortex is modulated by norepinephrine and this interaction has been the subject of multiple studies. Norepinephrine application in the auditory cortex improves frequency tuning in response to pure tones[80,81]. If auditory stimuli are paired with artificial stimulation of the locus coeruleus, neurons in the auditory cortex showed increases and decreases in frequency tuning that lasted for up to 15 minutes[82]. Norepinephrine has been shown to affect inhibitory synaptic transmission in the auditory cortex, with α_2 and β adrenergic receptors facilitating GABAergic post-synaptic currents while α_1 receptor mediated activity decreases responses to GABAergic synaptic activity[83]. Norepinephrine modulation in the IC has also been linked to auditory cortex responses during rewarding behavioral tasks. Following pairing of LC stimulation with the presentation of a rewarding auditory cue, areas of the auditory cortex that were

initially unresponsive begin showing activity when the animal is presented with the conditioned auditory stimulus[84].

The nuclei of the ascending auditory pathway compose a complex sensory processing network that demonstrates increasing complexity and feature detection from the initial mechanotransduction of sound into electrical signals in the cochlea to higher cognitive processing in the cortex (Figure 1.3). Many of the components of this system receive noradrenergic projections from the locus coeruleus and are modulated by norepinephrine.

1.3 The inferior colliculus

The primary midbrain nucleus of the central auditory pathway is the inferior colliculus (IC). The IC is a site of integration of the divergent pathways of auditory processing that arise in the brainstem. Nearly all of the ascending auditory pathways converge and make synapses in the IC, with only a small portion or axons bypassing it to the MGN[85,86] (Figure 1.3). The IC also receives extensive descending projections from the auditory cortex and MGN. Morphologically, the IC is composed of two bilateral lobes on the dorsal surface of the midbrain. Each lobe of the IC can be divided into three subregions, based on the patterns on ascending and descending inputs, neuronal composition, and function. These subregions are the central nucleus (ICc), the dorsal cortex (ICd), and the external cortex (ICx) (Figure 1.4). Neurons in the IC show an increased complexity of responses to auditory stimuli in comparison to brainstem auditory nuclei, indicating that the IC functions as a distinct processing center itself and more than a simple site of relay. For example, the IC is the first nucleus in the ascending auditory pathway that shows specialization for vocalizations[87–90].

The ICc is required for hearing[91] and is the primary auditory nucleus of the IC. The ICc receives the majority of the ascending auditory afferents, including projections from multiple subregions the cochlear nucleus[92,93], lateral superior olive, medial superior olive[94], and all of the nuclei of the lateral lemniscus[95]. These inputs are glutamatergic, GABAergic, and glycinergic[62,96]. Each ICc also receives input from the contralateral IC[97]. The ascending fibers and dendrites of intrinsic ICc neurons form layers in the ICc. Ascending projections that carry information regarding auditory stimuli of specific frequency ranges merge in the same layer of the ICc, even if those projections originate in different brainstem nuclei. Thus, the laminar structure of the ICc is formed. The layers of the ICc are known as isofrequency layers and contain neurons that show high levels of responsiveness to similar frequencies of auditory stimuli. The isofrequency layers that are more dorsal show the strongest responses to auditory stimuli of low frequencies. Layers more ventral and medial show representations of progressively higher stimulus frequencies[98]. The neurons of the ICc contribute to the laminar structure as well. 80% of neurons in the ICc are classified as “disc-shaped”, and have dendritic and axonal projections that do not cross isofrequency lamina[98]. The remaining 20% of neurons are classified as “stellate” cells. Stellate neuron projections readily cross laminae, presumably coordinating activity across multiple isofrequency layers. There are numerous intrinsic connections within the ICc and other IC subregions[99]. The ICc sends projections primarily to the ipsilateral auditory thalamus, MGN[100–102].

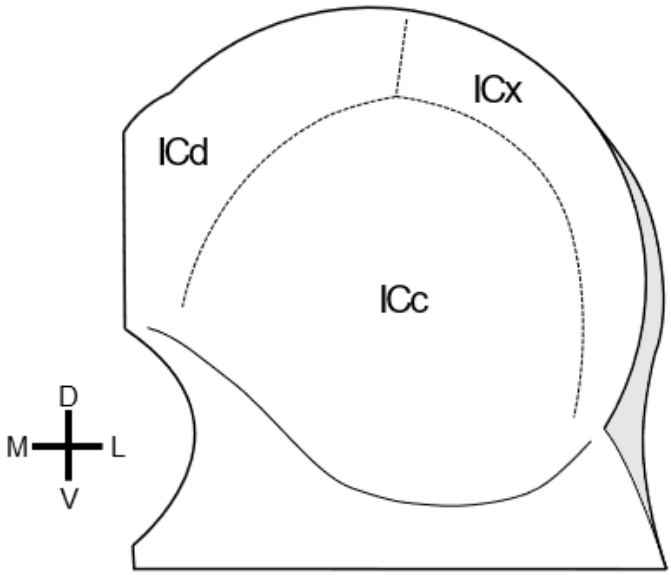

Figure 1.4: The subregions of the inferior colliculus

Diagram of the inferior colliculus and its subregions. ICc: central nucleus, ICd: dorsal cortex, ICx, external cortex. D: dorsal, L: lateral, V: ventral, M: medial.

Further categorization of ICc neurons remains elusive. Neurochemically, 30% of ICc neurons are GABAergic, with the remaining 70% glutamatergic[103]. GABAergic neurons in the ICc show variation in cell body size, and can be divided into four groups[104–106]. Despite this, glutamatergic and GABAergic neurons in the ICc do not show distinct types of responses to auditory stimulation[107]. Electrophysiologically, ICc neurons show a variety of responses to depolarizing current injection[108,109]. Both disc-shaped and stellate neurons in the ICc can project either intrinsically within the IC or to the MGN and the same is the case for ICc glutamatergic and GABAergic neurons. No correlations between intrinsic electrophysiological properties, neurotransmitter expression, cell morphology, or projection pattern have yet been firmly established. Some success in categorizing IC neurons has been seen using expression of vasoactive intestinal peptide (VIP)

expression. VIP cells in the IC exhibit a uniform type of firing, are glutamatergic, and show similar patterns in projections[110].

The dorsal cortex of the IC (ICd) has is less well studied than the ICc. Neurons in the ICd form layers but not the isofrequency-specialized layers of the ICc[111]. The ICd receives no direct input from the ascending auditory fibers from the auditory brainstem or lemniscal nuclei but receives extensive intrinsic connections from the rest of the IC[112]. The ICd receives large descending inputs from the auditory cortex as well[79], which are likely the primary drivers of auditory stimulus-evoked responses in ICd neurons[113]. The function of the ICd is also relatively unexplored, however links have been made between the ICd and attention to auditory stimuli[114] and the auditory startle reflex[111]. ICd neurons also show strong responses to novel stimuli and stimulus-specific adaptation, indicating the ICd might show specialization for detecting novel auditory stimuli[115,116].

The external cortex of the IC (ICx) is a site of multimodal integration The ICx receives inputs from intrinsic IC connections, the somatosensory regions of the dorsal column nuclei and spinal trigeminal nucleus[117], superior colliculus, and auditory cortex[79]. The somatosensory inputs to the ICx appear to be especially important, accounting for a simplistic representation of body position in ICx neurons[118]. There have been suggestions of a map of auditory space being represented in the mammalian ICx[119], similar to what has been established in the homologous lateral dorsal mesencephalic nucleus of the owl[120,121]. The IC also projects to the superior colliculus, which is important for orientation behaviors and visual attention. It is likely that the somatosensory and auditory information

integrated in the ICx assists with behavioral responses and orientation. Throughout the ICx, distinct groupings of neurons have been described. These patches of neurons have been identified based on their staining for a variety of metabolic and neurotransmitter markers, including glutamic acid decarboxylase-76 (GAD-67, a marker of GABAergic neurons), acetylcholinesterase (AChE), parvalbumin, nicotinamide adenine dinucleotide phosphate-diaphorase (NADPH-d), and cytochrome oxidase[122]. These patches coincide with somatosensory input terminations, and largely do not overlap with auditory inputs to the ICx.

1.4 Neuromodulation in the IC

Due to its role as a site of integration of ascending and descending inputs, the IC has long been hypothesized to be a location for efficient neuromodulation. Serotonergic (5-HT) fibers are present in the IC[123,124] and originate in the raphe nucleus. Serotonin alters ICc neuron responses to tones[125] and shifts response latencies[126]. Serotonin also reduces GABAergic synaptic activity in the IC[127] and robustly increases spontaneous GABAergic post-synaptic currents in slices of IC[128]. Interestingly, serotonin release in the IC is greater and faster in male mice exposed to an unfamiliar male compared with exposure to a familiar male[129]. These results suggest an interaction between social experiences and serotonergic modulation of auditory processing. Dopamine is also present in the IC[130,131]. Unlike serotonin, which arises from the primary serotonergic center of the brainstem, dopamine innervation of the IC originates from a thalamic dopaminergic region, the subparafascicular region (SPF)[131] instead of the principal dopaminergic centers, the

ventral tegmental area (VTA) or substantia nigra. Dopamine is released in the IC with electrical or optogenetic stimulation of the SPF[132] but its function remains unknown. When applied during presentation of auditory stimuli, dopamine alters the response rate, timing, and bursting of IC neurons[133]. Acetylcholine is also present in the IC, originating in the midbrain tegmental nuclei[134]. Cholinergic agonists bimodally affect responses to tones in IC neurons[135] but further exploration has not been completed. Overall, the IC is a rich target of modulatory systems in the mammalian brain. An exception in modulatory research in the IC is norepinephrine.

1.5 Norepinephrine in the IC

Little is currently understood of noradrenergic modulation in the IC. Projections from the locus coeruleus that are immunoreactive for DBH were found in the IC[123,136]. Evidence of adrenergic receptors in the IC has come from studies utilizing autoradiographic binding and *in situ* hybridization. Binding studies indicated the presence of α_1 and α_2 adrenergic receptors in the IC but not β[137–140]. *In situ* hybridization studies were able to assess distributions of adrenergic receptor subtypes more accurately and reported low levels of α_1 mRNA in the IC[141,142]. A later study utilizing a transgenic mouse line driving a reporter gene under the control of the α_{1A} promoter showed high expression levels in the IC[143]. α_{2A} and α_{2C} receptor encoding mRNA is expressed in the IC[144]. Consistent with autoradiographic binding studies, no expression of β_1 or β_2 has been described in the IC[145]. These anatomical studies focused on brain-wide expression patterns of adrenergic receptors, with few examining expressions at cellular-level resolution and none examining

co-expression of one or more adrenergic receptor subtypes (i.e. between α_2, α_2, and β). Despite evidence for the presence of presynaptic and postsynaptic mechanisms enabling noradrenergic modulation in the IC, the topic remains unexplored.

The functional roles of the IC and noradrenergic modulation show several overlaps. Norepinephrine is important for attention and novel stimuli orientation. Similarly, the ICx and ICd subregions have been implicated in modulating auditory attention and orientation to auditory stimuli Norepinephrine modulates other auditory processing centers in the brainstem, thalamus, and cortex. These regions receive projections from the LC, similar to the IC. Given the role of norepinephrine in modulating sensory processing in numerous locations in the brain, across sensory modalities, it is likely norepinephrine is providing a similar function in the IC.

Here, I detail experiments examining noradrenergic modulation in the mouse inferior colliculus. I used widefield calcium imaging to investigate how norepinephrine modulates calcium activity in cells of the IC. I used tri-channel *in situ* hybridization to examine the expression patterns of adrenergic receptors in the IC to understand where and in what combination cells in the IC express adrenergic receptors.

1.6 References

1. Hokfelt, T., Johansson, O. & Goldstein, M. Chemical anatomy of the brain. *Science (80-.).* **225**, 1326–1335 (1984).
2. Briand, L. A., Gritton, H., Howe, W. M., Young, D. A. & Sarter, M. Modulators in concert for cognition: Modulator interactions in the prefrontal cortex. *Prog. Neurobiol.* **83**, 69–91 (2007).
3. Dahlstom, A. & Fuxe, L. Evidence for existence of monoamine-containing neurons in central nervous system. I. Demonstration of monoamines in the cell bodies of brain stem neurons. *Acta Physiol. Scand.* **62**, 1–55 (1964).
4. Ungerstedt, U. Stereotaxic Mapping of the Monoamine Pathways in the Rat Brain*. *Acta Physiol. Scand.* **82**, 1–48 (1971).
5. Fuxe, K., Hökfelt, T. & Ungerstedt, U. Morphological and Functional Aspects of Central Monoamine Neurons. *Int. Rev. Neurobiol.* **13**, 93–126 (1970).
6. Maeda, T. & Shimizu, N. Projections ascendantes du locus coeruleus et d'autres neurones aminergiques pontiques au niveau du prosencéphale du rat. *Brain Res.* **36**, 19–35 (1972).
7. Guyenet, P. G. Central noradrenergic neurons: the autonomic connection. *Prog. Brain Res.* **88**, 365–380 (1991).
8. Byrum, C. E. & Guyenet, P. G. Afferent and efferent connections of the A5 noradrenergic cell group in the rat. *J. Comp. Neurol.* **261**, 529–542 (1987).
9. Coote, J. H. Noradrenergic projections to the spinal cord and their role in cardiovascular control. *J. Auton. Nerv. Syst.* **14**, 255–262 (1985).
10. Jones, B. E., Halaris, A. E., McIlhany, M. & Moore, R. Y. Ascending projections of the locus coeruleus in the rat. I. axonal transport in central noradrenaline neurons. *Brain Res.* **127**, 1–21 (1977).
11. Berridge, C. W. & Waterhouse, B. D. The locus coeruleus–noradrenergic system: modulation of behavioral state and state-dependent cognitive processes. *Brain Res. Rev.* **42**, 33–84 (2003).
12. *Principles of Neural Science*. (McGraw-Hill Education / Medical, 2012).
13. Waterhouse, B. D. & Navarra, R. L. The locus coeruleus-norepinephrine system and sensory signal processing: A historical review and current perspectives. *Brain Res.* (2018). doi:10.1016/J.BRAINRES.2018.08.032
14. Aston-Jones, G. & Bloom, F. E. Activity of norepinephrine-containing locus coeruleus neurons in behaving rats anticipates fluctuations in the sleep-waking cycle. *J. Neurosci.* **1**, 876–86 (1981).
15. Aston-Jones, G. & Cohen, J. D. An Integrative Theory of Locus Coeruleus-Norepinephrine Function: Adaptive Gain and Optimal Performance. *Annu. Rev. Neurosci* **28**, 403–50 (2005).
16. Sara, S. J., Roullet, P. & Przybyslawski, J. Consolidation of memory for odor-reward association: beta-adrenergic receptor involvement in the late phase. *Learn. Mem.* **6**, 88–96 (1999).
17. Tronel, S., Feenstra, M. G. P. & Sara, S. J. Noradrenergic action in prefrontal cortex in the late stage of memory consolidation. *Learn. Mem.* **11**, 453–8 (2004).
18. McGaugh, J. L. & Roozendaal, B. Drug enhancement of memory consolidation: historical perspective and neurobiological implications. *Psychopharmacology*

(Berl). **202**, 3–14 (2009).
19. Foote, S. L., Freedman, R. & Oliver, A. P. Effects of putative neurotransmitters on neuronal activity in monkey auditory cortex. *Brain Res.* **86**, 229–242 (1975).
20. Aston-Jones, G. & Bloom, F. E. Norepinephrine-containing locus coeruleus neurons in behaving rats exhibit pronounced responses to non-noxious environmental stimuli. *J. Neurosci.* **1**, 887–900 (1981).
21. Devilbiss, D. M. & Waterhouse, B. D. The effects of tonic locus ceruleus output on sensory-evoked responses of ventral posterior medial thalamic and barrel field cortical neurons in the awake rat. *J. Neurosci.* **24**, 10773–85 (2004).
22. Foote, S. L., Aston-Jones, G. & Bloom, F. E. Impulse activity of locus coeruleus neurons in awake rats and monkeys is a function of sensory stimulation and arousal. *Proc. Natl. Acad. Sci. U. S. A.* **77**, 3033–7 (1980).
23. Aston-Jones, G., Rajkowski, J., Kubiak, P. & Alexinsky, T. Locus coeruleus neurons in monkey are selectively activated by attended cues in a vigilance task. *J. Neurosci.* **14**, 4467–80 (1994).
24. Korf, J., Bunney, B. S. & Aghajanian, G. K. Noradrenergic neurons: Morphine inhibition of spontaneous activity. *Eur. J. Pharmacol.* **25**, 165–169 (1974).
25. Hobson, J. A., McCarley, R. W. & Wyzinski, P. W. Sleep cycle oscillation: reciprocal discharge by two brainstem neuronal groups. *Science* **189**, 55–8 (1975).
26. Rasmussen, K., Morilak, D. A. & Jacobs, B. L. Single unit activity of locus coeruleus neurons in the freely moving cat: I. During naturalistic behaviors and in response to simple and complex stimuli. *Brain Res.* **371**, 324–334 (1986).
27. Berridge, C. W. & Foote, S. L. Effects of locus coeruleus activation on electroencephalographic activity in neocortex and hippocampus. *J. Neurosci.* **11**, 3135–45 (1991).
28. Olschowka, J. A., Molliver, M. E., Grzanna, R., Rice, F. L. & Coyle, J. T. Ultrastructural demonstration of noradrenergic synapses in the rat central nervous system by dopamine-beta-hydroxylase immunocytochemistry. *J. Histochem. Cytochem.* **29**, 271–280 (1981).
29. Bouret, S. & Sara, S. J. Reward expectation, orientation of attention and locus coeruleus-medial frontal cortex interplay during learning. *Eur. J. Neurosci.* **20**, 791–802 (2004).
30. Usher, M., Cohen, J. D., Servan-Schreiber, D., Rajkowski, J. & Aston-Jones, G. The role of locus coeruleus in the regulation of cognitive performance. *Science* **283**, 549–54 (1999).
31. BLASCHKO, H. CATECHOLAMINE BIOSYNTHESIS. *Br. Med. Bull.* **29**, 105–109 (1973).
32. Farb, C. R., Chang, W. & LeDoux, J. E. Ultrastructural Characterization of Noradrenergic Axons and Beta-Adrenergic Receptors in the Lateral Nucleus of the Amygdala. *Front. Behav. Neurosci.* **4**, 162 (2010).
33. Kobilka, B. Adrenergic Receptors as Models for G Protein-Coupled Receptors. *Annu. Rev. Neurosci.* **15**, 87–114 (1992).
34. Strosberg, A. D. Structure, function, and regulation of adrenergic receptors. *Protein Sci.* **2**, 1198–1209 (1993).
35. Rohrer, D. K. Physiological consequences of β-adrenergic receptor disruption. *J.*

Mol. Med. **76**, 764–772 (1998).
36. Marshall, I., Burt, R. P. & Chapple, C. R. Signal Transduction Pathways Associated with α₁-Adrenoceptor Subtypes in Cells and Tissues Including Human Prostate. *Eur. Urol.* **36**, 42–47 (1999).
37. Ramos, B. P. & Arnsten, A. F. T. Adrenergic pharmacology and cognition: Focus on the prefrontal cortex. *Pharmacol. Ther.* **113**, 523–536 (2007).
38. Ordway, G. A., O'Donnell, J. M. & Frazer, A. Effects of clenbuterol on central beta-1 and beta-2 adrenergic receptors of the rat. *J. Pharmacol. Exp. Ther.* **241**, (1987).
39. Madison, D. V. & Nicoll, R. A. Noradrenaline blocks accommodation of pyramidal cell discharge in the hippocampus. *Nature* **299**, 636–638 (1982).
40. Madison, D. V & Nicoll, R. A. Actions of noradrenaline recorded intracellularly in rat hippocampal CA1 pyramidal neurones, in vitro. *J. Physiol.* **372**, 221–244 (1986).
41. Madison, D. V. & Nicoll, R. A. Cyclic adenosine 3',5'-monophosphate mediates beta-receptor actions of noradrenaline in rat hippocampal pyramidal cells. *J. Physiol.* **372**, 245–259 (1986).
42. Kawaguchi, Y. & Shindou, T. Noradrenergic excitation and inhibition of GABAergic cell types in rat frontal cortex. *J. Neurosci.* **18**, 6963–76 (1998).
43. Paukert, M. *et al.* Norepinephrine Controls Astroglial Responsiveness to Local Circuit Activity. *Neuron* **82**, 1263–1270 (2014).
44. Rogawski, M. A. & Aghajanian, G. K. Norepinephrine and serotonin: Opposite effects on the activity of lateral geniculate neurons evoked by optic pathway stimulation. *Exp. Neurol.* **69**, 678–694 (1980).
45. Collins, G. G., Probett, G. A., Anson, J. & McLaughlin, N. J. Excitatory and inhibitory effects of noradrenaline on synaptic transmission in the rat olfactory cortex slice. *Brain Res* **294**, 211–223 (1984).
46. Waterhouse, B. D. *et al.* New evidence for a gating action of norepinephrine in central neuronal circuits of mammalian brain. *Brain Res. Bull.* **21**, 425–432 (1988).
47. Ciombor, K. ., Ennis, M. & Shipley, M. . Norepinephrine increases rat mitral cell excitatory responses to weak olfactory nerve input via alpha-1 receptors in vitro. *Neuroscience* **90**, 595–606 (1999).
48. Winer, J. A. & Schreiner, C. E. The Central Auditory System: A Functional Analysis. in *The Inferior Colliculus* 1–68 (Springer-Verlag, 2005). doi:10.1007/0-387-27083-3_1
49. Pickles, J. O. *An introduction to the physiology of hearing.* (Emerald Group Pub, 2012).
50. Ryugo, D. K. The Auditory Nerve: Peripheral Innervation, Cell Body Morphology, and Central Projections. in 23–65 (Springer, New York, NY, 1992). doi:10.1007/978-1-4612-4416-5_2
51. Osen, K. K. Course and termination of the primaryafferents in the cochlear nuclei of the cat. *Arch. Ital. Biol.* **108**, 21–51 (1970).
52. Osen, K. K. Projection of the cochlear nuclei on the inferior colliculus in the cat. *J. Comp. Neurol.* **144**, 355–371 (1972).
53. Osen, K. K. Cytoarchitecture of the cochlear nuclei in the cat. *J. Comp. Neurol.*

136, 453–483 (1969).
54. Cant, N. B. The Cochlear Nucleus: Neuronal Types and Their Synaptic Organization. in 66–116 (Springer, New York, NY, 1992). doi:10.1007/978-1-4612-4416-5_3
55. Adams, J. C. & Mugnaini, E. Patterns of glutamate decarboxylase immunostaining in the feline cochlear nuclear complex studied with silver enhancement and electron microscopy. *J. Comp. Neurol.* **262**, 375–401 (1987).
56. Kane, E. S. & Conlee, J. W. Descending inputs to the caudal cochlear nucleus of the cat: Degeneration and autoradiographic studies. *J. Comp. Neurol.* **187**, 759–783 (1979).
57. Kuo, S. P. & Trussell, L. O. Spontaneous spiking and synaptic depression underlie noradrenergic control of feed-forward inhibition. *Neuron* **71**, 306–18 (2011).
58. Schwartz, I. R. The Superior Olivary Complex and Lateral Lemniscal Nuclei. in 117–167 (Springer, New York, NY, 1992). doi:10.1007/978-1-4612-4416-5_4
59. Yin, T. C. & Chan, J. C. Interaural time sensitivity in medial superior olive of cat. *J. Neurophysiol.* **64**, 465–88 (1990).
60. Guinan, J. J. & Li, R. Y.-S. Signal processing in brainstem auditory neurons which receive giant endings (calyces of Held) in the medial nucleus of the trapezoid body of the cat. *Hear. Res.* **49**, 321–334 (1990).
61. Hirao, K. *et al.* Noradrenergic refinement of glutamatergic neuronal circuits in the lateral superior olivary nucleus before hearing onset. *J. Neurophysiol.* **114**, 1974–1986 (2015).
62. Kelly, J. B., van Adel, B. A. & Ito, M. Anatomical projections of the nuclei of the lateral lemniscus in the albino rat (*rattus norvegicus*). *J. Comp. Neurol.* **512**, 573–593 (2009).
63. Oliver, D. L. & Morest, D. K. The central nucleus of the inferior colliculus in the cat. *J. Comp. Neurol.* **222**, 237–264 (1984).
64. Glendenning, K. K. & Masterton, R. B. Acoustic chiasm: efferent projections of the lateral superior olive. *J. Neurosci.* **3**, 1521–37 (1983).
65. MOREST, D. K. THE LAMINAR STRUCTURE OF THE MEDIAL GENICULATE BODY OF THE CAT. *J. Anat.* **99**, 143–60 (1965).
66. Imig, T. J. & Morel, A. Topographic and cytoarchitectonic organization of thalamic neurons related to their targets in low-, middle-, and high-frequency representations in cat auditory cortex. *J. Comp. Neurol.* **227**, 511–539 (1984).
67. Calford, M. B. & Aitkin, L. M. Ascending projections to the medial geniculate body of the cat: evidence for multiple, parallel auditory pathways through thalamus. *J. Neurosci.* **3**, 2365–80 (1983).
68. Winer, J. A., Diehl, J. J. & Larue, D. T. Projections of auditory cortex to the medial geniculate body of the cat. *J. Comp. Neurol.* **430**, 27–55 (2001).
69. Blum, P. S., Abraham, L. D. & Gilman, S. Vestibular, auditory, and somatic input to the posterior thalamus of the cat. *Exp. Brain Res.* **34**, 1–9 (1979).
70. Niimi, K. & Matsuoka, H. Thalamocortical organization of the auditory system in the cat studied by retrograde axonal transport of horseradish peroxidase. *Adv. Anat. Embryol. Cell Biol.* **57**, 1–56 (1979).
71. Shinonaga, Y., Takada, M. & Mizuno, N. Direct projections from the non-

laminated divisions of the medial geniculate nucleus to the temporal polar cortex and amygdala in the cat. *J. Comp. Neurol.* **340**, 405–426 (1994).
72. Jones, E. G. & Powell, T. P. S. Anatomical Organization of the Somatosensory Cortex. in 579–620 (Springer, Berlin, Heidelberg, 1973). doi:10.1007/978-3-642-65438-1_16
73. Edeline, J.-M. & Weinberger, N. M. Subcortical adaptive filtering in the auditory system: Associative receptive field plasticity in the dorsal medial geniculate body. *Behav. Neurosci.* **105**, 154–175 (1991).
74. Smith, P. H., Uhlrich, D. J., Manning, K. A. & Banks, M. I. Thalamocortical projections to rat auditory cortex from the ventral and dorsal divisions of the medial geniculate nucleus. *J. Comp. Neurol.* **520**, 34–51 (2012).
75. Tebēcis, A. K. Effects of monoamines and amino acids on medial geniculate neurones of the cat. *Neuropharmacology* **9**, 381–390 (1970).
76. Torda, C. Effects of noradrenaline and serotonin on activity of single lateral and medial geniculate neurons. *Gen. Pharmacol. Vasc. Syst.* **9**, 455–462 (1978).
77. Huang, C. L. & Winer, J. A. Auditory thalamocortical projections in the cat: Laminar and areal patterns of input. *J. Comp. Neurol.* **427**, 302–331 (2000).
78. Kelly, J. P. & Wong, D. Laminar connections of the cat's auditory cortex. *Brain Res.* **212**, 1–15 (1981).
79. Winer, J. A., Larue, D. T., Diehl, J. J. & Hefti, B. J. Auditory cortical projections to the cat inferior colliculus. *J. Comp. Neurol.* **400**, 147–174 (1998).
80. Manunta, Y. & Edeline, J.-M. Effects of Noradrenaline on Frequency Tuning of Rat Auditory Cortex Neurons. *Eur. J. Neurosci.* **9**, 833–847 (1997).
81. Manunta, Y. & Edeline, J.-M. Effects of noradrenaline on frequency tuning of auditory cortex neurons during wakefulness and slow-wave sleep. *Eur. J. Neurosci.* **11**, 2134–2150 (1999).
82. Edeline, J.-M., Manunta, Y. & Hennevin, E. Induction of selective plasticity in the frequency tuning of auditory cortex and auditory thalamus neurons by locus coeruleus stimulation. *Hear. Res.* **274**, 75–84 (2011).
83. Salgado, H. *et al.* Pre- and postsynaptic effects of norepinephrine on γ-aminobutyric acid-mediated synaptic transmission in layer 2/3 of the rat auditory cortex. *Synapse* **66**, 20–28 (2012).
84. Martins, A. R. O. & Froemke, R. C. Coordinated forms of noradrenergic plasticity in the locus coeruleus and primary auditory cortex. *Nat. Neurosci.* **18**, 1483–1492 (2015).
85. Adams, J. C. Ascending projections to the inferior colliculus. *J. Comp. Neurol.* **183**, 519–538 (1979).
86. Malmierca, M. S., Merchán, M. A., Henkel, C. K. & Oliver, D. L. Direct projections from cochlear nuclear complex to auditory thalamus in the rat. *J. Neurosci.* **22**, 10891–7 (2002).
87. Xie, R., Meitzen, J. & Pollak, G. D. Differing Roles of Inhibition in Hierarchical Processing of Species-Specific Calls in Auditory Brainstem Nuclei. *J. Neurophysiol.* **94**, 4019–4037 (2005).
88. Holmstrom, L. A., Eeuwes, L. B. M., Roberts, P. D. & Portfors, C. V. Efficient Encoding of Vocalizations in the Auditory Midbrain. *J. Neurosci.* **30**, 802–819 (2010).

89. Mayko, Z. M., Roberts, P. D. & Portfors, C. V. Inhibition shapes selectivity to vocalizations in the inferior colliculus of awake mice. *Front. Neural Circuits* **6**, 73 (2012).
90. Felix, R. A., Gourévitch, B. & Portfors, C. V. Subcortical pathways: Towards a better understanding of auditory disorders. *Hear. Res.* **362**, 48–60 (2018).
91. Jenkins, W. M. & Masterton, R. B. Sound localization: effects of unilateral lesions in central auditory system. *J. Neurophysiol.* **47**, 987–1016 (1982).
92. Oliver, D. L. Dorsal cochlear nucleus projections to the inferior colliculus in the cat: A light and electron microscopic study. *J. Comp. Neurol.* **224**, 155–172 (1984).
93. Oliver, D. L. Projections to the inferior colliculus from the anteroventral cochlear nucleus in the cat: Possible substrates for binaural interaction. *J. Comp. Neurol.* **264**, 24–46 (1987).
94. Glendenning, K. K., Baker, B. N., Hutson, K. A. & Masterton, R. B. Acoustic chiasm V: Inhibition and excitation in the ipsilateral and contralateral projections of LSO. *J. Comp. Neurol.* **319**, 100–122 (1992).
95. Saint Marie, R. L., Shneiderman, A. & Stanforth, D. A. Patterns of gamma-aminobutyric acid and glycine immunoreactivities reflect structural and functional differences of the cat lateral lemniscal nuclei. *J. Comp. Neurol.* **389**, 264–76 (1997).
96. Cant, N. B. & Benson, C. G. Parallel auditory pathways: projection patterns of the different neuronal populations in the dorsal and ventral cochlear nuclei. *Brain Res. Bull.* **60**, 457–474 (2003).
97. Aitkin, L. M. & Phillips, S. C. The interconnections of the inferior colliculi through their commissure. *J. Comp. Neurol.* **228**, 210–216 (1984).
98. Morest, D. K. & Oliver, D. L. The neuronal architecture of the inferior colliculus in the cat: Defining the functional anatomy of the auditory midbrain. *J. Comp. Neurol.* **222**, 209–236 (1984).
99. Oliver, D. L., Kuwada, S., Yin, T. C. T., Haberly, L. B. & Henkel, C. K. Dendritic and axonal morphology of HRP-injected neurons in the inferior colliculus of the cat. *J. Comp. Neurol.* **303**, 75–100 (1991).
100. Anderse, R. A., Roth, G. L., Aitkin, L. M. & Merzenich, M. M. The efferent projections of the central nucleus and the pericentral nucleus of the inferior collculus in the cat. *J. Comp. Neurol.* **194**, 649–662 (1980).
101. Wenstrup, J. J. The Auditory Thalamus in Bats. in 368–415 (Springer, New York, NY, 1995). doi:10.1007/978-1-4612-2556-0_8
102. Malmierca, M. S., Rees, A. & Le Beau, F. E. N. Ascending Projections to the Medial Geniculate Body from Physiologically Identified Loci in the Inferior Colliculus. in *Acoustical Signal Processing in the Central Auditory System* 295–302 (Springer US, 1997). doi:10.1007/978-1-4419-8712-9_28
103. Merchán, M., Aguilar, L. A., Lopez-Poveda, E. A. & Malmierca, M. S. The inferior colliculus of the rat: Quantitative immunocytochemical study of GABA and glycine. *Neuroscience* **136**, 907–925 (2005).
104. Ito, T., Bishop, D. C. & Oliver, D. L. Two Classes of GABAergic Neurons in the Inferior Colliculus. *J. Neurosci.* **29**, 13860–13869 (2009).
105. Ito, T. & Oliver, D. L. The basic circuit of the IC: tectothalamic neurons with

different patterns of synaptic organization send different messages to the thalamus. *Front. Neural Circuits* **6**, 48 (2012).
106. Beebe, N. L., Young, J. W., Mellott, J. G. & Schofield, B. R. Extracellular Molecular Markers and Soma Size of Inhibitory Neurons: Evidence for Four Subtypes of GABAergic Cells in the Inferior Colliculus. *J. Neurosci.* **36**, 3988–3999 (2016).
107. Ono, M., Bishop, D. C. & Oliver, D. L. Identified GABAergic and Glutamatergic Neurons in the Mouse Inferior Colliculus Share Similar Response Properties. *J. Neurosci.* **37**, 8952–8964 (2017).
108. Peruzzi, D., Sivaramakrishnan, S. & Oliver, D. L. Identification of cell types in brain slices of the inferior colliculus. *Neuroscience* **101**, 403–416 (2000).
109. Sivaramakrishnan, S. & Oliver, D. L. Distinct K currents result in physiologically distinct cell types in the inferior colliculus of the rat. *J. Neurosci.* **21**, 2861–2877 (2001).
110. Goyer, D. *et al.* A novel class of inferior colliculus principal neurons labeled in vasoactive intestinal peptide-Cre mice. *Elife* **8**, (2019).
111. Aitkin, L. M. The Auditory Midbrain. in *The Auditory Midbrain* 201–204 (Humana Press, 1986). doi:10.1007/978-1-59259-460-3_12
112. Aitkin, L. M. & Phillips, S. C. Is the inferior colliculus and obligatory relay in the cat auditory system? *Neurosci. Lett.* **44**, 259–264 (1984).
113. Barnstedt, O., Keating, P., Weissenberger, Y., King, A. J. & Dahmen, J. C. Functional Microarchitecture of the Mouse Dorsal Inferior Colliculus Revealed through In Vivo Two-Photon Calcium Imaging. *J. Neurosci.* **35**, 10927–10939 (2015).
114. Jane, J. A., Masterton, R. B. & Diamond, I. T. The function of the tectum for attention to auditory stimuli in the cat. *J. Comp. Neurol.* **125**, 165–191 (1965).
115. Lumani, A. & Zhang, H. Responses of neurons in the rat's dorsal cortex of the inferior colliculus to monaural tone bursts. *Brain Res.* **1351**, 115–129 (2010).
116. Patel, C. R., Redhead, C., Cervi, A. L. & Zhang, H. Neural sensitivity to novel sounds in the rat's dorsal cortex of the inferior colliculus as revealed by evoked local field potentials. *Hear. Res.* **286**, 41–54 (2012).
117. Li, H. & Mizuno, N. Single neurons in the spinal trigeminal and dorsal column nuclei project to both the cochlear nucleus and the inferior colliculus by way of axon collaterals: a fluorescent retrograde double-labeling study in the rat. *Neurosci. Res.* **29**, 135–142 (1997).
118. Aitkin, L. M., Dickhaus, H., Schult, W. & Zimmermann, M. External nucleus of inferior colliculus: auditory and spinal somatosensory afferents and their interactions. *J. Neurophysiol.* **41**, 837–47 (1978).
119. Binns, K. E., Grant, S., Withington, D. J. & Keating, M. J. A topographic representation of auditory space in the external nucleus of the inferior colliculus of the guinea-pig. *Brain Res.* **589**, 231–242 (1992).
120. Knudsen, E. I. & Konishi, M. A neural map of auditory space in the owl. *Science* **200**, 795–7 (1978).
121. Gutfreund, Y. & Knudsen, E. I. Adaptation in the Auditory Space Map of the Barn Owl. *J. Neurophysiol.* **96**, 813–825 (2006).
122. Lesicko, A. M. H., Hristova, T. S., Maigler, K. C. & Llano, D. A. Connectional

Modularity of Top-Down and Bottom-Up Multimodal Inputs to the Lateral Cortex of the Mouse Inferior Colliculus. *J. Neurosci.* **36**, 11037–11050 (2016).
123. Klepper, A. & Herbert, H. Distribution and origin of noradrenergic and serotonergic fibers in the cochlear nucleus and inferior colliculus of the rat. *Brain Res.* **557**, 190–201 (1991).
124. Thompson, G. C., Thompson, A. M., Garrett, K. M. & Britton, B. H. Serotonin and Serotonin Receptors in the Central Auditory System. *Otolaryngol. Neck Surg.* **110**, 93–102 (1994).
125. Hurley, L. M. & Pollak, G. D. Serotonin differentially modulates responses to tones and frequency-modulated sweeps in the inferior colliculus. *J. Neurosci.* **19**, 8071–82 (1999).
126. Hurley, L. M. Serotonin Shifts First-Spike Latencies of Inferior Colliculus Neurons. *J. Neurosci.* **25**, 7876–7886 (2005).
127. Hurley, L. M., Tracy, J. A. & Bohorquez, A. Serotonin 1B receptor modulates frequency response curves and spectral integration in the inferior colliculus by reducing GABAergic inhibition. *J. Neurophysiol.* **100**, 1656–1667 (2008).
128. OBARA, N., KAMIYA, H. & FUKUDA, S. Serotonergic modulation of inhibitory synaptic transmission in mouse inferiorcolliculus. *Biomed. Res.* **35**, 81–84 (2014).
129. Keesom, S. M., Sloss, B. G., Erbowor-Becksen, Z. & Hurley, L. M. Social experience alters socially induced serotonergic fluctuations in the inferior colliculus. *J. Neurophysiol.* **118**, 3230–3241 (2017).
130. Tong, L., Altschuler, R. A. & Holt, A. G. Tyrosine hydroxylase in rat auditory midbrain: Distribution and changes following deafness. *Hear. Res.* **206**, 28–41 (2005).
131. Nevue, A. A., Elde, C. J., Perkel, D. J. & Portfors, C. V. Dopaminergic Input to the Inferior Colliculus in Mice. *Front. Neuroanat.* **9**, 1–9 (2016).
132. Batton, A. D., Blaha, C. D., Bieber, A., Lee, K. H. & Boschen, S. L. Stimulation of the subparafascicular thalamic nucleus modulates dopamine release in the inferior colliculus of rats. *Synapse* **73**, e22073 (2019).
133. Gittelman, J. X., Perkel, D. J. & Portfors, C. V. Dopamine modulates auditory responses in the inferior colliculus in a heterogeneous manner. *JARO - J. Assoc. Res. Otolaryngol.* **14**, 719–729 (2013).
134. Motts, S. D. & Schofield, B. R. Sources of Cholinergic Input to the Inferior Colliculus. *Neuroscience* **160**, 103 (2009).
135. Farley, G. R., Morley, B. J., Javel, E. & Gorga, M. P. Single-unit responses to cholinergic agents in the rat inferior colliculus. *Hear. Res.* **11**, 73–91 (1983).
136. Levitt, P. & Moore, R. Y. Origin and organization of brainstem catecholamine innervation in the rat. *J. Comp. Neurol.* **186**, 505–528 (1979).
137. Jones, L. S., Gauger, L. L. & Davis, J. N. Anatomy of brain alpha1-adrenergic receptors: In vitro autoradiography with [125I]-heat. *J. Comp. Neurol.* **231**, 190–208 (1985).
138. Palacios, J. M., Hoyer, D. & Cortés, R. α1-adrenoceptors in the mammalian brain: similar pharmacology but different distribution in rodents and primates. *Brain Res.* **419**, 65–75 (1987).
139. Boyajian, C. L., Loughlin, S. E. & Leslie, F. M. *Anatomical Evidence forAlpha-2 Adrenoceptor Heterogeneity: Differential Autoradiographic Distributions of*

[3H]Rauwolscine and [3H]Idazoxan in Rat Brain1. **241**, (1987).
140. Rainbow, T. C., Parsons, B. & Wolfe, B. B. Quantitative autoradiography of beta 1- and beta 2-adrenergic receptors in rat brain. *Proc. Natl. Acad. Sci. U. S. A.* **81**, 1585–9 (1984).
141. Day, H. E. ., Campeau, S., Watson, S. J. & Akil, H. Distribution of α1a-, α1b- and α1d-adrenergic receptor mRNA in the rat brain and spinal cord. *J. Chem. Neuroanat.* **13**, 115–139 (1997).
142. Domyancic, A. V. & Morilak, D. A. Distribution of ?1A adrenergic receptor m RNA in the rat brain visualized by in situ hybridization. *J. Comp. Neurol.* **386**, 358–378 (1997).
143. Papay, R. *et al.* Localization of the mouse α1A-adrenergic receptor (AR) in the brain: α1AAR is expressed in neurons, GABAergic interneurons, and NG2 oligodendrocyte progenitors. *J. Comp. Neurol.* **497**, 209–222 (2006).
144. Scheinin, M. *et al.* Distribution of α2-adrenergic receptor subtype gene expression in rat brain. *Mol. Brain Res.* **21**, 133–149 (1994).
145. Nicholas, A. P., Pieribone, V. A. & Hökfelt, T. Cellular localization of messenger RNA for beta-1 and beta-2 adrenergic receptors in rat brain: An in situ hybridization study. *Neuroscience* **56**, 1023–1039 (1993).

Chapter 2. Noradrenergic modulation of intracellular calcium in the mouse inferior colliculus

2.1 Abstract

Norepinephrine is a modulator of diverse processes in the brain, with roles in arousal, attention, memory, and fear. Norepinephrine modulates multiple sensory processing modalities in the brain, including the auditory system. The central noradrenergic modulatory region, the locus coeruleus, projects noradrenergic fibers to the principal auditory midbrain region, the inferior colliculus (IC). We examined the modulatory effects of norepinephrine in the IC using widefield calcium imaging. We found that norepinephrine reliably and robustly increases intracellular levels of calcium in cells in the IC. This occurred in all three subregions of the IC, with greater effects observed in the external subregions of the IC. Norepinephrine's effects were mediated by all three adrenergic receptor subtypes (α_1, α_2, and β). α_1 receptor-mediated effects were indirect, requiring intact purinergic signaling. α_2 and β receptor-mediated effects were direct. All of the observed effects of norepinephrine did not require action potentials but were prevented by the exclusion of extracellular calcium. We found that the effects of norepinephrine did not occur in excitatory neurons in the IC. Together, these results provide the first evidence for the modulatory actions of norepinephrine in the IC, implicating noradrenergic modulation in auditory processing.

2.2 Introduction

Modulation of sensory processing is an important mechanism by which the central nervous system can adapt incoming information to differing internal and external states.

Norepinephrine is a powerful neuromodulator that is released widely throughout the brain and is implicated in a broad range of functions, such as arousal, attention, and memory. The locus coeruleus (LC), provides the majority of noradrenergic fibers that project throughout the mammalian brain[1,2]. Norepinephrine can modulate sensory processing as well, with effects on the majority of central sensory processing systems, including visual, olfactory, somatosensory, gustatory, and auditory[3]. Norepinephrine modulates synaptic activity in the auditory cortex[4–7] resulting in improved signal relative to noise. Pairing the presentation of an auditory stimulus with stimulation of the LC results in facilitation of auditory cortical responses[8], highlighting the links between attention and noradrenergic modulation. In the auditory brainstem, norepinephrine is critical for development of lateral superior olive networks[9] and increases signal-to-noise ratio in the dorsal cochlear nucleus[10].

The inferior colliculus (IC) is the primary auditory nucleus of the mammalian midbrain. The IC functions as a relay and integration site for nearly all ascending auditory signals and receives descending projections from multiple regions, including the auditory cortex and thalamus[11–15]. The merging of ascending auditory information gives rise to an increased complexity of neuronal responses to auditory stimuli. As a gatekeeper for ascending and descending auditory pathways, the IC is positioned to be a powerful site

of broad modulatory effects. Dopamine exerts diverse actions on tone-evoked responses in IC neurons[16]. Serotonin affects the timing of auditory responses in IC neurons[17–19] and changes inhibitory synaptic activity[20].

Little is currently known of norepinephrine's actions in the IC. The IC contains fibers that express dopamine β-hydroxylase (DBH), the enzyme required for the synthesis of norepinephrine. The vast majority of DBH-positive fibers in the IC originate from the locus coeruleus[21]. Neural activity in the IC has been linked to LC activity via pupil diameter, suggesting noradrenergic release in the IC during bouts of increased LC activity[22].

Here we examine the effects of norepinephrine application in brain slices of the IC using calcium imaging. We find that norepinephrine evokes intracellular calcium increases throughout the IC, with larger amplitude effects observed in the external cortices of the IC. These effects are mediated by all three noradrenergic receptor subtypes (α1, α2, and β), with distinct patterns of activity elicited by activation of each subtype. These results implicate a diverse role for noradrenergic modulation in the IC.

2.3 Materials and methods

Animals

All procedures were done in accordance with the University of Washington Institutional Animal Care and Use Committee. Male and female CBA/CaJ mice aged postnatal day 12 through 15 were used for all experiments. Mice were housed with foster mothers until the day of experiments, under a 12:12 light dark cycle with unlimited access to food and

water. Mice expressing GCaMP6s under the control of Camk2a-cre were bred by crossing Camk2a-cre/ERT2 (Jackson labs catalog number 012362) with Ai162D (TIT2L-GC6s-ICL-tTA2, Jackson labs catalog number 031562). Pups aged 10 days were injected intraperitoneally with tamoxifen (1 mg in corn oil vehicle, Sigma) to induce cre expression. Camk2a-GCaMP6s pups were then sacrificed five to eight days later for experiments.

Brain slice preparation

Mice were anesthetized by isoflurane inhalation and quickly decapitated. Brains were removed and transferred to an ice-cold slicing solution composed of (in mM): sucrose (180), KCl (2.5), MgCl2 (7.5), NaH2PO4·H2O (1), NaHCO3 (26.2), glucose (11), CaCl2 (0.5), HEPES (20), and ascorbate (5). The slicing solution osmolarity was adjusted to 300 mOsm by addition of sucrose and was bubbled with a 95% O2/5% CO2 mixture for the duration of slicing. Brains were blocked rostral to the IC and coronal slices of the IC were made using a vibrating microtome (Leica). Slices were made at 250 μm thickness. Some slices were bisected into hemispheres to increase experimental yield per animal. Slices were transferred using a glass pipette to warmed recovery solution composed of (in mM): NaCl (94), KCl (2.5), MgSO4·7H2O (1.3), NaH2PO4·H2O (1), NaHCO3 (26.2), glucose (11), CaCl2 (2.5), HEPES (20), and ascorbate (5). The recovery solution osmolarity was 300 mOsm and was bubbled with a 95% O2/5% CO2 mixture at room temperature for the duration of the recording day. Slices were rested for a minimum of 45 min before use in experiments.

Calcium imaging

After resting, slices were transferred to a small petri dish containing 0.07% pluronic (Sigma), 1 μM Fluo-4 AM (Invitrogen), and recovery solution that was continuously bubbled with 95% O2/5% CO2 for calcium indicator dye loading. The slices were loaded for 40 minutes then returned to the original recovery bath until recording. For recording, slices were transferred to a bath that was continuously perfused with warmed (30° C) bath solution containing (in mM): NaCl (119), KCl (2.5), MgSO4·7H2O (1.3), NaH2PO4·H2O (1), NaHCO3 (26.2), glucose (11), and CaCl2 (2.5). The bath solution osmolarity was 300 mOsm and bubbled with a 95% O2/5% CO2 mixture for the duration of experiments. A bath solution containing zero calcium and EGTA was composed of (in mM): NaCl (119), KCl (2.5), MgSO4·7H2O (3.8), NaH2PO4·H2O (1), NaHCO3 (26.2), glucose (11), and EGTA (0.5). Slices were secured using a small patch of porous membrane (12 micron, Nucleopore) and a platinum harp. Slices were allowed to rest for 10 minutes in the recording bath prior to the start of an experiment. Experiments were performed using a Nikon AZ100 upright microscope with AZ Plan Fluor 2x objective. Photomultipliers or 2x or 3x in the light path were used to frame the IC and maximize the tradeoff between area recorded and cellular resolution. Recordings were captured at one frame per second at a resolution of 1920x1440 pixels using an ORCA-Flash2.8 camera (Hamamatsu) and NIS-elements (Nikon) software. Drugs for pharmacological manipulations were bath applied with the following concentrations: Norepinephrine (10 μM, Sigma), cirazoline (30 μM, Tocris), clonidine (50 μM, Sigma), isoproterenol (15 μM, Sigma), prazosin (10 μM, Tocris), yohimbine (20 μM, Sigma), propranolol (30 μM, Tocris), tetrodotoxin (TTX, 500 nM, Calbiochem), NBQX (10 μM, Tocris), DL AP-V (50 μM,

Sigma), SR-95531 (GABAzine, 10 μM, Sigma), strychnine (1 μM, Sigma), suramin (150 μM, Sigma), PPADS (50 μM, Tocris), forskolin (10 μM, Sigma), TTAP-2 (20 μM, Alomone labs), nifedipine (50 μM, Sigma), ATP (100 μM, Sigma), Carbenoxolone (100 μM, Sigma).

SR101

For labeling of astrocytes, slices were loaded with sulforhodamine 101 (SR101, Sigma). Immediately following slicing, slices were placed in a small petri dish containing recovery solution with 1 μM SR101, warmed to 34°C. This loading protocol effectively labels astrocytes[23] Slices were loaded for 20 minutes before a brief wash in recovery solution and transfer to a recovery chamber. Slices were then allowed to rest for an additional 10 minutes before normal Fluo-4 loading and subsequent recordings. During imaging of SR101 loaded slices, SR101 fluorescence images were taken before and after Fluo4 imaging and compared for movement. Slices that exhibited inconsistencies attributed to swelling and/or movement between the two SR101 images were not used for analysis.

Data analysis

All imaging analysis was performed with FIJI[24] and Matlab (Mathworks).

Captured time courses were first exported from NIS-elements (Nikon) as image stacks for further processing in ImageJ. Time course stacks were then spatially down sampled by a factor of 2. Masks of the inferior colliculus were then drawn by hand to limit analysis to the IC.

Constrained non-negative matrix factorization (CNMF) was then performed as described in Pnevmatikakis et al, 2016[25]. The Matlab implementation of this analysis was used. This analysis allowed for objective detection of cells and neuropil captured in our time courses based on fluctuations in calcium and resulting indicator fluorescence.

Specifically, temporal and spatial components of cells and neuropil were first estimated, along with background components. We utilized the 'greedy' method provided by Pnevmatikakis and colleagues, followed by HALs refinement. First estimations of spatial and temporal components were then further refined by using initial spatial estimates to build a subsequent set of temporal components, and initial temporal components to build a subsequent set of spatial components. At this point, cellular components were correlated with raw fluorescence activity to estimate their accuracy in representing the raw data. Overlapping spatial components that had similarly correlated temporal activity were then merged. Spatial and temporal components were then refined again, before being ordered based on the maximum values in their spatial and temporal components. ΔF/F values were then measured for each cellular component.

Primary functions used: *preprocess_data, initialize_components, update_spatial_components, update_temporal_components, classify_comp_corr, merge_components, order_ROIs*, and *extract_DF_F*. *plot_contours* and *plot_components_GUI* were also used for aid in analysis and data visualization.

Component ΔF/F traces were used for all subsequent measurements. Initial estimates of the number of spatial components were high (~1000), often resulting in a large number

of spurious components detected. To select non-spurious components for further analysis, we calculated the sum of the absolute values of differences within each ΔF/F trace to eliminate components that showed little to no (< 1%) total change in fluorescence. All presented data were measured from the selected ΔF/F traces.

Mean ΔF/F increases for each slice experiment were measured by calculating the difference in maximum mean ΔF/F during drug application vs baseline period for across all components. Baseline period was defined as the initial 10-20 seconds of each time series (~10% of the full duration). ΔF/F peak values were calculated as the difference between peak ΔF/F and baseline for each component. ΔF/F halfwidths were calculated by measuring the width of the ΔF/F response at half peak ΔF/F value, and in some cases were truncated due to sustained increases that surpassed the length of recording. This was the case for primarily the IC surface noradrenergic effects and rarely observed within the ICc, ICx, and ICd subregions. Component distance from edge was calculated by measuring the distance from the centroid coordinates of each CNMF-detected component and nearest edge of the IC mask region of interest (ROI) drawn initially to limit analysis to the IC.

Subregion specific effects were assessed by limiting measurements of CNMF-detected components to manually determined IC subregions. Subregion ROIs were drawn based on comparison of anatomical markers in slices to a reference atlas (Allen brain institute) and borders discernible by variations in Fluo4 loading.

We measured overlap between agonist-evoked ΔF/F increases and SR101 label manually. For examining overlap between agonist effects, only slices where effects were observed from each adrenergic receptor agonist were used. 200 by 200 pixel regions of ICc, ICx, and ICd were cropped and CNMF-detected components were overlaid using custom Matlab scripts for manual assessment of the number of overlapping components. For SR101 overlap, we used ImageJ functions to find SR101 ROIs. First, a gaussian blur with a radius of 2 pixels was applied. Next, background was subtracted using the rolling ball technique (radius = 10 pixels). Images were then thresholded and ROIs detected with a minimum area of 10 pixels to help eliminate spurious ROIs arising from trapped air bubbles or other artifacts. SR101 ROIs were then imported into Matlab and overlaid with CNMF-detected components for manual counting of overlap.

Statistical analysis and plotting

All images shown were made using Matlab or ImageJ. All data plots were made using GraphPad Prism. All statistical analyses were made using GraphPad Prism. Unless otherwise noted, individual slices and hemislices were treated as independent observations. Images presented in figures represent maximum-intensity z-projections produced in ImageJ, unless otherwise noted.

2.4 Results

Norepinephrine elicits calcium increases throughout the inferior colliculus

To examine the effects of norepinephrine in the inferior colliculus (IC), we bath applied norepinephrine to coronal slices of IC loaded with Ca indicator while imaging. Norepinephrine application (10 μM) reliably produced increases in calcium in the IC with

a mean ΔF/F increase of 5.8% (n=15, p-value < 0.001, one-sample T test) (Figure 2.1). The norepinephrine effect was observed in all subregions of the IC as well as the external surface of the IC (Figure 2.1a). To quantify the differences in norepinephrines effects in the subregions of the IC, we selected 5 slices where the subregions were able to be

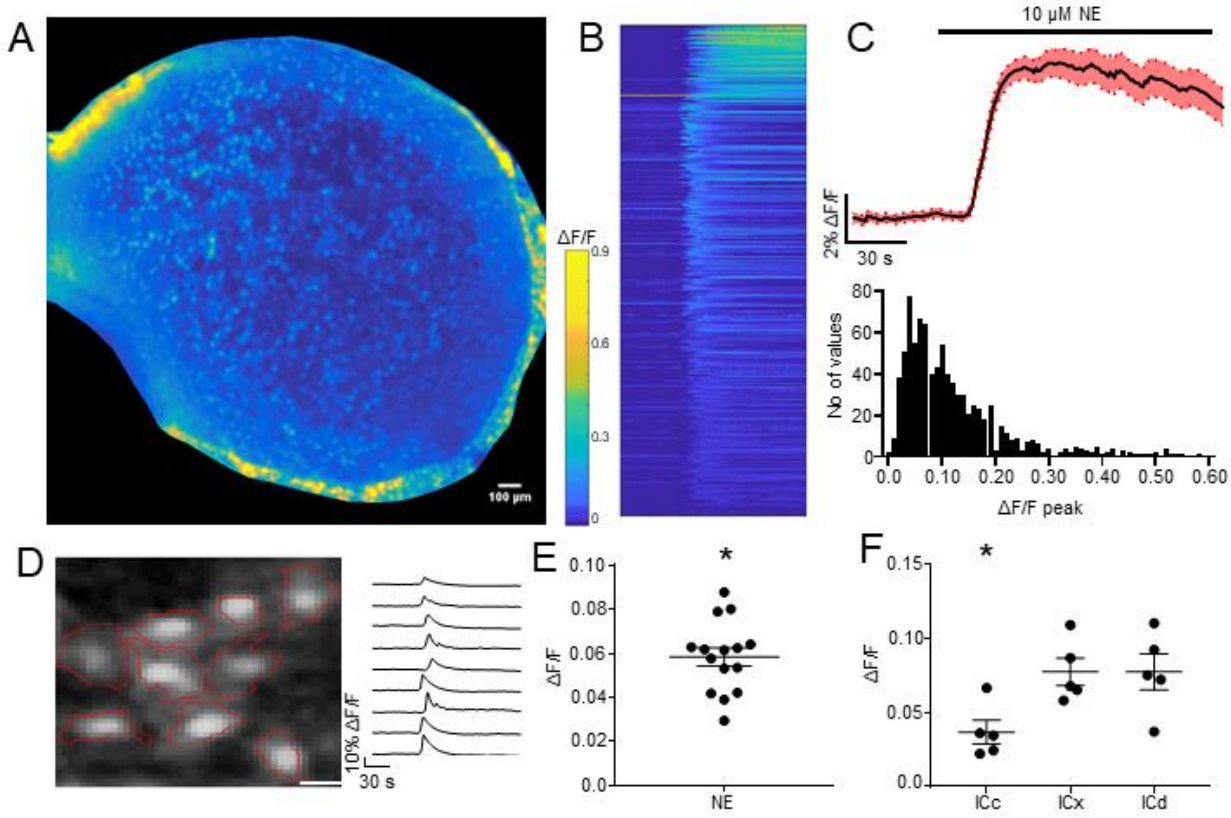

Figure 2.1: Norepinephrine evokes calcium increases in the IC

A: ΔF/F max projection of norepinephrine's (10 μM) effects in a representative coronal slice of IC. Scale bar = 100 microns. B: Carpet plot of ΔF/F responses in detected regions of interest across time of the representative effect shown in A. Each row represents a ROI's change in fluorescence over time coded by color. Total time = 180 s. C: *Upper:* Mean trace of ΔF/F responses shown in B with standard error of the mean cloud in red. *Lower:* Histogram of the peak ΔF/F effects observed in the representative effect shown in A and B. n = 881. D: *Left:* Crop of the max projection ΔF/F image shown in A with CNMF-detected ROIs outlined in red. Scale bar = 15 microns. *Right:* ΔF/F traces over time of the ROIs shown on the right. E: Summary plot of all mean ΔF/F responses to norepinephrine application. Error bars represent mean ± standard error of the mean. F: Summary of mean ΔF/F responses to norepinephrine application across IC subregions in 5 slices with well-defined subregions. ICc: central nucleus ICx: external cortex, ICd: dorsal cortex.

differentiated by anatomical landmarks visible due to baseline fluorescence of the calcium indicator After measuring subregion-specific ΔF/F, greater increases in fluorescence in response to norepinephrine were observed in the dorsal cortex of the IC (ICd) (mean 7.74%, n=5) and external cortex of the IC (ICx) (mean 7.74, n=5) than in the primary auditory processing central nucleus (ICc) (mean 3.67%, n=5). ΔF/F increases in the ICd and ICx were not significantly different (p-value > 0.999, Tukey's multiple comparisons) but both were significantly greater than the ΔF/F increase observed in the ICc (p-values 0.0337 and 0.0337 respectively, Tukey's multiple comparisons).

Norepinephrine-evoked responses exhibit different time courses.

We observed that cells on the external surface of the IC and in the ICx and ICd subregions showed longer-lasting responses to NE application than did cells in the ICc (Figure 2.1b). We measured the half-width of ΔF/F responses and observed a clear bimodal distribution (Figure 2.2a). Examining the time course of ΔF/F responses of these two populations revealed different responses to norepinephrine (Figure 2.2b). Examining the spatial distribution of ROIs with respect to their halfwidths confirmed that longer lasting ΔF/F responses were concentrated on the edges and surface of the IC (Figure 2.2c, d, e). Across slices, halfwidths were the shortest in the ICc (mean 25.14s, n=5) and longer in the ICx (58.82s, n=5) and ICd (mean 44.12s, n=5). ICc halfwidths were significantly shorter than ICx halfwidths (p-value = 0.0232, Tukey's multiple comparisons) (Figure 2.2f). Differing responses to norepinephrine suggested the presence of multiple types of norepinephrine-sensitive cells in the IC.

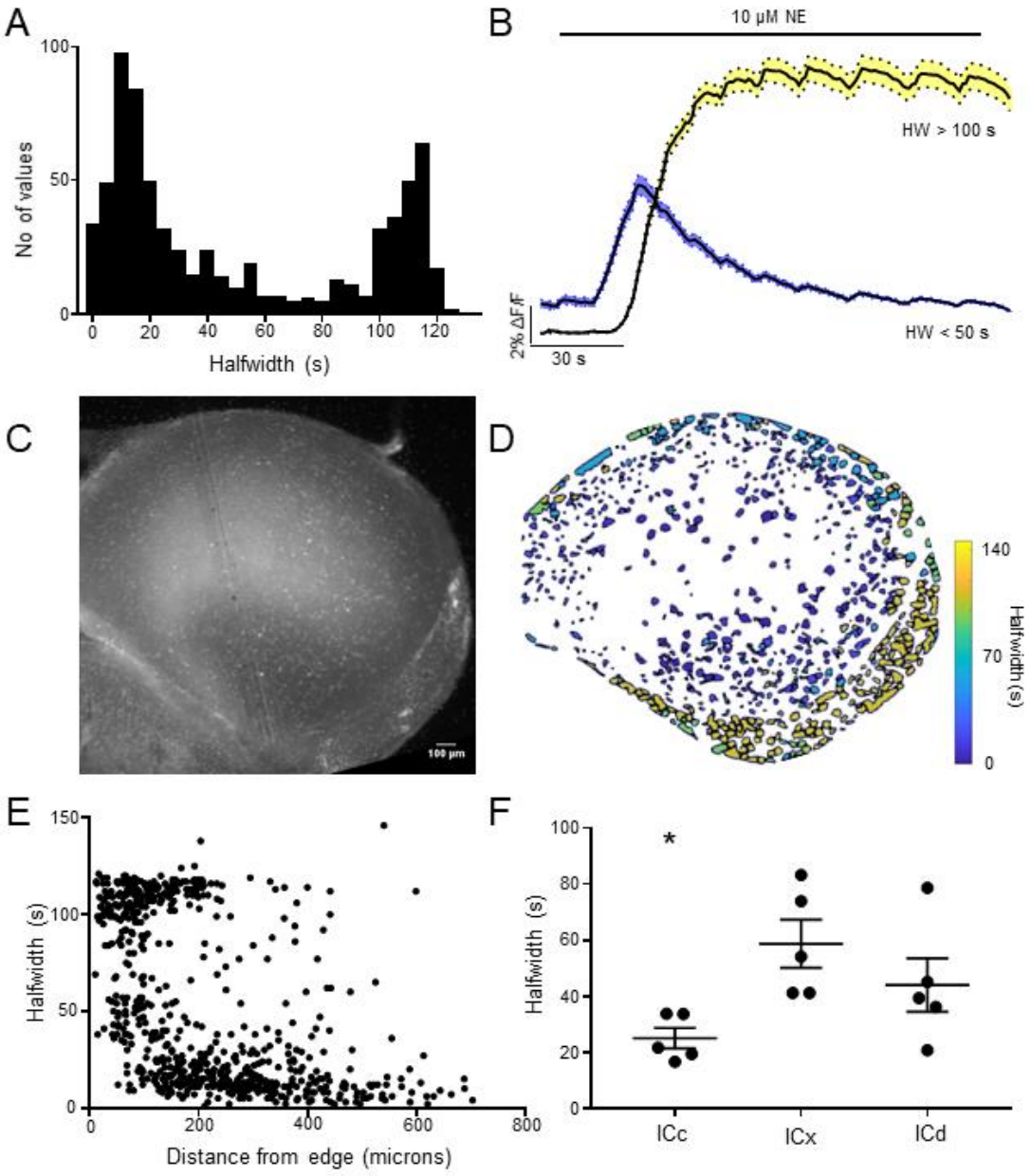

Figure 2.2: Noradrenergic effects are longer in the exterior regions of the IC

A: Histogram of ΔF/F response halfwidths in a representative experiment. n= 717. B: Mean ΔF/F traces with standard error of the mean clouds of ΔF/F responses with halfwidths greater than 100s in yellow, and less than 50s in blue. C: Image of coronal slice of IC from which ΔF/F responses shown in A, B, D, E were recorded. Scale bar = 100 microns. D: ΔF/F ROIs plotted spatially in the IC with halfwidth color coded (range 0 – 140 s). E: ΔF/F responses plotted with distance from IC edge by halfwidth F: Summary mean halfwidths of ICc, ICx, and ICd IC subregions. Error bars represent mean ± standard error of the mean. Mean ICc halfwidths were significantly lower than ICx halfwidths.

Norepinephrine's effects in the IC are direct

We next examined whether the observed effect of norepinephrine on cells in the IC was direct by applying norepinephrine in the presence of TTX and inhibitors of synaptic transmission. Norepinephrine-evoked calcium increases were not blocked by 500 nM TTX (mean 8.213%, n=4) (Figure 2.3a, b), indicating that voltage gated sodium channels and action potential generation are not required for the observed calcium signal.

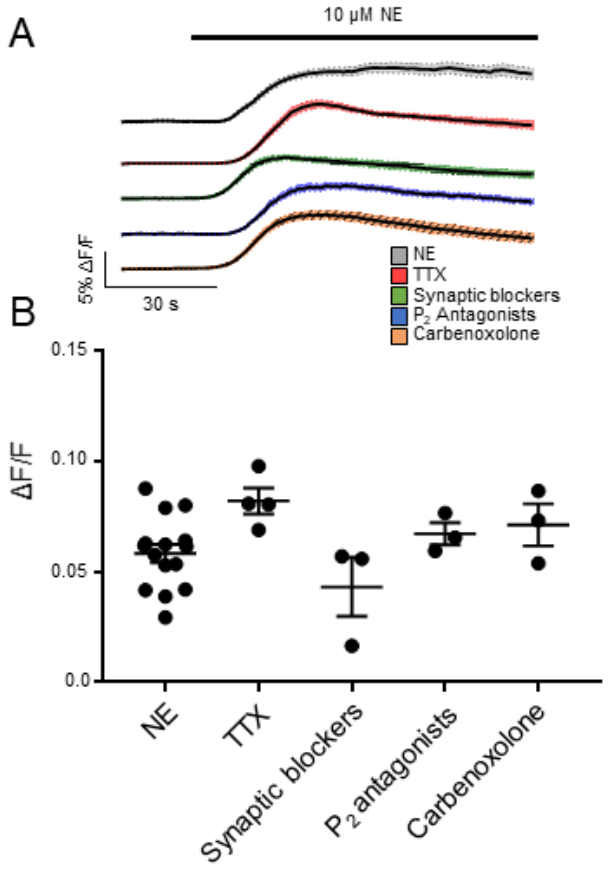

Figure 2.3: Norepinephrine's effects on IC cells is direct

A: Traces of mean ΔF/F responses with standard error of the mean clouds of norepinephrine application in the presence of: control ACSF, 500 nM TTX, fast glutamatergic, GABAergic, and glycinergic synaptic blockers (NBQX 10 µM, AP-V 50 µM, GABAzine 10 µM, and strychnine 1 µM), purinergic receptor antagonists (suramin 150 µM, PPADS 50 µM), and gap junction blocker carbenoxolone (100 µM). B: Summary dot plots of mean ΔF/F responses to NE application in the conditions listed above. Error bars represent mean ± standard error of the mean.

Interestingly, the average fluorescence increase in the presence of TTX appeared to be greater than without. The IC is known to contain GABAergic, glutamatergic, and glycinergic synapses that originate from intrinsic and extrinsic sources. We applied NBQX (10 μM), AP-V (50 μM), GABAzine (10 μM), and strychnine (1 μM) to slices of IC before the addition of norepinephrine. These synaptic blockers did not result in a significant change in norepinephrine-induced calcium transients (mean = 4.32%, n=3) (Figure 2.3a, b). To our knowledge, purinergic signaling has not been observed in the IC but has been linked to noradrenergic modulation elsewhere in the brain. Blocking purinergic signaling with the nonspecific P2 antagonists suramin and PPADs (150 μM and 50 μM) did not significantly alter norepinephrine's effects in the IC (mean 6.73%, n=3) (Figure 2.3a, b). The gap junction inhibitor carbenoxolone also did not have an appreciable effect on norepinephrine-evoked calcium responses (mean 7.13%, n=3) (Figure 2.3a, b). Norepinephrine application in the presence of TTX, fast synaptic blockers, purinergic blockers or carbenoxolone did not differ significantly from control conditions (p-values of 0.096, 0.566, 0.903, and 0.709 respectively, Tukey's multiple comparisons test).

An antagonist cocktail of α1, α2, and β adrenergic receptor blockers eliminated norepinephrine's effects

There is evidence for the expression of multiple adrenergic receptors in the IC, including α1 subtypes and α2 subtypes. To test whether the effect of norepinephrine is mediated by adrenergic receptors, we applied norepinephrine in the presence of a cocktail of adrenergic receptor antagonists. Broadly, adrenergic receptors are divided into three types, α1, α2, and β. We blocked all three receptors with a combination of the α1

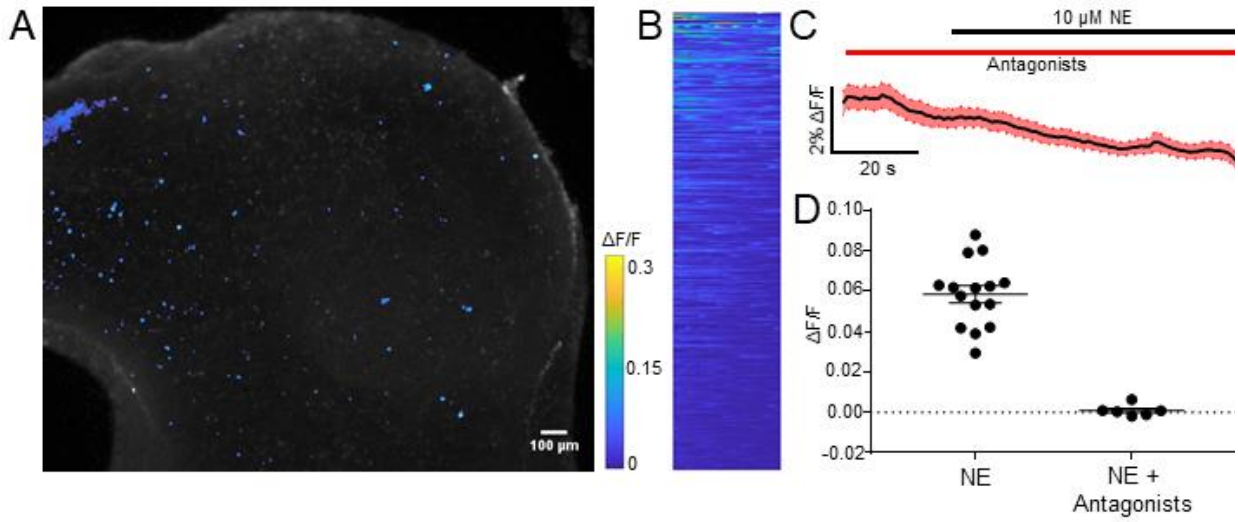

Figure 2.4: Noradrenergic receptor antagonists block norepinephrine's effects in the IC

A: Representative ΔF/F response of NE application in the presence of α_1 receptor antagonist prazosin (10 μM), α_2 receptor antagonist yohimbine (20 μM), and β receptor antagonist propranolol (30 μM) in a coronal slice of the IC. ΔF/F max projection superimposed with raw fluorescence for anatomical reference. Scale bar = 100 microns. B: Carpet plot of ΔF/F responses in detected regions of interest across time of the representative effect shown in A. Each row represents a ROI's change in fluorescence over time coded by color. Total time = 90 s. C: Mean trace of ΔF/F responses shown in A and B with standard error of the mean cloud in red. D: Summary of mean ΔF/F responses in control conditions and with a cocktail of adrenergic receptor antagonists.

antagonist prazosin (10 μM), α2 antagonist yohimbine (20 μM), and β antagonist propranolol (30 μM). The cocktail of adrenergic receptor antagonists fully blocked the calcium increases in response to norepinephrine application (mean 0.01%, n=6, p-value < 0.0001) (Figure 2.4). This confirms that the observed activity with norepinephrine application is mediated by adrenergic receptors.

α1, α2, and β adrenergic agonists elicit calcium responses in the IC

To examine which adrenergic receptors mediate the effects of norepinephrine, we applied subtype specific adrenergic receptor agonists. Surprisingly, we observed fluorescence

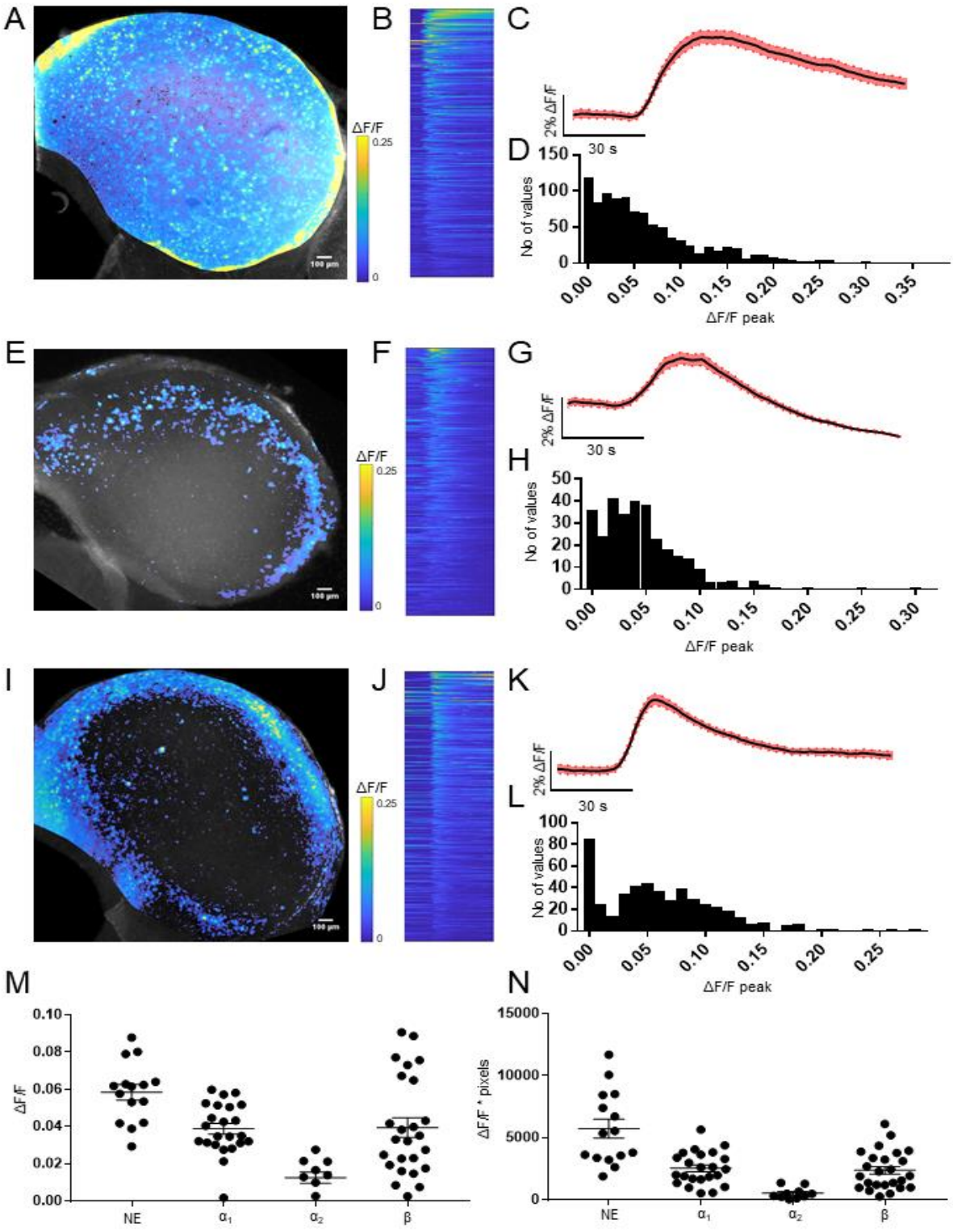

Figure 2.5: α1, α2, and β receptor specific agonists elicit calcium increases in the IC

Figure 2.5 continued. A-D: Representative effects of α_1 adrenergic receptor agonist (cirazoline 30 μM) in the IC. A: ΔF/F max projection superimposed with raw fluorescence for anatomical reference. Scale bars = 100 microns. B: Carpet plots of ΔF/F responses in detected regions of interest across time of the representative effect shown in A. Each row represents a ROI's change in fluorescence over time coded by color. Total time = 120 s. C: Mean trace of cirazoline-induced ΔF/F responses shown in A with standard error of the mean cloud in red. D: Histogram of the peak ΔF/F effects observed in the representative effect shown in A. n = 982. E-H: Representative effects of α_2 adrenergic receptor agonist (clonidine 50 μM) in the IC. E: ΔF/F max projection superimposed with raw fluorescence for anatomical reference. Scale bars = 100 microns. F: Carpet plot of responses in ROIs detected from the representative effect shown in E. Total time = 120 s. G: Mean trace of clonidine-induced ΔF/F responses shown in E with standard error of the mean cloud in red. H: Histogram of peak ΔF/F effects observed in the representative effect shown in E. n = 320. I-L: Representative effects of β adrenergic receptor agonist (isoproterenol 15 μM) in the IC. I: ΔF/F max projection superimposed with raw fluorescence for anatomical reference. Scale bars = 100 microns. J: Carpet plot of responses in ROIs detected from the representative effect shown in I. Total time = 120 s. K: Mean trace of isoproterenol-induced ΔF/F responses shown in I with standard error of the mean cloud in red. H: Histogram of peak ΔF/F effects observed in the representative effect shown in I. n = 527. M: Summary of mean ΔF/F responses elicited by NE or agonist application. Error bars represent mean ± standard error of the mean. N: Summary of mean ΔF/F responses multiplied by total ROI area observed in NE or agonist application. Error bars represent mean ± standard error of the mean.

increases with activation of any of the three adrenergic receptor subtypes (Figure 2.5). The α1 agonist cirazoline (30 μM) (Figure 2.5a, b, c, d), α2 agonist clonidine (50 μM) (Figure 2.5e, f, g, h), and β agonist isoproterenol (15 μM) (Figure 2.5i, j, k, l) each elicited a significant increase in calcium signal (α1 : mean 3.88%, n=23, p-value < 0.0001, α2: mean 1.26%, n=10, p-value=0.002, β: mean 3.945%, n=25, p-value < 0.0001, one sample t-tests). On average, activation of α2 receptors produced the smallest increase in fluorescence, while α1 and β agonists elicited more moderate increases. These agonist-induced signals were all smaller than those caused by NE application (α1 : p-value=0.015, α2: p-value < 0.0001, β: p-value=0.017, Tukey's multiple comparisons test) and α1 and β agonists differed significantly from α2 (p-values=0.003 and 0.002 respectively, Tukey's multiple comparisons test) while not being significantly different from each other (p-

value=0.999, Tukey's multiple comparisons test). Similar average ΔF/F values can be obtained from differing numbers of cells. To account for this possibility, we compared the products of average ΔF/F and total CNMF-detected component area for each agonist. Similar trends were exhibited while comparing ΔF/F * total area values to solely ΔF/F values, confirming that α1 and β agonist applications produced larger ΔF/F effects across more cells in the IC than did α2 receptors.

α1, α2, and β adrenergic agonists differentially activate subregions of the IC

Subregions of the IC perform different functions in auditory processing. We next examined whether noradrenergic receptor specific agonists affected IC subregions differently (Figure 2.6). We observed that α1 receptor activation was more evenly distributed across all three IC subregions (ICc mean 3.22%, n=5, ICx mean 4.26%, n=5, ICd mean 3.96%, n=5, p-value=0.308, one-way ANOVA) (Figure 2.6a, b, c). α1 receptor agonist application also replicated the IC external surface effect (Figure 2.5a**,** Figure 2.6a) previously noted with norepinephrine application (Figure 2.1a). α2 receptor agonist-evoked activity was consistently weak, with its limited effects spread across the IC (ICc mean 1.61%, n=5, ICx mean 1.88%, n=5, ICd mean 1.72%, n=5, p-value=0.953, one-way ANOVA) **(**Figure 2.6a, b, c). Interestingly, α2 effects were concentrated near the borders between the ICc and ICx or ICd (Figure 2.6a). β receptor specific agonist elicited effects were concentrated in the ICx and ICd while being significantly lower in the ICc (ICc mean 2.56%, n=5, ICx mean 5.91%, n=5, ICd mean 6.76%, n=5, p-value=0.018, one-way ANOVA) (Figure 2.6a, b, c). Controlling for total ROI area, the patterns of adrenergic agonist activation hold, with α1 activity being widespread throughout the IC, α2 activity

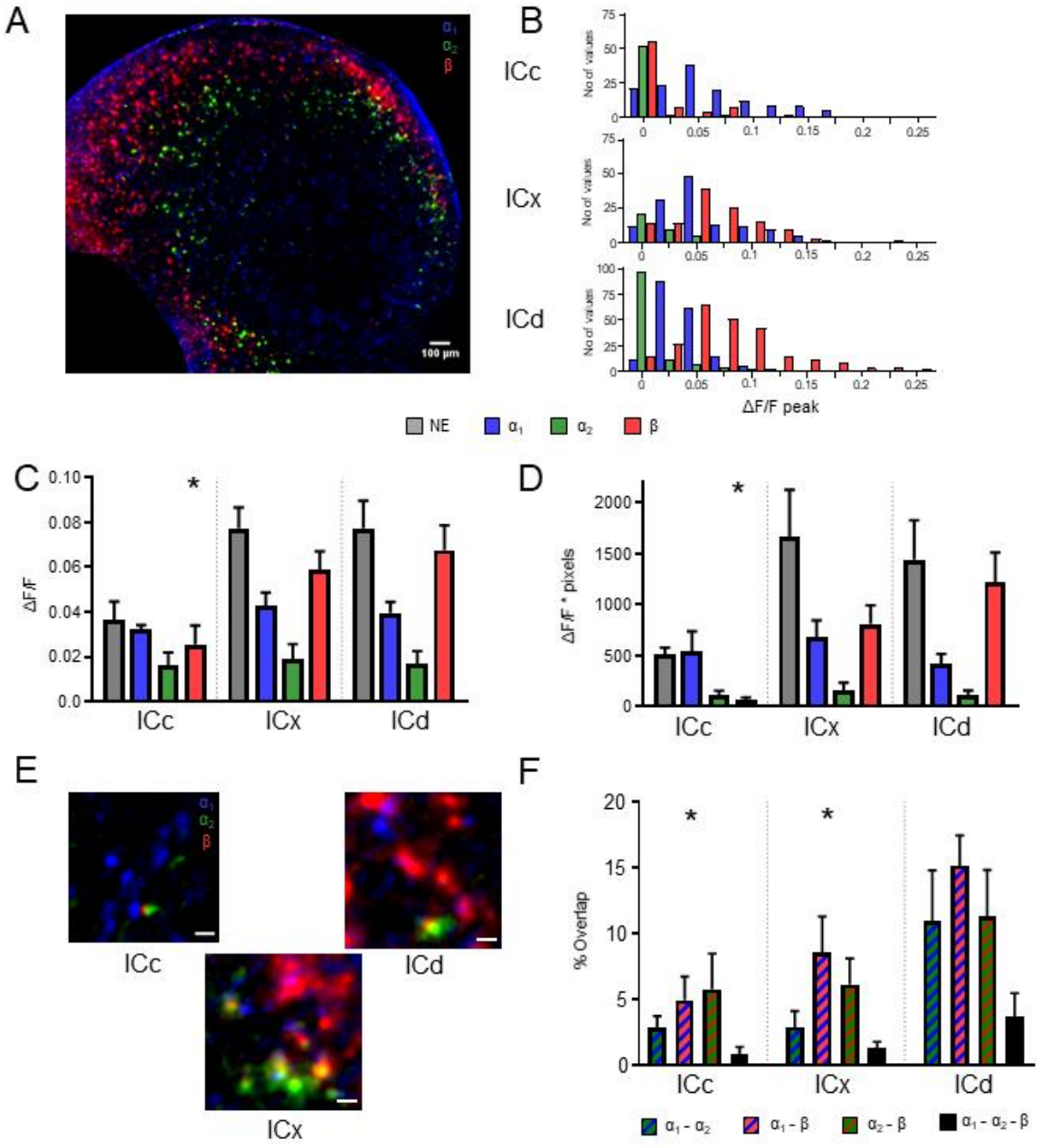

Figure 2.6: Adrenergic specific agonists excite different populations of cells in the IC with little overlap

A: ΔF/F responses of three adrenergic receptor agonists in a coronal slice of IC. Max projections of each agonist-elicited ΔF/F effect superimposed. Scale bar = 100 microns. Brightness and contrast adjusted independently for each agonist-elicited ΔF/F effect. B: Histograms of peak ΔF/F effects shown in A across IC subregions. C: Summary of peak mean ΔF/F responses in IC subregions. n = 5 for each subregion. Summary of peak mean ΔF/F responses multiplied by total ROI area across IC subregions. n = 5 for each subregion. E: Example crops of IC subregions and maximum agonist-elicited ΔF/F effect projected and

Figure 2.6 continued. superimposed. Scale bars = 20 microns. Brightness and contrast adjusted independently for each agonist-elicited ΔF/F effect. F: Summary of agonist ΔF/F effect overlap across IC subregions. n = 5 for each subregion.

weak and focused on the borders of ICc, and β activity being limited to the ICx and ICd subregions (α1 p-value=0.539, α2 p-value=0.822, β p-value=0.0048, one-way ANOVAs) (Figure 2.6d). Different adrenergic receptors exert spatially distinct patterns of calcium activity in the IC.

α1, α2, and β adrenergic agonists activate largely distinct populations of IC cells

Despite the gross differences in spatial patterns of adrenergic receptor action, there is some level of agonist-specific activity in all three subregions of the IC. We next asked if cells in each IC subregion had calcium responses provoked by more than one noradrenergic receptor agonist. We applied all three agonists to seven slices of IC and examined to what extent the agonist-evoked patterns of activity overlapped. Overall, we found small fractions of overlap between agonist-induced effects (α1+α2: mean 0.05 n=18, α1+β: mean 0.09 n=22, α2+β: mean 0.07 n=18, α1+α2+β: mean 0.01 n=18). The least amount of overlap occurred between the α1 and α2 adrenergic receptors and more occurring in between α1 and β receptors and α2 and β receptors (p-value = 0.001, one-way ANOVA). There were small amounts of agonist-induced activity overlap in all three IC subregions, with the largest amount of overlap occurring in the ICd, and least amount in the ICc (ICc: mean 0.03 n=25, ICx: mean 0.04m n=29, ICd: mean=0.11, n=22, p-value = 0.0003, one-way ANOVA) (Figure 2.6f). These results show that while largely distinct populations, some cells show calcium increases in response to application of more than one adrenergic receptor.

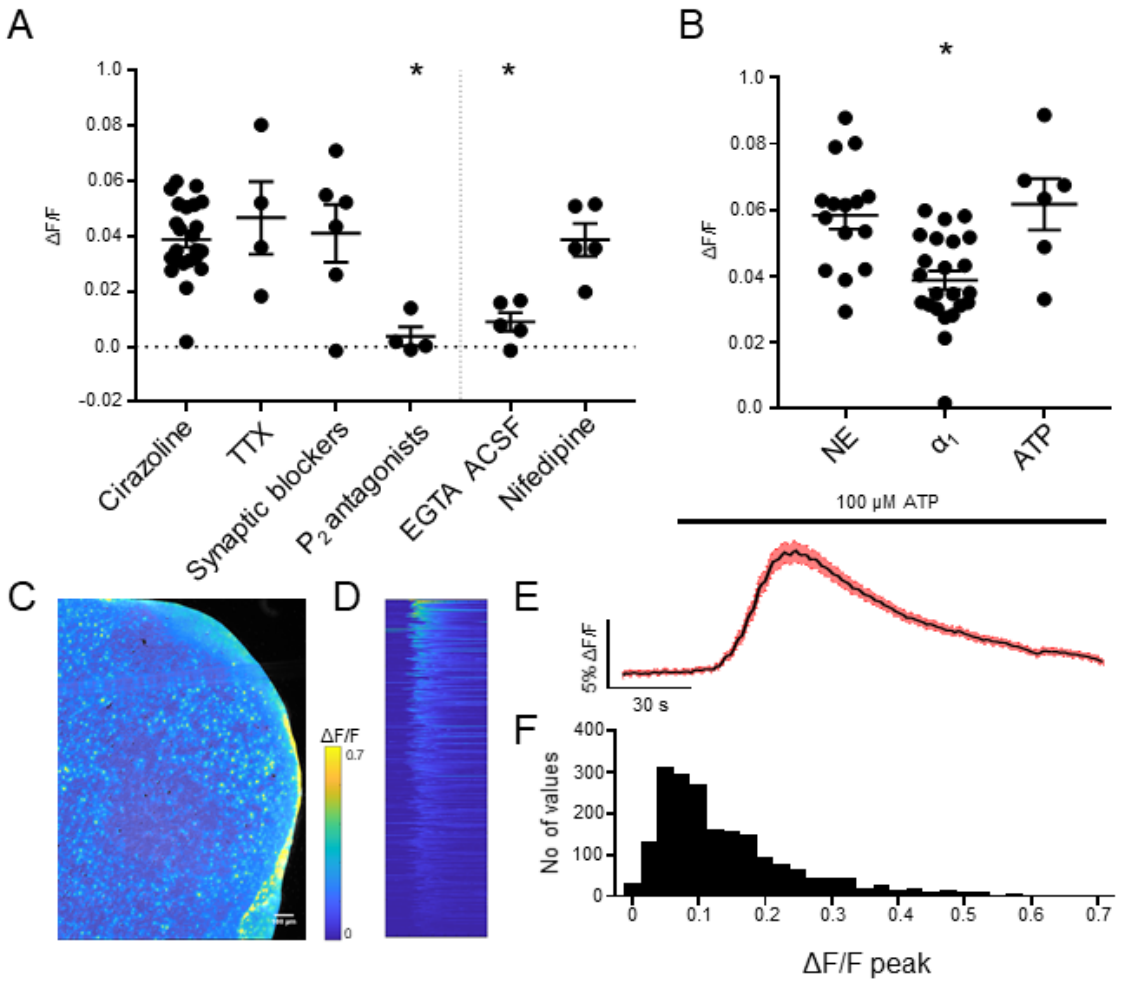

Figure 2.7: α1 effects in the IC require purinergic signaling and extracellular calcium

A: Summary plot of mean ΔF/F responses of α_1 agonist cirazoline (30 μM) in the presence of TTX (500 nM), synaptic blockers (NBQX 10 μM, AP-V 50 μM, GABAzine 10 μM, and strychnine 1 μM), purinergic antagonists (suramin 150 μM, PPADS 50 μM), 0 mM Ca^{2+} ACSF with 0.5 mM EGTA, and L-type calcium channel blocker nifedipine (50 μM). Error bars represent mean ± standard error of the mean. B: Summary mean ΔF/F responses to norepinephrine (10 μM), cirazoline, and ATP (100 μM). Error bars represent mean ± standard error of the mean. C: Representative ΔF/F response of ATP application in coronal slices of the IC. Scale bar = 100 microns. D: Carpet plot of ΔF/F responses in detected regions of interest across time of the representative effect shown in A. Each row represents a ROI's change in fluorescence over time coded by color. Total time = 170 s. E: Mean trace of ΔF/F responses shown in C and D with standard error of the mean cloud in red. F: Histogram of the peak ΔF/F effects observed in the representative effect shown in C and D. n = 1014.

α1 receptor mediated activity requires purinergic signaling and extracellular calcium

We next tested if α1 receptor specific agonist-induced activity was direct and required extracellular calcium (Figure 2.7). Blocking action potentials with TTX had no effect (mean 4.67%, n=4, p-value=0.961, Tukey's multiple comparisons). Blocking fast synaptic transmission also did not affect the response to norepinephrine (mean 4.11%, n=6, p-value=0.999, Tukey's multiple comparisons). Broad inhibition of P2 receptors significantly decreased activity produced in the IC by application of the α1 specific agonist (mean 0.38%, n=4, p-value=0.002, Tukey's multiple comparisons), indicating that an intermediate purine release is required for the observed calcium effects. Zero calcium, EGTA-containing ACSF lowered the average ΔF/F increase significantly (mean 0.09%, n=5, p-value=0.0002, Tukey's multiple comparisons). Surprisingly, pretreatment of slices with the L-type blocker nifedipine often led to a slow and steady increase in fluorescence. Despite this unexpected effect of L-type blockade, α1 agonist evoked ΔF/F increases were not reduced (mean 3.88%, n=5, p-value > 0.999, Tukey's multiple comparisons). We next tested whether an agonist of P2 receptors could produce a similar effect to what is observed with α1 receptor activation. Application of ATP (100 μM) elicited a widespread calcium increase, similar to that observed with α1 agonist application (Figure 2.7b, c). Interestingly, we found that the overall level of fluorescence increased more with ATP application than with α1 agonist (mean 6.18%, n=6, p-value=0.006, Tukey's multiple comparisons), similar to the level of response observed with norepinephrine (p-value=0.894, Tukey's multiple comparisons) (Figure 2.7b). Our results indicate that

intracellular calcium modulation by α1 adrenergic receptors requires purinergic signaling and extracellular calcium.

α2 and β receptor mediated activity is direct, produces faster transient calcium responses, and requires extracellular calcium

Neither α2 nor β receptor mediated activity was significantly reduced by preventing the generation of action potentials with TTX (α2 mean 1.10%, n=4, p-value=0.858; β mean 5.77%, n=2, p-value=0.709, Tukey's multiple comparisons) or blocking fast synaptic transmission (α2 mean 1.23%, n=4, p-value=0.949; β mean 2.78%, n=6, p-value=0.688, Tukey's multiple comparisons) (Figure 2.8a, b). Additionally, β receptor mediated activity was unaffected by the presence of nonspecific purinergic blockers (mean 6.56%, n=4, p-value=0.176, Tukey's multiple comparisons) (Figure 2.8b), in contrast to α1 receptor mediated activity (Figure 2.7a). Pretreatment of slices with zero calcium, EGTA-containing ACSF lowered the responses to α2 and β agonists significantly (α2 mean -0.3%, n=2, p-value=0.036, β mean 0.8%, n=5, p-value=0.036, Tukey's multiple comparisons) (Figure 2.8a, b). The L-type calcium channel blocker nifedipine did not affect the average response to α2 and β receptor agonists significantly (α2 mean 0.03%, n=4, p-value=0.054; β mean 2.35%, n=4, p-value=0.451, Tukey's multiple comparisons) (Figure 2.8a, b). The average length of α2 and β responses as measured by halfwidth were significantly shorter than responses elicited by norepinephrine and α1 agonist applications (NE mean 52.07 s, n=5; α1 mean 58.63 s, n=5; α2 mean 18.8 s, n=5, p-value=0.001; β mean 29.94 s, n=5, p-value=0.036, Tukey's multiple comparisons) (Figure 2.8c).

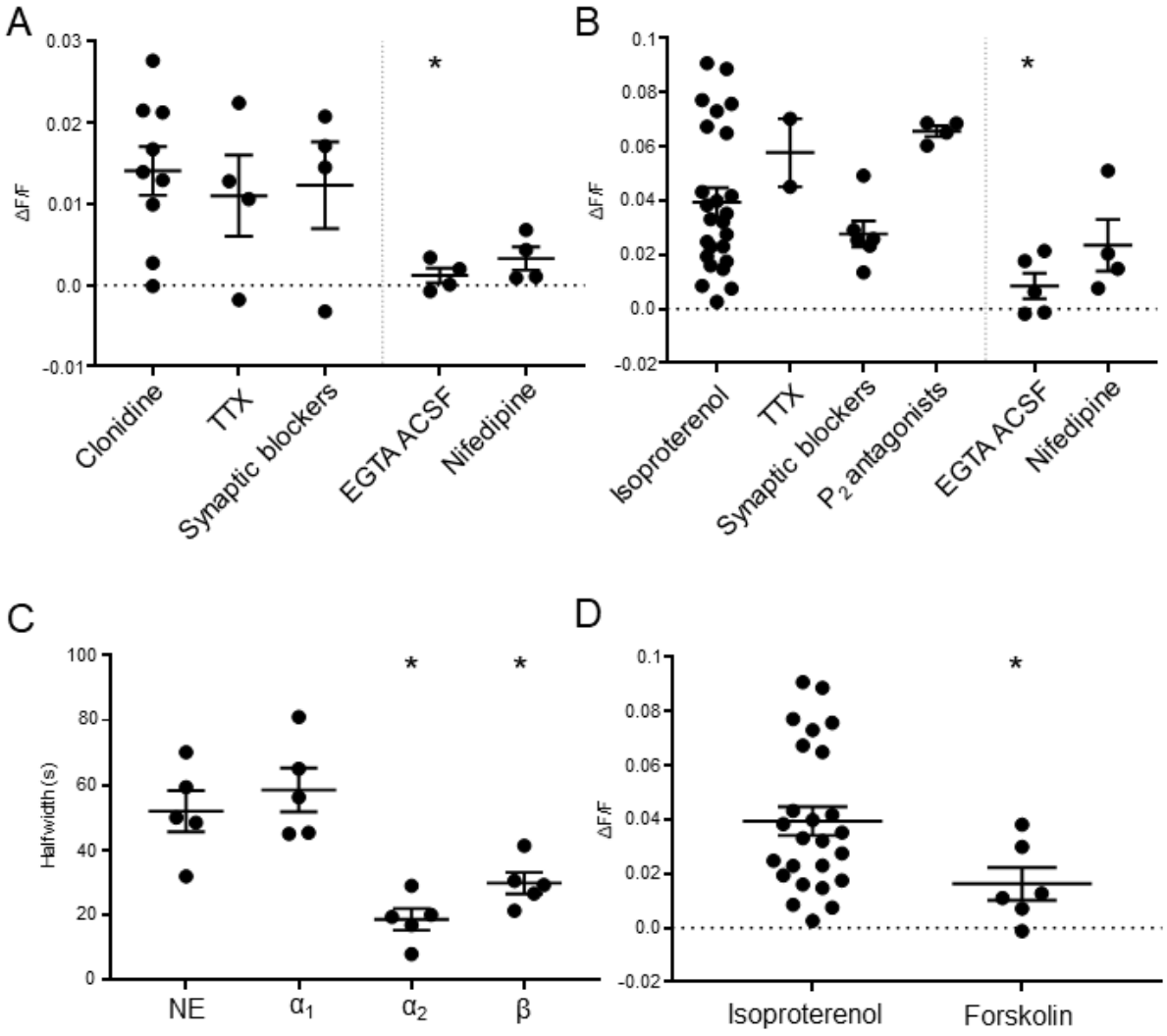

Figure 2.8: α2 and β receptor mediated effects are direct and shorter-lived than α1 effects and require extracellular calcium

A, B: Summary plot of mean ΔF/F responses of α_2 agonist clonidine (A) and β agonist isoproterenol (B) in the presence of TTX (500 nM), synaptic blockers (NBQX 10 μM, AP-V 50 μM, GABAzine 10 μM, and strychnine 1 μM), 0 mM Ca^{2+} ACSF with 0.5 mM EGTA, and L-type calcium channel blocker nifedipine (50 μM). Error bars represent mean ± standard error of the mean. Additionally, isoproterenol was tested against nonspecific purinergic receptor blockade (suramin 150 μM, PPADS 50 μM). C: Summary of mean ΔF/F response halfwidths elicited by NE, a1, a2, or B agonist application. D: Summary of mean ΔF/F responses evoked by β agonist isoproterenol or forskolin application.

Forskolin produces a weaker effect in IC cells compared to β receptor specific activation

β adrenergic receptor activity is canonically mediated through activation of the Gs GPCR subunits and subsequent increase in adenylyl cyclase (AC) activity that results in increased levels of intracellular cAMP. Forskolin is a modulator of AC that causes an increase in AC activity and cAMP production. We hypothesized that the observed effects accompanying β adrenergic receptor activation were due to its actions via Gs and AC. We applied forskolin to slices of the IC and found a significant transient increase in ΔF/F (mean 1.63%, n=6, p-value=0.042, one sample T-test). Surprisingly, the forskolin effect had an average calcium increase that was smaller than the effect of β receptor application (p-value=0.049, unpaired T-test) (Figure 2.8d). These results suggest that the Gs - AC second messenger pathway is not solely responsible for mediating the effects of β receptor activation in the IC.

Camk2a expressing cells do not contribute to the observed noradrenergic effects

Calcium/calmodulin-dependent protein kinase II alpha (Camk2a) is an important regulator of glutamatergic signaling in the brain. We asked whether Camk2a-expressing cells in the IC are sensitive to norepinephrine by crossing mice that express cre recombinase under the control of the Camk2a promoter with mice that express the

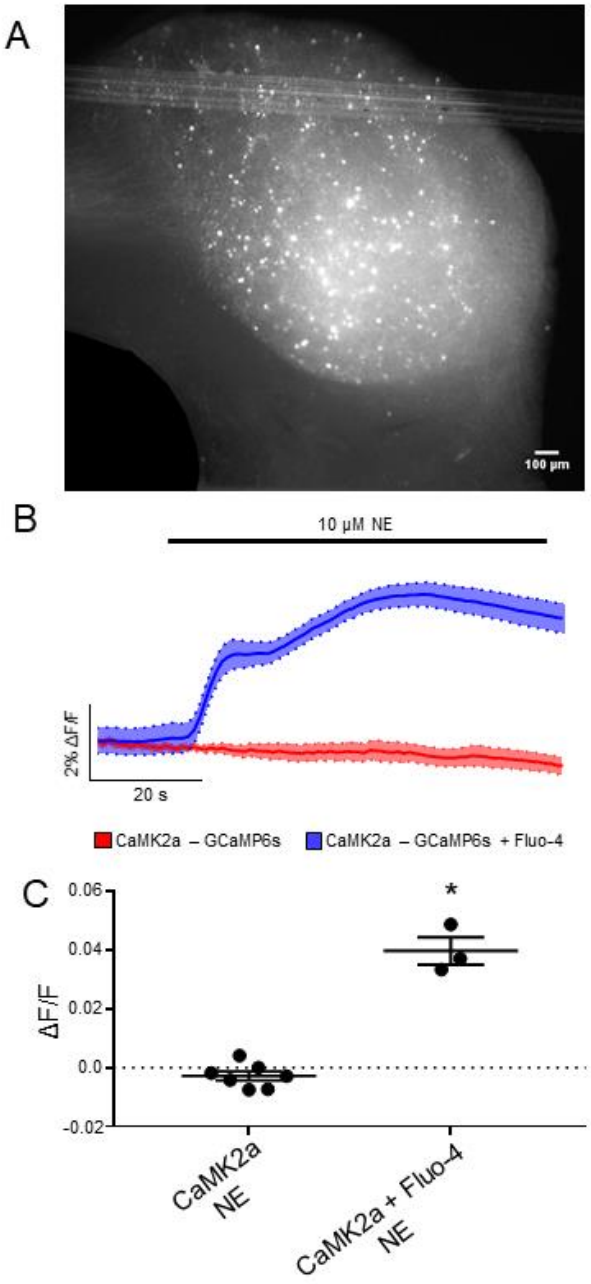

Figure 2.9: Camk2a expressing cells in the IC do not exhibit calcium increases in response to norepinephrine

A: Representative image of a coronal slice of IC from an animal expressing GCaMP6s under the control of Camk2a. Scale bar = 100 microns. B: Traces of ΔF/F responses in matching hemispheres of Camk2a - GCaMP6s IC, one also loaded with Fluo-4. C: Summary data of mean ΔF/F responses to norepinephrine application in Camk2a-GCaMP6s slices without and with additional Fluo-4 loading. Error bars represent mean ± standard error of the mean.

genetically encoded calcium sensor GCaMP6s in a cre-dependent manner. We found Camk2a-expressing cells across the IC (Figure 2.9a). No increases in fluorescence were detected with application of norepinephrine to GCaMP6s expressing slices (mean -0.28%, n=7, p-value=0.120, one-sample T test) (Figure 2.9c). Camk2a-GCaMP6s slices were exposed to ACSF containing high potassium (20 mM) to control for slice health. High potassium ACSF elicited large calcium increases in Camk2a-GCaMP6s slices (mean 52.93%, n=4, p-value=0.040, one-sample T test). Some Camk2a-GCaMP6s slices of IC were loaded with Fluo-4, and in these slices norepinephrine elicited a significantly greater response than what was observed in GCaMP6s-expressing slices with no Fluo4 (mean 3.98%, n=3, p-value < 0.0001, unpaired T test) (Figure 2.9b, c). Putatively excitatory, Camk2a-expressing cells in the IC do not exhibit calcium increases in response to norepinephrine.

Adrenergic effects are not solely neuronal or astrocytic

Norepinephrine increases intracellular calcium in astrocytes in multiple regions of the brain[26–30]. Fluo4 loads into glia as well as neurons. We examined if the observed effects of noradrenergic agonist application occurred in astrocytes by loading slices with sulforhodamine 101 (SR101) followed by Fluo4. SR101 preferentially labels astrocytes in the brain, with minimal loading into other cell types[23]. We compared overlap of agonist-evoked ΔF/F signals and SR101 in small patches of the IC that showed strong signals from both channels. Because apparent overlap could reflect two cells at distinct depths in the slice, we determined the expected rate of overlap assuming random

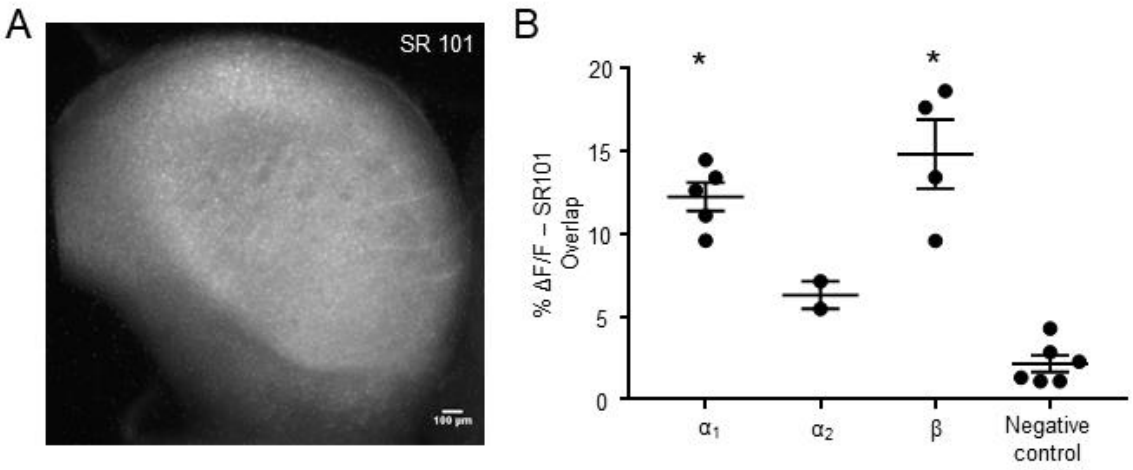

Figure 2.10: A portion of norepinephrine-sensitive cells in the IC are astrocytes

A: Representative image of SR101 loading in a coronal slice of the IC. Scale bar = 100 microns. B: Percentages of overlap between SR101 ROIs and CNMF-detected ΔF/F components. Error bars represent mean ± standard error of the mean.

placement of astrocytes and cells exhibiting a calcium response to noradrenergic agonist. We did so by determining the degree of overlap using astrocyte and calcium-response components from different fields of view. We found that mean overlap percentage for α1 and β receptor mediated activity and astrocyte label was significantly greater than the space-offset control (α1 mean 12.25%, n=5, p-value < 0.0001, β mean 14.83%, n=4, p-value < 0.0001, Tukey's multiple comparisons test) while α2 receptor mediated activity did not differ significantly from the control (mean 6.31%, n=2, p-value = 0.204) (Figure 2.10). These results indicate that a subset of astrocytes is sensitive to norepinephrine in the IC but the majority of cells responding to norepinephrine are not astrocytes.

2.5 Discussion

These findings show that norepinephrine evokes intracellular calcium increases in the mouse inferior colliculus. These effects occur throughout all subregions of the IC. Agonists of the three adrenergic receptor subtypes elicit responses, suggesting that the noradrenergic effect is an amalgamation of responses arising from activity mediated via all three adrenergic receptor subtypes. Each adrenergic agonist produced differing spatial and temporal patterns of calcium increases with small levels of cellular overlap. These results show that norepinephrine is well placed to modulate auditory processing the IC.

The IC can be divided into three anatomically and functionally distinct subregions and norepinephrine elicits different effects across all three. Norepinephrine shows the smallest level of calcium increase in the primary auditory region of the IC, the central nucleus. The ICc receives the bulk of ascending auditory information and is the source of thalamic-directed outputs. The ICc also receives comparably fewer dopamine β-hydroxylase (DBH) positive fibers that originate in the locus coeruleus[21]. α1 receptor-mediated activity is responsible for the majority of activity observed in the ICc. The relatively lower levels of calcium increase in the ICc could indicate lower levels of modulatory action. Alternatively, the nature of the ICc and its collated ascending auditory information means any level of modulatory activity in the ICc could have wide-ranging effects.

In contrast, average ΔF/F values were greater in the ICd and ICx regions of the IC. The ICd receives descending projections from the auditory cortex and is important for the

generation of auditory stimulus driven defensive behavior[31]. It also receives projections from the contralateral IC[32]. The ICd also shows a denser innervation of fibers from the locus coeruleus, aligning with the higher levels of activity we have observed. β receptor-mediated effects evoked the largest calcium increases in the ICd out of the three adrenergic receptor subtypes. Modulation of cells and/or synapses that are the targets of the corticofugal projections from the auditory cortex could allow for tuning the level of control the auditory cortex can exert.

The ICx also exhibited higher average ΔF/F responses than the ICc. β receptor-mediated effects evoked the largest calcium increases in the ICx. This effect appeared to be limited to the more superficial layers of the ICx, layers 1 and 2[33]. These ICx layers receive multimodal innervation from the superior colliculus, dorsal columns, and trigeminal nuclei[34] as opposed to contributions from ascending projections that terminate in the deeper layer 3 of the ICx (also called the ventrolateral nucleus)[33]. Studies suggest that the ICx is organized into cellular patches, which have higher levels of GAD, NADPH-d, parvalbumin, acetylcholinesterase, and cytochrome oxidase[35]. We observed some nonuniformity in the pattern of norepinephrine and beta agonist, but not in discrete patches as described previously for GAD, NADPH-d, and other ICx markers. The lack of modular patterning in adrenergic beta-receptor mediated activity indicates that modulation by the locus coeruleus is likely not organized compartmentally the ICx. Modulation of the more multimodal ICx likely contributes to norepinephrine's brain-wide roles in arousal and attention. Together, the effects observed in the ICx and ICd indicate

that the role of norepinephrine in the IC is not limited to modulating ascending auditory information.

ΔF/F effects elicited by α2 specific agonists were more limited than those elicited by α1 and β receptor agonists. Small effects were observed in every subregion of the IC but most consistently and strongly on the outer edges of the ICc. These regions constitute the borders of the ICc with the ICx and ICd. It is difficult accurately defining the edges of the ICc with its neighbors which in turn is difficult to correlate activity observed during calcium recording to specifically the ICc border as opposed to a balance of ICc and ICx/ICd responses. The relative smaller amplitudes of α2 receptor mediated effects make reaching conclusions regarding its neuromodulator potential challenging.

It is important to note that neuromodulatory actions of norepinephrine do not necessarily result in fluctuations of intracellular calcium and would therefore be undetectable using calcium indicators. This fact makes it likely that we are underestimating the number of cells, synapses, and neuropil that may be affected by norepinephrine.

Interestingly, we observed little overlap in adrenergic receptor-mediated ΔF/F effects among different receptor subtypes. In the ICc, α1 receptor mediated effects were significantly greater than α2 and β receptor-mediated effects, making the lack of overlap unsurprising. In the ICx and ICd, overlap was significantly greater than zero but nonetheless the majority of cells did not show ΔF/F increases to more than one adrenergic receptor-specific agonist. Technically, overlap assessment is imperfect, given the multiple

cellular layers that contribute to images. This makes overassessment of overlap likely, suggesting that our measurements are an overestimation of true overlap between these populations of cells. A possible source of underestimation of overlap is the possibility that sequential application of agonists leads to cross-desensitization among receptor subtypes.

Increases in calcium were also observed in cellular regions in the surface of the IC. These responses were distinct from what was observed in the rest of the IC via the coronal view of the IC slice. The activity observed in surface regions exhibited longer halfwidths, often not returning to baseline for several minutes after washout of norepinephrine. These responses were mimicked by the application of α1 receptor agonists. The superficial location of these responses suggests they are meningeal and are less likely to contribute directly to auditory processing. Unlike in the periphery, α1A and α1B adrenergic receptors are not expressed in cerebral blood vessels[36], making it unlikely that this surface effect is the response of blood vessels to noradrenergic application.

Noradrenergic effects are not significantly affected by the inhibition of action potential generation with TTX. Average levels of ΔF/F appeared to be higher in the presence of TTX, although not significantly, perhaps suggesting a contribution of spontaneous activity. The lack of a similar increased effect with blockade of fast glutamatergic, GABAergic, and glycinergic synaptic transmission or purinergic signaling makes spontaneous activity contributions at the circuit level unlikely however. While we cannot fully rule out contributions of gap junctions to indirect effects of norepinephrine, carbenoxolone did not

have any detrimental effect on norepinephrine-evoked activity. These results suggest that noradrenergic modulation of action-potential driven circuit activity in GABAergic and glutamatergic neurons does not indirectly cause the observed increases in calcium.

While broad activation of adrenergic receptors with norepinephrine is resistant to any synaptic blockade, α1 receptor-mediated activity is prevented with co-treatment with non-specific purinergic receptor antagonists (Figure 2.7). Noradrenergic and purinergic signaling have been linked in other brain regions[37,38]. Purinergic receptors have been shown to mediate calcium influx in astrocytes[39]. Purinergic antagonist-mediated blockade of α1 receptor-mediated calcium increases indicate that α1 receptors are not directly causing calcium increases in all the cells observed in control conditions. Elimination of extracellular calcium resulted in a significant decrease of effect with α1 receptor agonist application, suggesting that increases in cytosolic calcium are likely the result of primarily P2X receptors. P2X receptors are nonspecific cation channels that allow for the flow of calcium down its electrochemical gradient, which could explain the inhibited effects of α1 agonists in zero calcium conditions. It is also possible that P2Y receptors are mediating the purinergic effects seen, as zero calcium conditions could block the release of purines from α1 sensitive cells. These results provide the first evidence of a connection between purinergic and noradrenergic activity in the IC.

α2 and β receptor-mediated effects in the IC are direct. We find no significant effects of TTX or synaptic blockade indicating that it is likely that the observed cellular increases in calcium are occurring in cells that express α2 and β receptors. α2 and β receptors do not

contribute to the superficial, long lasting effects seen with norepinephrine and α1 agonist application, and overall show shorter ΔF/F responses. α2 and β receptor activity can lead to the opening of extracellular membrane bound calcium channels. We find that α2 agonist effects do not persist in the absence of extracellular calcium, and β agonist effects are similarly inhibited. The L-type calcium channel blocker nifedipine reduces the observed effects of α2 and β agonist applications but not to significant degrees, making it unclear if L-type calcium channels are necessary for α2 and β agonist mediated effects. L-type calcium current has been measured in the IC and shown to be involved in regulating IC responses to intensity of stimuli[40].

Stimulation of adenylyl cyclase by forskolin produces similar effects seen with β agonist application but with a lower average amplitude of ΔF/F increase. β receptors canonically mediate their effects via Gs and subsequent activation of adenylyl cyclase and increased levels of cAMP. Recent evidence indicates that β receptors can activate phospholipase C and release calcium from internal stores[41]. A combination of canonical and non-canonical second messenger pathways by β adrenergic receptors could account for the moderate effects of forskolin and β agonists in the presence of zero calcium extracellular ACSF or L-type calcium channel blockers.

Norepinephrine has been shown to increase intracellular calcium levels in astrocytes via the activity mediated through α1 and β adrenergic receptors[26,28,30]. Fluo-4 AM loads into astrocytes in addition to neurons. We observed a small amount of overlap in the spatial patterning of agonist-evoked ΔF/F responses and SR101 labeled astrocytes. Greater

levels of overlap were observed in α1 and β receptor-mediated activity. Astrocytes have been shown to affect synaptic signaling and plasticity[42]. While we observed only small levels of astrocytic ΔF/F increases, it is possible astrocytes in the IC are providing similar functional roles as to what has been observed elsewhere in the brain.

We used calcium/calmodulin dependent protein kinase 2 alpha (CaMk2a) expression as a marker for excitatory neurons[43] in the IC. An estimated 70% of the neurons in the IC are glutamatergic, with the remaining 30% being GABAergic[44]. Previous tracing experiments have shown that glutamatergic neurons in the cortices of the IC (ICd and ICx) receive more inputs from the locus coeruleus compared to GABAergic neurons[45]. Here, we find no norepinephrine-elicited ΔF/F increases in CaMk2a positive cells, indicating that excitatory neurons in the IC are not targets of direct noradrenergic modulation. GABAergic neurons in the ICc are a combination of inhibitory interneurons and projection neurons that target the auditory medial geniculate nucleus[46]. Norepinephrine has been shown to have modulatory effects on GABAergic signaling in the auditory cortex[7] and these results suggest a similar role in the IC.

This work provides evidence for a role for noradrenergic modulation in the mammalian auditory midbrain. The spatial patterns of direct noradrenergic activity in the IC make it likely that norepinephrine is playing a role in controlling ascending and descending projections through the IC. The modulation of auditory sensory information in the IC could play a role in the greater modulation of attention and arousal throughout the brain by the locus coeruleus and noradrenergic release.

2.6 References

1. Jones, B. E., Halaris, A. E., McIlhany, M. & Moore, R. Y. Ascending projections of the locus coeruleus in the rat. I. axonal transport in central noradrenaline neurons. *Brain Res.* **127**, 1–21 (1977).
2. Berridge, C. W. & Waterhouse, B. D. The locus coeruleus–noradrenergic system: modulation of behavioral state and state-dependent cognitive processes. *Brain Res. Rev.* **42**, 33–84 (2003).
3. Waterhouse, B. D. & Navarra, R. L. The locus coeruleus-norepinephrine system and sensory signal processing: A historical review and current perspectives. *Brain Res.* (2018). doi:10.1016/J.BRAINRES.2018.08.032
4. Manunta, Y. & Edeline, J.-M. Effects of Noradrenaline on Frequency Tuning of Rat Auditory Cortex Neurons. *Eur. J. Neurosci.* **9**, 833–847 (1997).
5. Manunta, Y. & Edeline, J.-M. Effects of noradrenaline on frequency tuning of auditory cortex neurons during wakefulness and slow-wave sleep. *Eur. J. Neurosci.* **11**, 2134–2150 (1999).
6. Edeline, J.-M., Manunta, Y. & Hennevin, E. Induction of selective plasticity in the frequency tuning of auditory cortex and auditory thalamus neurons by locus coeruleus stimulation. *Hear. Res.* **274**, 75–84 (2011).
7. Salgado, H. *et al.* Pre- and postsynaptic effects of norepinephrine on γ-aminobutyric acid-mediated synaptic transmission in layer 2/3 of the rat auditory cortex. *Synapse* **66**, 20–28 (2012).
8. Martins, A. R. O. & Froemke, R. C. Coordinated forms of noradrenergic plasticity in the locus coeruleus and primary auditory cortex. *Nat. Neurosci.* **18**, 1483–1492 (2015).
9. Hirao, K. *et al.* Noradrenergic refinement of glutamatergic neuronal circuits in the lateral superior olivary nucleus before hearing onset. *J. Neurophysiol.* **114**, 1974–1986 (2015).
10. Kuo, S. P. & Trussell, L. O. Spontaneous spiking and synaptic depression underlie noradrenergic control of feed-forward inhibition. *Neuron* **71**, 306–18 (2011).
11. Adams, J. C. Ascending projections to the inferior colliculus. *J. Comp. Neurol.* **183**, 519–538 (1979).
12. Oliver, D. L. & Morest, D. K. The central nucleus of the inferior colliculus in the cat. *J. Comp. Neurol.* **222**, 237–264 (1984).
13. Glendenning, K. K. & Masterton, R. B. Acoustic chiasm: efferent projections of the lateral superior olive. *J. Neurosci.* **3**, 1521–37 (1983).
14. Winer, J. A., Larue, D. T., Diehl, J. J. & Hefti, B. J. Auditory cortical projections to the cat inferior colliculus. *J. Comp. Neurol.* **400**, 147–174 (1998).
15. Kuwabara, N. & Zook, J. M. Geniculo-collicular descending projections in the gerbil. *Brain Res.* **878**, 79–87 (2000).
16. Gittelman, J. X., Perkel, D. J. & Portfors, C. V. Dopamine modulates auditory responses in the inferior colliculus in a heterogeneous manner. *JARO - J. Assoc. Res. Otolaryngol.* **14**, 719–729 (2013).
17. Hurley, L. M. & Pollak, G. D. Serotonin differentially modulates responses to tones and frequency-modulated sweeps in the inferior colliculus. *J. Neurosci.* **19**, 8071–82 (1999).

18. Hurley, L. M. Serotonin Shifts First-Spike Latencies of Inferior Colliculus Neurons. *J. Neurosci.* **25**, 7876–7886 (2005).
19. Hurley, L. M. & Sullivan, M. R. From behavioral context to receptors: serotonergic modulatory pathways in the IC. *Front. Neural Circuits* **6**, 58 (2012).
20. OBARA, N., KAMIYA, H. & FUKUDA, S. Serotonergic modulation of inhibitory synaptic transmission in mouse inferiorcolliculus. *Biomed. Res.* **35**, 81–84 (2014).
21. Klepper, A. & Herbert, H. Distribution and origin of noradrenergic and serotonergic fibers in the cochlear nucleus and inferior colliculus of the rat. *Brain Res.* **557**, 190–201 (1991).
22. Joshi, S., Li, Y., Kalwani, R. M. & Gold, J. I. Relationships between Pupil Diameter and Neuronal Activity in the Locus Coeruleus, Colliculi, and Cingulate Cortex. *Neuron* **89**, 221–34 (2016).
23. Hülsmann, S., Hagos, L., Heuer, H. & Schnell, C. Limitations of Sulforhodamine 101 for Brain Imaging. *Front. Cell. Neurosci.* **11**, 44 (2017).
24. Schindelin, J. *et al.* Fiji: an open-source platform for biological-image analysis. *Nat. Methods* **9**, 676–82 (2012).
25. Pnevmatikakis, E. A. *et al.* Simultaneous Denoising, Deconvolution, and Demixing of Calcium Imaging Data. *Neuron* **89**, 285–299 (2016).
26. Salm, A. K. & McCarthy, K. D. Norepinephrine-Evoked Calcium Transients in Cultured Cerebral Type 1 Astroglia. *Glia* **3**, 529–538 (1990).
27. Bekar, L. K., He, W. & Nedergaard, M. Locus Coeruleus a-Adrenergic-Mediated Activation of Cortical Astrocytes In Vivo. *Cereb. Cortex December* **18**, 2789–2795 (2008).
28. Ding, F. *et al.* α1-Adrenergic receptors mediate coordinated Ca2+ signaling of cortical astrocytes in awake, behaving mice. *Cell Calcium* **54**, 387–394 (2013).
29. Paukert, M. *et al.* Norepinephrine Controls Astroglial Responsiveness to Local Circuit Activity. *Neuron* **82**, 1263–1270 (2014).
30. Horvat, A., Zorec, R. & Vardjan, N. Adrenergic stimulation of single rat astrocytes results in distinct temporal changes in intracellular Ca2+ and cAMP-dependent PKA responses. *Cell Calcium* **59**, 156–163 (2016).
31. Xiong, X. R. *et al.* Auditory cortex controls sound-driven innate defense behaviour through corticofugal projections to inferior colliculus. *Nat. Commun.* **6**, 7224 (2015).
32. Aitkin, L. M. & Phillips, S. C. The interconnections of the inferior colliculi through their commissure. *J. Comp. Neurol.* **228**, 210–216 (1984).
33. Loftus, W. C., Malmierca, M. S., Bishop, D. C. & Oliver, D. L. The cytoarchitecture of the inferior colliculus revisited: A common organization of the lateral cortex in rat and cat. *Neuroscience* **154**, 196–205 (2008).
34. Li, H. & Mizuno, N. Single neurons in the spinal trigeminal and dorsal column nuclei project to both the cochlear nucleus and the inferior colliculus by way of axon collaterals: a fluorescent retrograde double-labeling study in the rat. *Neurosci. Res.* **29**, 135–142 (1997).
35. Lesicko, A. M. H., Hristova, T. S., Maigler, K. C. & Llano, D. A. Connectional Modularity of Top-Down and Bottom-Up Multimodal Inputs to the Lateral Cortex of the Mouse Inferior Colliculus. *J. Neurosci.* **36**, 11037–11050 (2016).
36. Papay, R. *et al.* Mouse ?1B-adrenergic receptor is expressed in neurons and NG2 oligodendrocytes. *J. Comp. Neurol.* **478**, 1–10 (2004).

37. Gordon, G. R. J. *et al.* Norepinephrine triggers release of glial ATP to increase postsynaptic efficacy. *Nat. Neurosci.* **8**, 1078–1086 (2005).
38. Pinho, D., Quintas, C., Sardo, F., Cardoso, T. M. & Queiroz, G. Purinergic modulation of norepinephrine release and uptake in rat brain cortex: contribution of glial cells. *J. Neurophysiol.* **110**, 2580–2591 (2013).
39. Helen, C., Kastritsis, C., Salm, A. K. & McCarthy, K. Stimulation of the P_{2Y} Purinergic Receptor on Type 1 Astroglia Results in Inositol Phosphate Formation and Calcium Mobilization. *J. Neurochem.* **58**, 1277–1284 (1992).
40. Alex Grimsley, C., Brian Green, D. & Sivaramakrishnan, S. L-type calcium channels refine the neural population code of sound level. *J Neuro-physiol* **116**, 2550–2563 (2016).
41. Galaz-Montoya, M., Wright, S. J., Rodriguez, G. J., Lichtarge, O. & Wensel, T. G. β2-Adrenergic receptor activation mobilizes intracellular calcium via a non-canonical cAMP-independent signaling pathway. *J. Biol. Chem.* **292**, 9967 (2017).
42. Araque, A. *et al.* Gliotransmitters Travel in Time and Space. *Neuron* **81**, 728–739 (2014).
43. Tsien, J. Z. *et al.* Subregion- and cell type-restricted gene knockout in mouse brain. *Cell* **87**, 1317–26 (1996).
44. Merchán, M., Aguilar, L. A., Lopez-Poveda, E. A. & Malmierca, M. S. The inferior colliculus of the rat: Quantitative immunocytochemical study of GABA and glycine. *Neuroscience* **136**, 907–925 (2005).
45. Chen, C., Cheng, M., Ito, T. & Song, S. Neuronal Organization in the Inferior Colliculus Revisited with Cell-Type-Dependent Monosynaptic Tracing. *J. Neurosci.* **38**, 3318–3332 (2018).
46. Ito, T., Bishop, D. C. & Oliver, D. L. Two Classes of GABAergic Neurons in the Inferior Colliculus. *J. Neurosci.* **29**, 13860–13869 (2009).

Chapter 3. Distribution and co-expression of adrenergic receptor-encoding mRNA in the mouse inferior colliculus

3.1 Abstract

Adrenergic receptors are important mediators of adrenergic and noradrenergic modulation in the brain. Previous studies have provided evidence for the expression of adrenergic receptors in the midbrain auditory nucleus, the inferior colliculus (IC), but have not examined the cellular patterns of expression in detail. Here, we utilize multi-channel fluorescent in situ hybridization to detect the expression of adrenergic receptor-encoding mRNA in the mouse inferior colliculus. We found expression of α1, α2A, and β2 receptor-encoding mRNA throughout all areas of the IC. We observed similar levels of expression of α1 and α2A receptor-encoding mRNA across the IC, while β2 receptor-encoding mRNA was expressed in a higher proportion of cells in the outer subregions of the dorsal cortex of the IC (ICd) and external nucleus of the IC (ICx). To account for developmental changes in noradrenergic receptor expression, we measured expression levels in mice aged P15, P20, and P60. We observed no changes in levels of expression across these ages, indicating noradrenergic modulatory potential is likely mature by P15. By utilizing multi-channel fluorescent in situ hybridization, we measured co-expression of α1, α2A, and β2 receptor-encoding mRNA. We found greater proportions of cells in the IC that expressed no adrenergic receptor-encoding mRNA, α1 and α2A adrenergic receptor-encoding mRNA, and α1, α2A, and β2 receptor-encoding mRNA than predicted. These data suggest a coordinated pattern of adrenergic receptor expression in the IC and

provide the first evidence for adrenergic receptor expression and co-expression in the subregions of the mouse auditory midbrain.

3.2 Introduction

The interior colliculus (IC) is the primary auditory region of the mammalian midbrain. Nearly all of the ascending auditory information that originates from the brainstem and lateral lemniscus is integrated in the IC before projection to the medial geniculate nucleus of the thalamus[1–3]. The IC is made up of bilateral spherical lobes on the dorsal surface of the midbrain. Each lobe is constructed of a central subregion (central nucleus: ICc), which receives the bulk of ascending projections, wrapped in layered tissue that makes up the dorsal cortex (ICd) and external cortex (ICx)[4]. The IC also receives extensive descending projections from the auditory cortex[5], thalamus[6], and nonauditory sensory regions[7,8]. The IC also receives neuromodulatory input. The subparafascicular nucleus of the thalamus supplies dopaminergic input to the IC[9]. IC serotonergic projections originate in the raphe[10,11].

Noradrenergic fibers in the IC originate in the locus coeruleus[10]. While there is evidence for the presence of noradrenergic fibers in the IC, adrenergic receptors in the IC have not been examined in detail. Adrenergic receptors can be broadly classified into three groups, α1, α2, and β. Each receptor type can be further broken down into subtypes, based on molecular genetic origin (α1A, α1B, and α1D; α2A, α2B, and α2C; β1, β2, and β3) with each group mediating its modulatory effects through the same second messenger system (Gq, Gi, and Gs, respectively). Patterns of adrenergic receptor expression have been examined across the brain with a variety of techniques, many indicating expression of

adrenergic receptors in the IC. Detection of α1 subtypes in the IC has been mixed. Detection of adrenergic receptor mRNA using *in situ* hybridization has provided no evidence for expression of α1A and α1B and weak expression of α1D[12,13]. A transgenic model that expressed a fluorophore under the control of the α1A promoter showed expression in the IC[14]. α2 adrenergic receptors are likely expressed in the IC. Studies using the binding of labeled pharmacological ligands have shown α2 signal in the IC[15]. Using *in situ* hybridization, a study showed moderate levels of α2A and α2C expression[16]. Little evidence for β adrenergic receptors has been found, with autoradiographical[17] and *in situ* hybridization[18,19] results suggesting little to no expression in the IC.

Studies of adrenergic receptor expression have focused on patterns of expression across the entire brain. While these techniques are excellent for measuring the broad expression patterns of adrenergic receptors, they often do not provide cellular resolution. Moreover, these studies to not address differential expression across the different IC subregions. Thus, evidence about adrenergic expression in the IC is mixed. Here, we examined the expression and overlap of α1, α2A, and β2 adrenergic receptors in the IC with triple-channel fluorescent *in situ* hybridization. We found strong levels of expression of α1 and α2A receptor-encoding mRNA and weaker levels of β2 mRNA. These levels did not significantly differ across age (P15, P20, and P60) and α1 and α2A expression did not differ across IC subregions. β2 expression was weaker in the ICC compared to ICx and ICd subregions. We observed higher levels of overlap among receptor subtype than would be predicted by chance, indicating that cells in the IC are likely to express multiple adrenergic receptors.

3.3 Materials and methods

Animals

All procedures were approved by the University of Washington Institute for Animal Care and Use Committee. CBA/CaJ mice of both sexes (9 male, 4 female) across ages P15, P20, and P60 (n = 5, 4, 4 respectively) were used for these experiments. Mice were anesthetized with isoflurane (inhalation) and euthanized by decapitation. Brains were quickly removed, flash frozen, and embedded in Tissue-Tek OCT compound (Sakura Finetek). Brains were cryosectioned and 20-μm thick coronal sections were mounted on SuperFrost Plus slides (Fisher Scientific).

Fluorescent in situ hybridization

Sections were fixed in 4% paraformaldehyde for 30 minutes at 4° C and dehydrated in ethanol. Fluorescent *in situ* hybridizations (FISH) were accomplished using Advanced Cell Diagnostics RNAScope and hybridization protocols followed according to the manufacturer's specifications. In brief, sections were then air dried at room temperature and then treated with protease for 15 minutes. Hybridization probes were then applied and amplified. Probes were purchased from Advanced Cell Diagnostics. A combination of 3 α1 adrenergic receptor probes (subtypes α1A, α1B, and α1D) was custom made by Advanced Cell Diagnostics. α2A receptor probe (ACD Catalog 425341). β2 receptor probe (ACD Catalog 449771). Following FISH, sections were stained with a fluorescent Nissl (NeuroTrace – Invitrogen N21479) at a dilution of 1:50 for 30 minutes and rinsed

before being coverslipped with Fluoromount-G (Southern Biotech) and stored at 4°C until imaging.

Imaging

FISH-treated sections were imaged using a Leica SP8 confocal microscope. Images were captured with a 10x objective and 63x oil-immersion objective. Section overviews were first created using multiple 10x objective captured images and stitched together for confirmation of IC presence and identification of IC subregion using the fluorescent Nissl stain (Figure 3.1). Following identification of IC subregions, z-stacks were collected with a 63x objective. High power z-stacks were 185x185 microns in size, 0.9 microns in thickness with a resolution of 1024 x 1024 pixels. The four fluorescent channels were imaged sequentially with excitation wavelengths of 405, 488, 594, and 647 nm. Laser

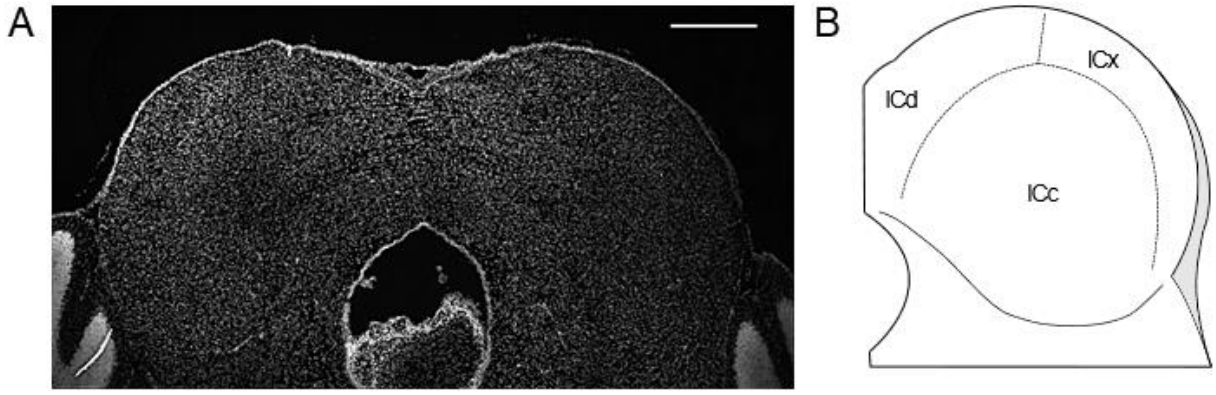

Figure 3.1: Fluorescent Nissl stain shows IC anatomy

A: Stitched 10x objective micrograph of fluorescent Nissl stain. Scale bar = 500 microns. B: Diagram of IC subregions.

power was adjusted for maximum signal for each excitation wavelength. Subregion high-power z-stacks were collected from 3 sections per animal.

Image analysis

Detection of *in situ* probe signal was accomplished using the FIJI distribution[20] of ImageJ[21] and Matlab (Mathworks).

Images were first imported into FIJI for detection of Nissl stain and receptor mRNA expression. Fluorescent channels were separated and converted to TIF stacks. Maximum intensity projections of each channel were then created. Nissl maximum intensity projections were blurred with a gaussian filter (radius = 5 pixels) and thresholded. The watershed function was then used to separate overlapping Nissl signals. Regions of interest (ROIs) were then detected to specify Nissl-defined cells and borders. In situ probe channels were thresholded to reduce background signal and ROIs representing *in situ* fluorescent probe signal were detected using the Analyze Particles function.

Nissl and probe ROIs were imported into Matlab for quantification and scoring. We followed Advanced Cell Diagnostics guidelines for scoring RNAscope results. Cells were scored based on the number of probe ROIs (“dots”) that overlapped each Nissl-derived ROI. A score of 0 was given to Nissl ROIs that contained no probe ROIs. A score of 1 was given to Nissl ROIs that contained 1-3 probe ROIs. Scores of 2-4 were given to cells that contained 4-9, 10-15, and greater than 15 probe ROIs, respectively. For quantification of results, we considered only cells that had a score of 2 or greater for analysis. Some Nissl overlap was too severe to separate with the watershed calculation. To control for this, we used only Nissl ROIs that had an area of 500 to 10,000 pixels. This

range captured single cell ROIs while excluding too small ROIs that were the result of weak Nissl signal and clusters of cells whose Nissl stains could not be differentiated.

Proportions of cells that expressed each probe were calculated by dividing the number of Nissl ROIs that had a score greater than 2 by the total number of Nissl ROIs for each field of view. Once scored for signal originating from each probe, overlaps of probe signals were detected for each Nissl-derived ROI. Proportions of cells that showed different overlaps were calculated by dividing the number of Nissl ROIs that had scores greater than 2 for different probes (or none) by the total number of Nissl ROIs for a given field of view.

Statistics and plotting

All plots were made using GraphPad Prism (GraphPad Software). With the exception of the chi-squared test, all statistical analyses were performed in GraphPad Prism. The chi-squared test was performed using the chi2gof() function in Matlab R2019a (Mathworks).

Example images shown were created using ImageJ, with brightness and contrast adjusted to highlight probe and Nissl signals. Only ROIs that passed thresholding were shown.

For calculating the predicted proportions of overlap, we took the products of total proportion of cells that exhibited a condition. For example, to calculate the predicted proportion of cells that would express no adrenergic mRNA, we multiplied the proportion

of cells that showed no α1 mRNA, no α2 mRNA, and no β2 mRNA. These predictions were used for comparison with the measured proportions of cells that showed various overlaps in a chi-squared test.

3.4 Results

α1 adrenergic receptor mRNA is expressed throughout the IC

Due to conflicting reports of α1 adrenergic receptor mRNA in the IC (CITES), we used a combination of mRNA probes that labeled α1A, α1B, and α1D α1 adrenergic receptor mRNA was detected in Nissl-body defined cells in all subregions of the IC (Figure 3.2). No significant difference in the proportion of cells that exhibited α1 mRNA expression was detected between ages P15, P20, and P60 (means 0.477, 0.547, and 0.565, respectively, p-value = 0.253, one-way ANOVA) (Figure 3.2e). α1 adrenergic receptor mRNA was similarly represented in the ICc, ICd, and ICc regions. No significant differences were observed in the proportion of cells in each IC subregion that showed α1 adrenergic receptor mRNA (means 0.464, 0.517, and 0.553, respectively, p-value = 0.284, one-way ANOVA). We also observed strong signal in the dense surface layer of the IC (Figure 3.2d).

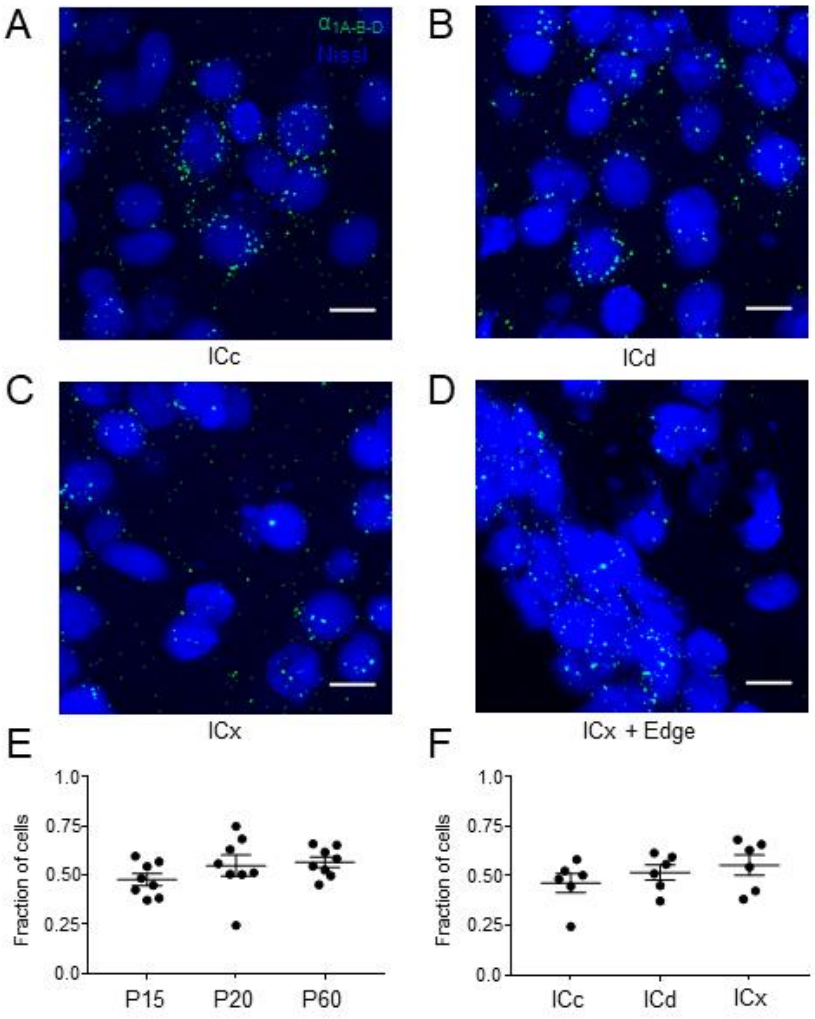

Figure 3.2: α1 adrenergic receptor mRNA is expressed throughout the IC

A-D: Representative high-power micrographs of α_1 mRNA and fluorescent Nissl stain. Scale bars = 10 microns. Not the clustering of α_1 mRNA around Nissl-labeled cells. E: Summary plot of fraction of cells that exhibited α_1 mRNA expression over the three age groups. F: Summary plot of fraction of cells that expressed α_1 mRNA in ICc, ICd, and ICx subregions. Summary plot bars represent the mean ± standard error of the mean. Also included is the ICx + edge. Note the high α_1 mRNA label in the Nissl-rich outer layer.

α2A adrenergic receptor mRNA is expressed throughout the IC

α2A adrenergic receptor mRNA was found in all IC subregions and at all ages tested (Figure 3.3). We found similar proportions of α2A mRNA positive cells in the IC of animals aged P15, P20, and P60 (means 0.315, 0.332, and 0.354, respectively, p = 0.768, one-

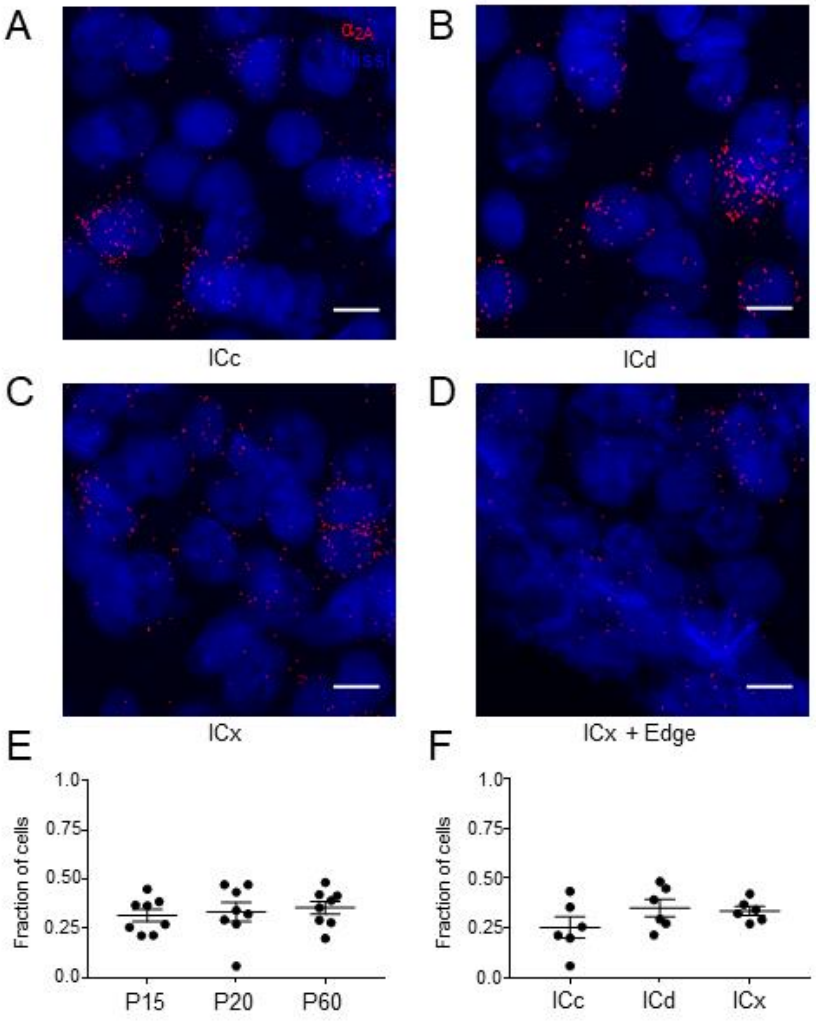

Figure 3.3: α2A adrenergic receptor mRNA is expressed throughout the IC

A-D: Representative images of overlap of α_{2A} mRNA and fluorescent Nissl stain. Scale bars = 10 microns. Note the clustering of α_{2A} mRNA around Nissl-labeled cells. Overall, fewer cells showed α_{2A} expression in comparison to α_1. E: Summary plot of fraction of cells that expressed α_{2A} mRNA across the three age groups. F: Summary plot of fraction of cells that expressed α_{2A} mRNA in ICc, ICd, and ICx subregions. Summary plot bars represent the mean ± standard error of the mean. Also included is the ICx + edge.

way ANOVA) (Figure 3.3e). No significant differences were observed in the proportions of α2A mRNA expressing cells in the ICc, ICd, and ICx subregions (means 0.252, 0.35, 0.335, respectively, p = 0.234, one-way ANOVA) (Figure 3.3f). Moderate levels of α2A mRNA positive cells were observed in the surface layer of IC (Figure 3.3d).

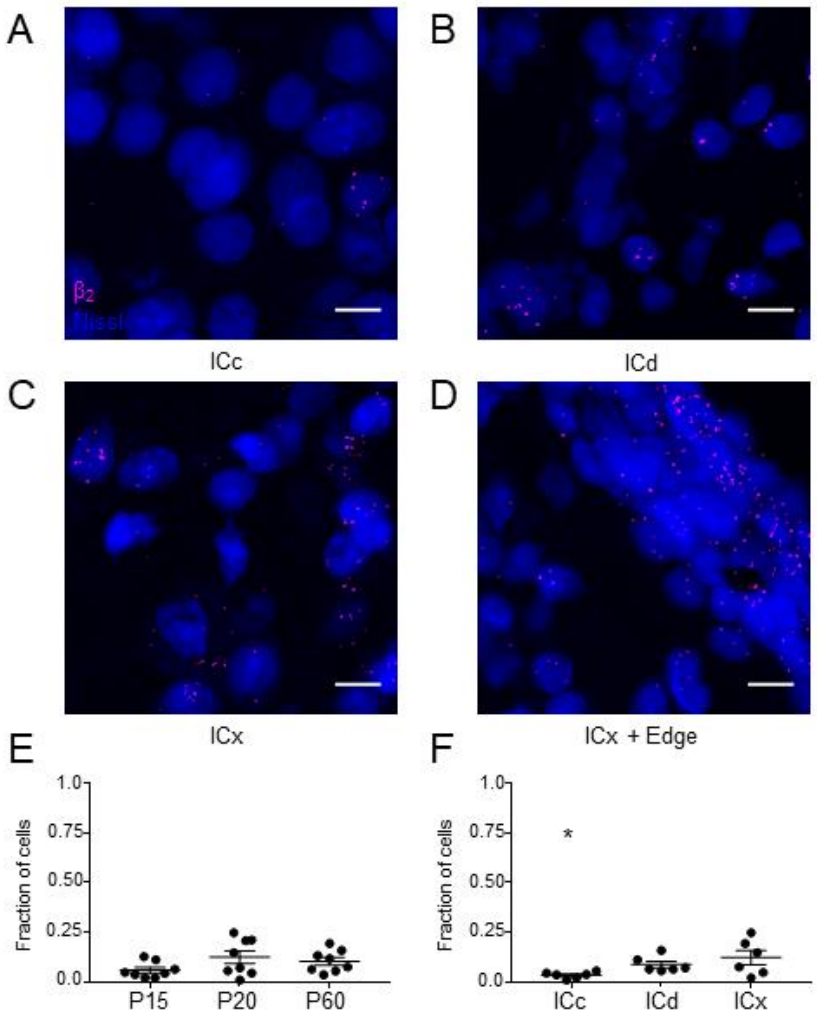

Figure 3.4: β2 adrenergic receptors show low levels of expression in the ICd and ICx subregions

A-D: Representative images of overlap of β_2 mRNA and fluorescent Nissl stain. Scale bars = 10 microns. Note the low levels of clustering and expression throughout. E: Summary plot of fraction of cells that expressed β_2 mRNA across the three age groups. F: Summary plot of fraction of cells that expressed β_2 mRNA in ICc, ICd, and ICx subregions. Summary plot bars represent the mean ± standard error of the mean. Also included is the ICx + edge. Average fraction of β_2 mRNA expressing cells in the ICc was significantly lower than cells in the ICx + edge (p-valye = 0.025, one-way ANOVA, Tukey's multiple comparisons test).

β2 adrenergic receptor mRNA expression is greatest in the ICx

We found low levels of β2 mRNA in all subregions of the IC (Figure 3.4). Across ages P15, P20, and P60, we observed no significant differences in the proportions of β2 mRNA expressing cells (means 0.058, 0.123, and 0.103, respectively, p-value = 0.152, one-way ANOVA) (Figure 3.4e). Examination of the expression levels of β2 mRNA in the IC subregions revealed lower proportions of β2 mRNA positive cells in the ICc compared to ICd and ICx subregions (means 0.033, 0.087, and 0.121, respectively, p = 0.026, one-way ANOVA) **(**Figure 3.4f). Similar to α1 and α2A receptor mRNA, we found β2 mRNA expressing cells in the Nissl-dense surface layer of the IC.

Cells in the IC are more likely to express α1 and α2A mRNA and α1, α2A, and β2 mRNA than predicted by chance

To examine co-expression of adrenergic receptors we mesured the overlap between α1, α2A, and β2 mRNA in Nissl-defined cells (Figure 3.5). We first determined the amount of co-expression we expected to observe by calculating the probability of observing a condition (α1 only, α1 + α2A, etc) (see Methods). We found that a greater proportion of cells expressed no adrenergic mRNA of any type than expected (mean 0.426 vs 0.283 predicted), while fewer cells expressed a single adrenergic receptor's mRNA than expected (α1: 0.229 vs 0.319 predicted, α2A: 0.057 vs 0.142 predicted, β2: 0.008 vs 0.029 predicted) (Figure 3.5b). We also found lower-than-expected overlap between α1 and β2 mRNA (mean 0.018 vs 0.033 predicted) and α2A and β2 mRNA (mean 0.001 vs 0.015 predicted). Interestingly, we found a higher proportion of cells that expressed both α1 and α2A mRNA than expected (mean 0.199 vs 0.160 predicted). Similarly, we

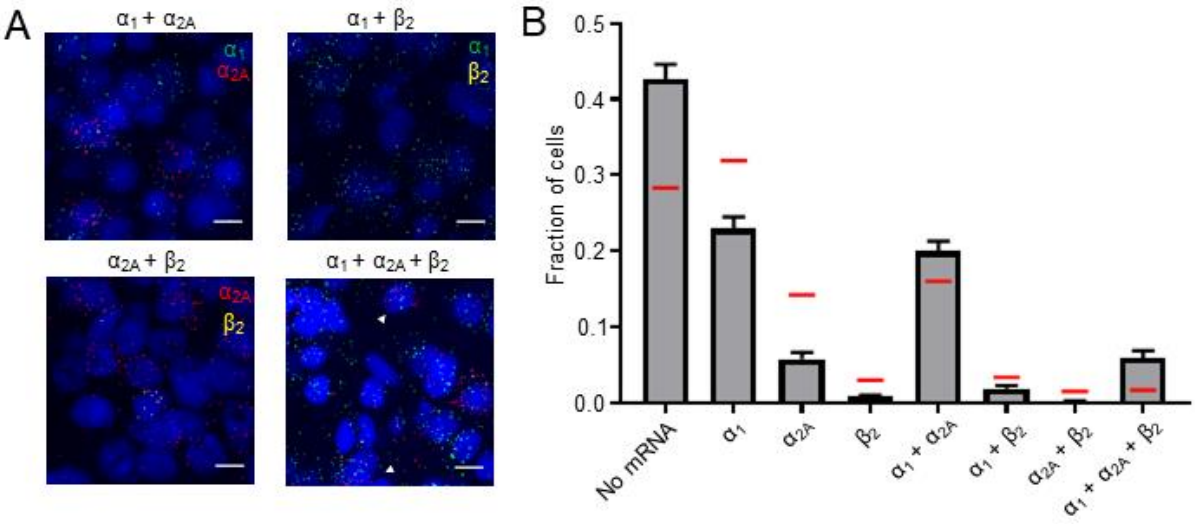

Figure 3.5: Co-expression of α1, α2A, and β2 adrenergic receptor mRNA is different than theoretical distribution

A: Representative images of overlap between the adrenergic receptor mRNA signals. Scale bars = 10 microns. The white arrowheads in the lower right indicate cells that display overlap of α_1, α_{2A}, and β_2 mRNA. B: Summary plot of fraction of cells that expressed no mRNA signal, α_1, α_{2A}, or β_2 mRNA solely, or overlaps. Bars represent the mean with error bars representing the standard error of the mean. N = 24 for each category. All ages and all subregions are combined. Horizontal red bars indicate the theoretical mean of fractional overlap based on percentages of cells predicted to exhibit each condition. These values were calculated by the product of probabilities for each condition based on total fraction of cells that exhibited α_1, α_{2A}, or β_2 mRNA.

observed a higher proportion of cells that expressed mRNA for all three receptors than predicted (mean 0.037 vs 0.016 predicted). These results show that there are cells that express mRNA for more than one type of adrenergic receptor in the IC, and suggest that cells have coordinate expression patterns for multiple receptor types.

Patterns of α1, α2A, and β2 mRNA overlap is similar across IC subregions and ages

We next compared the distributions of adrenergic receptor mRNA overlap across age groups and IC subregions (Figure 3.6). Overall, patterns of mRNA distribution across ages and subregions was similar to what was observed in the aggregate (Figure 3.6). We

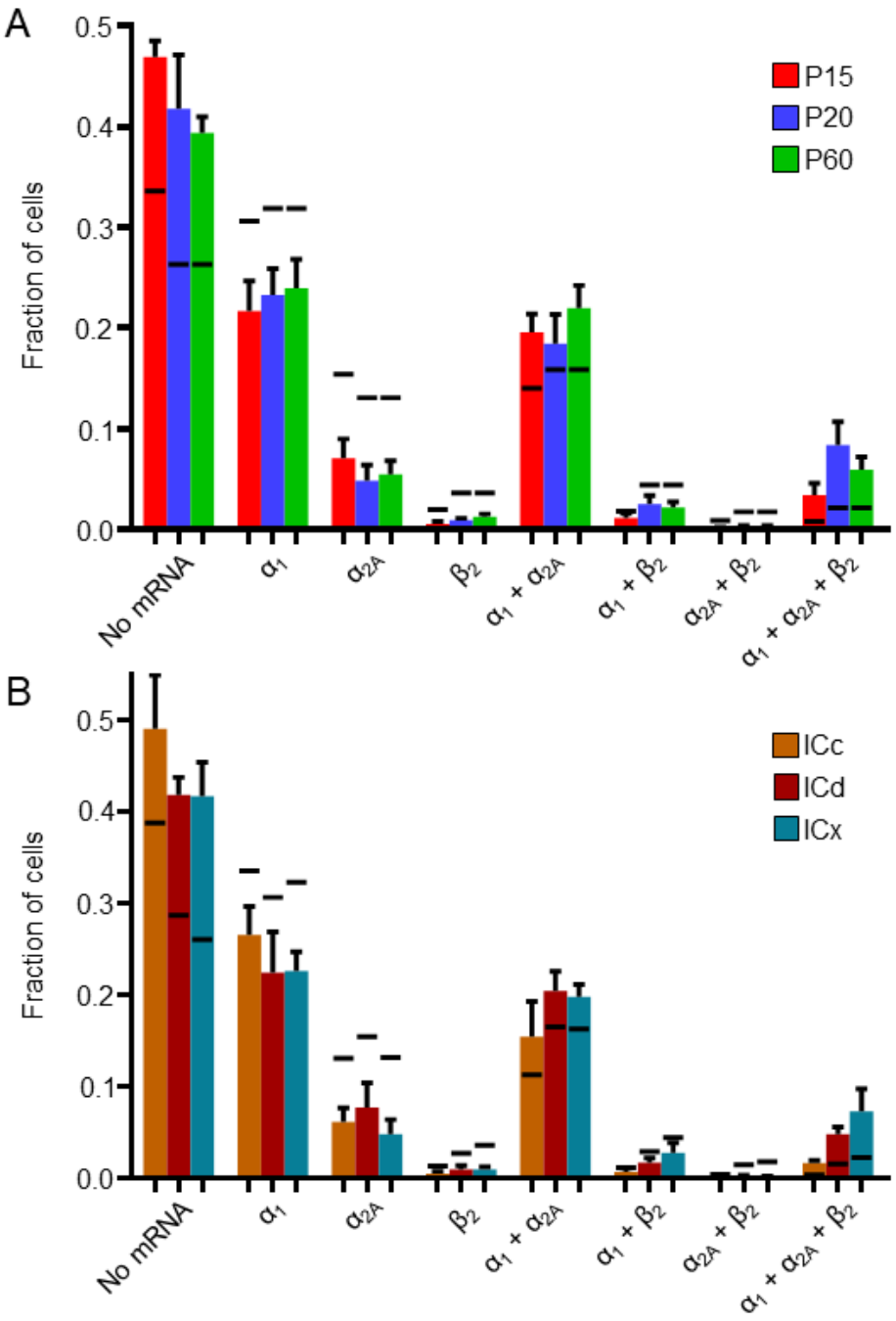

Figure 3.6: Co-expression of α1, α2A, and β2 adrenergic receptor mRNA is similar across ages and subregions

Figure 3.6 continued. A: Summary plot of fraction of cells that expressed no mRNA signal, α_1, α_{2A}, or β_2 mRNA solely, or overlaps in each age group. Bars represent the mean with error bars representing the standard error of the mean. N = 24 for each category. Horizontal black bars indicate the theoretical mean of fractional overlap based on percentages of cells predicted to exhibit each condition. B: Summary plot of fraction of cells that expressed no mRNA signal, α_1, α_{2A}, or β_2 mRNA solely, or overlaps in each IC subregion. Bars represent the mean with error bars representing the standard error of the mean. N = 24 for each category. Horizontal black bars indicate the theoretical mean of fractional overlap based on percentages of cells predicted to exhibit each condition.

observed greater than expected proportions of cells that expressed zero adrenergic receptor mRNA. Lower proportions of cells than expected were observed expressing only α1 mRNA, α2A mRNA, or β2 mRNA. Greater proportions of cells that expressed both α1 and α2A mRNA and cells that expressed all three tested adrenergic receptor mRNAs. These results indicate that expression patterns and overlap of α1, α2A, and β2 mRNA likely do not change over development from P15 to P60, nor do they differ between IC subregions.

3.5 Discussion

These results show that α1, α2A, and β2 adrenergic receptor mRNA are expressed in the mouse inferior colliculus. The proportion of cells in the IC that express mRNA encoding these receptors is not different at ages P15, P20, and P60. mRNA encoding the adrenergic receptor family α1 and adrenergic receptor α2A are expressed in similar proportions of cells in the three subregions of the IC (ICc, ICd, and ICx). β2 adrenergic receptor mRNA was expressed in a smaller proportion of cells compared to α1 and α2A mRNA. β2 adrenergic receptor mRNA was found to be lower in the ICc compared to ICd and ICx subregions. Compared to a random distribution of adrenergic mRNA in IC cells, we found more cells co-expressing α1 and α2A mRNA and cells that co-expressed α1,

α2A, and β2 mRNA. Similarly, we found more cells that expressed no adrenergic receptor mRNA than predicted These results indicate that the IC is subject to adrenergic modulation and that multiple receptors are positioned to mediate norepinephrine's effects.

Previous studies have provided evidence for the presence of α1 adrenergic receptors in the IC, using either *in situ* hybridization[12,13], autoradiography[22,23], or generation of a transgenic line in which the α1A adrenergic receptor promoter also drove a reporter gene[14]. Day et al. (1997) used *in situ* hybridization to examine expression patterns of α1A, α1B, and α1D, mRNA across the rat brain and found no expression of α1A and α1B in the rat inferior colliculus, but low levels of α1D mRNA. Similarly, Domyancic et al. (1997) reported no expression of α1A in the IC. In contrast, Papay et al. (2006), using an α1A transgenic line, found moderate expression levels in the IC. To ensure that we did not miss expression of α1 receptors in the IC, we opted to use a combination of α1A, α1B, and α1D probes for *in situ* hybridization detection. We detected expression of α1 mRNA in all age groups tested and across all IC subregions. α1 mRNA has been observed in a number of cell types in the brain[14]. α1 mRNA is not expressed in cerebral vasculature[24], in contrast with peripheral blood vessels. While our results are unable to differentiate cell types, the widespread nature of expression patterns implicates α1 receptors in a role of IC modulation.

We found expression of adrenergic receptor α2A mRNA in the IC, across all age groups and IC subregions. Previous *in situ* hybridization studies showed the expression of α2A and α2C mRNA in the IC and autoradiography studies implicated α2A, α2B, α2C type

receptors in the IC[15,16]. These early studies examined mRNA expression or ligand binding across the whole brain, resulting in a lack of cellular resolution. Our findings corroborate these previous results, indicating the potential for noradrenergic modulation in the mouse IC via activity of the α2A receptor and additionally allows us to estimate the prevalence of α2A expressing cells in the IC.

We observed low proportions of cells that express β2 adrenergic receptor mRNA. No evidence of β2 mRNA has been reported in previous *in situ* hybridization or autoradiography studies[17–19]. We find low, non-zero proportions of β2 expressing cells throughout all ages tested. Similarly, we find low, non-zero proportions of β2 expressing cells in all IC subregions. Unlike α1 and α2A receptor mRNA, we find differential expression across IC subregions. The IC subregions are functionally distinct, with the ICc being the primary target for ascending auditory afferents. The ICx is multimodal, receiving somatosensory inputs, and trading reciprocal connections with the superior colliculus. The ICd receives little to no ascending auditory information, while being the primary target for descending projections from the auditory cortex[5,25]. We find significantly higher levels of β2 adrenergic receptor mRNA in the ICx and ICd subregions than in the ICCc. These results suggest that β2 receptors may play a greater role in modulating multimodal integration of the ICx and the targets of descending projections in the ICd than in modulating ascending auditory.

We also observed strong label for all tested adrenergic receptor mRNAs in the Nissl-dense surface of the IC. While this layer is likely meningeal, without further testing it is unclear which layer of the meninges gives rise to the mRNA signal.

Sound-evoked signals in the auditory nerve can first be detected between ages P10-P12[26]. We examined the expression levels of α1, α2A, and β2 adrenergic receptor mRNA at ages P15, P20, and P60 to determine if the proportion of cells that showed receptor expression changed throughout the development of the auditory system. We found no differences in the proportion of cells that exhibited expression of α1, α2A, or β2 adrenergic receptor mRNA across these three ages. Noradrenergic fibers appear early in development[27]. Taken together, the early presence of noradrenergic fibers and unchanging levels of α1, α2A, or β2 adrenergic receptor mRNA, these findings indicate that noradrenergic modulatory systems are in place from the time of hearing onset.

Using triple-channel *in situ* hybridization, we were able to examine co-expression of α1, α2A, and β2 adrenergic receptor mRNA in cells in the IC. We compared the distribution of cells with no detected mRNA, mRNA encoding for a single adrenergic receptor, or co-expression of any combination of the three mRNAs studied. Compared to a random distribution of adrenergic mRNA, we found more cells that expressed combinations of α1 and α2A mRNA and cells that expressed mRNA for α1, α2A, and β2 mRNA probes. There were fewer cells than expected that expressed solely α1, α2A, or β2 mRNA. These results indicate that many cells in the IC are not sensitive to norepinephrine at all, while many express more than one type of adrenergic receptor, including a small population of cells

that express receptors from all three adrenergic receptor subtypes. The increased prevalence of co-expression of adrenergic receptor mRNA in IC cells suggests that the control of adrenergic receptor expression is non-independent. These patterns of mRNA overlap did not change throughout the ages we tested, nor did they differ across IC subregions. It is interesting that there were higher levels of cells that expressed β2 mRNA in conjunction with α1 and α2A compared to cells that expressed solely β2. Adrenergic receptors have been shown to be present both postsynaptically and presynaptically. The use of *in situ* hybridization makes intracellular localization of adrenergic receptors impossible but cells could be expressing certain classes of receptors in distinct cellular locales. Norepinephrine is thought to be released both synaptically and by volume transmission into extrasynaptic space[28,29]. Different patterns of adrenergic receptors in a single cell could be receptive to different patterns of norepinephrine release.

Together, these results suggest that multiple types of adrenergic receptors are expressed in the mouse IC. Cells can express more than one type of adrenergic receptor encoding mRNA. Further investigations are needed to determine the nature of these adrenergic receptor expressing cells in the IC. It is likely that auditory processing in the IC is modulated by norepinephrine release.

3.6 References

1. Adams, J. C. Ascending projections to the inferior colliculus. *J. Comp. Neurol.* **183**, 519–538 (1979).
2. Oliver, D. L. & Morest, D. K. The central nucleus of the inferior colliculus in the cat. *J. Comp. Neurol.* **222**, 237–264 (1984).

3. Glendenning, K. K. & Masterton, R. B. Acoustic chiasm: efferent projections of the lateral superior olive. *J. Neurosci.* **3**, 1521–37 (1983).
4. Loftus, W. C., Malmierca, M. S., Bishop, D. C. & Oliver, D. L. The cytoarchitecture of the inferior colliculus revisited: A common organization of the lateral cortex in rat and cat. *Neuroscience* **154**, 196–205 (2008).
5. Winer, J. A., Larue, D. T., Diehl, J. J. & Hefti, B. J. Auditory cortical projections to the cat inferior colliculus. *J. Comp. Neurol.* **400**, 147–174 (1998).
6. Kuwabara, N. & Zook, J. M. Geniculo-collicular descending projections in the gerbil. *Brain Res.* **878**, 79–87 (2000).
7. Tokunaga, A., Sugita, S. & Otani, K. Auditory and non-auditory subcortical afferents to the inferior colliculus in the rat. *J. Hirnforsch.* **25**, 461–72 (1984).
8. Li, H. & Mizuno, N. Single neurons in the spinal trigeminal and dorsal column nuclei project to both the cochlear nucleus and the inferior colliculus by way of axon collaterals: a fluorescent retrograde double-labeling study in the rat. *Neurosci. Res.* **29**, 135–142 (1997).
9. Nevue, A. A., Elde, C. J., Perkel, D. J. & Portfors, C. V. Dopaminergic Input to the Inferior Colliculus in Mice. *Front. Neuroanat.* **9**, 1–9 (2016).
10. Klepper, A. & Herbert, H. Distribution and origin of noradrenergic and serotonergic fibers in the cochlear nucleus and inferior colliculus of the rat. *Brain Res.* **557**, 190–201 (1991).
11. Thompson, G. C., Thompson, A. M., Garrett, K. M. & Britton, B. H. Serotonin and Serotonin Receptors in the Central Auditory System. *Otolaryngol. Neck Surg.* **110**, 93–102 (1994).
12. Domyancic, A. V. & Morilak, D. A. Distribution of A1A adrenergic receptor m RNA in the rat brain visualized by in situ hybridization. *J. Comp. Neurol.* **386**, 358–378 (1997).
13. Day, H. E. ., Campeau, S., Watson, S. J. & Akil, H. Distribution of α1a-, α1b- and α1d-adrenergic receptor mRNA in the rat brain and spinal cord. *J. Chem. Neuroanat.* **13**, 115–139 (1997).
14. Papay, R. *et al.* Localization of the mouse α1A-adrenergic receptor (AR) in the brain: α1AAR is expressed in neurons, GABAergic interneurons, and NG2 oligodendrocyte progenitors. *J. Comp. Neurol.* **497**, 209–222 (2006).
15. Boyajian, C. L., Loughlin, S. E. & Leslie, F. M. *Anatomical Evidence forAlpha-2 Adrenoceptor Heterogeneity: Differential Autoradiographic Distributions of [3H]Rauwolscine and [3H]Idazoxan in Rat Brain1*. **241**, (1987).
16. Scheinin, M. *et al.* Distribution of α2-adrenergic receptor subtype gene expression in rat brain. *Mol. Brain Res.* **21**, 133–149 (1994).
17. Rainbow, T. C., Parsons, B. & Wolfe, B. B. Quantitative autoradiography of beta 1- and beta 2-adrenergic receptors in rat brain. *Proc. Natl. Acad. Sci. U. S. A.* **81**, 1585–9 (1984).
18. Asanuma, M. *et al.* Distribution of the Beta-2 Adrenergic receptor messenger RNA in the rat brain by in situ hyrbridization histochemistry: Effects of chronic reserpine treatment. *Neurochemical Research* **16**, 1253–1256 (1991).
19. Nicholas, A. P., Pieribone, V. A. & Hökfelt, T. Cellular localization of messenger RNA for beta-1 and beta-2 adrenergic receptors in rat brain: An in situ hybridization study. *Neuroscience* **56**, 1023–1039 (1993).

20. Schindelin, J. *et al.* Fiji: an open-source platform for biological-image analysis. *Nat. Methods* **9**, 676–82 (2012).
21. Schneider, C. A., Rasband, W. S. & Eliceiri, K. W. NIH Image to ImageJ: 25 years of image analysis. *Nat. Methods* **9**, 671–5 (2012).
22. Palacios, J. M., Hoyer, D. & Cortés, R. α1-adrenoceptors in the mammalian brain: similar pharmacology but different distribution in rodents and primates. *Brain Res.* **419**, 65–75 (1987).
23. Jones, L. S., Gauger, L. L. & Davis, J. N. Anatomy of brain alpha1-adrenergic receptors: In vitro autoradiography with [125I]-heat. *J. Comp. Neurol.* **231**, 190–208 (1985).
24. Papay, R. *et al.* Mouse ?1B-adrenergic receptor is expressed in neurons and NG2 oligodendrocytes. *J. Comp. Neurol.* **478**, 1–10 (2004).
25. Winer, J. A. Decoding the auditory corticofugal systems. *Hear. Res.* **212**, 1–8 (2006).
26. Mikaelian, D. & Ruben, R. J. Development of Hearing in the Normal Cba-J Mouse: *Correlation of Physiological Observations with Behavioral Responses and with Cochlear Anatomy*. *Acta Otolaryngol.* **59**, 451–461 (1965).
27. Lauder, J. M. & Bloom, F. E. Ontogeny of monoamine neurons in the locus coeruleus, raphe nuclei and substantia nigra of the rat. I. Cell differentiation. *J. Comp. Neurol.* **155**, 469–481 (1974).
28. Olschowka, J. A., Molliver, M. E., Grzanna, R., Rice, F. L. & Coyle, J. T. Ultrastructural demonstration of noradrenergic synapses in the rat central nervous system by dopamine-beta-hydroxylase immunocytochemistry. *J. Histochem. Cytochem.* **29**, 271–280 (1981).
29. Farb, C. R., Chang, W. & LeDoux, J. E. Ultrastructural Characterization of Noradrenergic Axons and Beta-Adrenergic Receptors in the Lateral Nucleus of the Amygdala. *Front. Behav. Neurosci.* **4**, 162 (2010).

Chapter 4. Conclusions and future directions

4.1 Conclusions

Here we have provided the first evidence for noradrenergic modulation in the inferior colliculus (IC). We have also shown novel evidence of cellular co-expression of adrenergic receptor-encoding mRNA in the inferior colliculus. The IC is in a powerful position to modulate auditory processing in the brain. The IC is an obligatory synaptic relay for nearly all ascending auditory projections. The IC integrates and refines the auditory stimulus information and features detected by the brainstem auditory nuclei. The IC also receives extensive descending projections from the auditory cortex and thalamus, as well as non-auditory sensory and processing regions. Noradrenergic modulation in the IC could have wide-ranging and powerful effects by altering activity in the IC and the coalescence of ascending and descending information.

We observed expression of α1 and α2A adrenergic receptor-encoding mRNA throughout the IC and its subregions (ICc, ICd, and ICx). β2 adrenergic receptor mRNA is also expressed throughout the IC, albeit in a lower proportion of IC cells. Additionally, we found that β 2 adrenergic receptor mRNA is expressed in a higher proportion of cells in the outer IC subregions of the ICd and ICx in comparison to the ICc. We tested for any developmental changes in adrenergic receptor mRNA species and find no appreciable differences in the proportion of cells that express α1, α2A, or β2 receptor encoding mRNA across ages P15, P20, and P60. Mouse pups begin responding to auditory stimuli between ages P10-12, indicating that the noradrenergic modulatory potential is likely mature by age P15. By performing simultaneous in situ hybridizations

for each of these adrenergic receptor mRNAs, we were able to detect cellular co-expression between them. We found that there were higher levels of co-expression of adrenergic receptor-encoding mRNA than expected. This suggests a non-independent control for the expression of each receptor. The co-expression of adrenergic mRNA is similar across ages P15, P20, and P60. Higher levels of adrenergic receptor co-expression perhaps imply that certain cells form hubs of noradrenergic modulation in the IC. The cellular identity of these hotspots for noradrenergic modulation are currently unknown but potentially play an important role in the modulation of auditory processing in the IC.

Using widefield calcium imaging, we measured physiological changes in IC cell calcium levels across all three IC subregions. We found that application of norepinephrine results in robust and reliable increases in intracellular calcium across the IC. Cells responsive to norepinephrine were found in all three subregions of the IC. Greater increases in calcium signal were observed in the ICd and ICx subregions in comparison to the ICc. The observed calcium increases in IC cells are not the result of neuronal spiking but it is not known if the calcium fluctuations could lead to increased excitability or other action-potential related intrinsic change. Noradrenergic IC effects do not require glutamatergic, GABAergic, or glycinergic signaling in the IC, nor do they require activity mediated through carbenoxolone-blocked gap junctions. These data strongly suggest that the observed increases in calcium occur in cells that express noradrenergic receptors and that it is the physiological changes mediated by adrenergic receptor activity that directly cause calcium influx into the cytosol. We found that agonists

specific for each adrenergic receptor subtype all produce increases in calcium in the IC, similar to the effects observed with norepinephrine application. Adrenergic receptor antagonists blocked all norepinephrine-induced effects in the IC. α1 agonist application resulted in effects across the entire IC, and these effects were not dependent on action potentials. Interestingly, antagonists of purinergic receptors nearly abolished the observed α1 agonist induced effects. This suggests that α1 receptors induce a release of a purinergic transmitter which in turn binds to P2 receptors and induce an increase in intracellular calcium. On average, α2 agonist application resulted in weaker increases in calcium. α2 receptor mediated effects were direct and showed shorter duration responses on average. α2 effects were spatially limited to a region that bordered the ICc and its surrounding ICd and ICx regions. β receptor mediated effects are also direct and shower shorter response durations on average. Strikingly, β effects were limited to the ICd and ICx regions, inducing very little effect in the ICc. While the neuronal composition of the IC is 70% glutamatergic, we observed no norepinephrine-induced calcium effects when we limited calcium indicator expression to solely excitatory cells in the IC.

Together, the results of the *in situ* hybridization and calcium imaging experiments largely agree. Expression patterns of α1 receptor mRNA and physiological responses to α1 receptor specific agonists are similar. Both implicate the presence of α1 receptors across the IC, in all subregions. The spatial patterns of β receptor mRNA and β agonist-induced activity were largely the same as well. We observed higher expression and calcium increases in the ICd and ICx subregions in comparison to the ICc.

There were, however, some aspects of the two studies that are harder to fit together. For example, we observed high expression of α2A receptor-encoding mRNA throughout the IC but observed α2 agonist induced activity in a more limited region. The largest discrepancy in these results is the difference in co-expression of adrenergic receptor mRNA and overlap in cellular responses to sequential application of specific adrenergic receptor agonists. We observed moderate proportions of cells that express mRNA for multiple adrenergic receptors and observed little overlap in single cells of agonist-induced calcium activity. There are several potential explanations for this difference. The principal explanation for the differing results is methodological. In situ hybridization examines the expression of mRNA while calcium imaging is measuring the physiological changes in levels of intracellular calcium. Detection of mRNA in the cell body does not necessarily indicate expression of the resulting protein in the same location. Expression of an adrenergic receptor in the synaptic terminal or dendrites would appear the same as receptor expression in the cell body as measured by the presence of mRNA. IC neurons project to numerous targets, many of which would not be in the same coronal plane as IC and therefore not be measured in live imaging experiments. Another possible explanation for the discrepancy between adrenergic mRNA expression and agonist-induced calcium transients is that not all adrenergic receptor-mediated effects would lead to calcium mobilization. Noradrenergic signaling is frequently tied to increases in intracellular calcium, as we have demonstrated here, but many examples in other systems and cells do not. For example, modulation of the

excitability of neurons would not necessarily be reflected in changes in calcium while the neuron is at rest, as they were in the experiments described here.

The data presented here gives evidence for noradrenergic modulation in the inferior colliculus. What role might norepinephrine release in the IC play in modulating auditory processing and behavior? While the data described here do not directly address this question, we can make predictions based on the spatial patterns of noradrenergic effects in the IC. α1 adrenergic receptor encoding mRNA and α1 receptor specific agonist-induced effects were found throughout the IC. This suggests that α1 activity may exert a broader modulatory role in IC processing, one that is not limited to the functions of each subregion. At the same time, α1 receptor agonists regularly increased calcium levels in the ICc, the principal ascending auditory processing region of the IC. An additional factor to consider is that the calcium effects caused by α1 receptor application depend on actions of the P2 class of purinergic receptors. In the visual and olfactory sensory systems, intracellular calcium mobilization in response to purinergic receptor activity has been observed in a variety of glial cell types, including astrocytes, microglia, and Müller glia of the retina[1]. Purinergic activation of glia can then regulate homeostatic processes of neurons and blood flow. Release of transmitters from glia, gliotransmission, can then in turn modulate neuronal processing. A portion of the responses with α1 agonist application occurred in cells that also showed label for an astrocyte-labeling dye but this was a minority of the responses observed. It is likely that some of the observed calcium transients occur in glia but would require further

experimentation to precisely determine the identity of α1 agonist sensitive cells in the IC.

Hypothesizing the role of α2 receptors in auditory processing is difficult. Out of the three adrenergic receptors, α2 receptor mediated activity was the lowest. However, as noted above, not all adrenergic receptor activity results in changes to calcium levels as detected by a cytosolic calcium indicator. The spatial pattern of α2 mediated effects is interesting, regularly appearing on the outer edges of the ICc, spilling over into the ICd and ICx regions. To our knowledge, no distinctions have been made regarding cells occupying this space in other IC research. This pattern of calcium responses in the IC likely indicates a new subtype of IC cell that has yet to be described.

β receptor mediated effects observed via calcium imaging occur almost exclusively in the ICx and ICd subregions of the IC. The ICd is the target of the majority of descending projections from the auditory cortex, suggesting that β mediated effects are more important for modulating these processing pathways. The ICd shows strong responses to novel auditory stimuli, a response that is shared with the source of norepinephrine in the IC, the locus coeruleus. Release of norepinephrine and subsequent modulatory actions in the ICd via the β receptor could account for or enhance the responsiveness to auditory stimuli in ICd neurons. β mediated activity in the ICx could serve a similar purpose, albeit in the multi-modal integration of the ICx. The ICx sends and receives connections from the superior colliculus, an important nucleus for orientation, as well as

from brainstem somatosensory regions. β mediated activity in these regions could enhance the responsiveness to salient auditory stimuli.

4.2 Future directions

While the data shown here provide a solid first step in understanding how norepinephrine modulates activity in the IC, future experiments would be useful for attaining a deeper understanding of how norepinephrine alters IC circuits and auditory processing. One of the primary challenges in the field of IC research is the seemingly inscrutable nature of types of IC neurons. Differentiation based on classical properties such as neurotransmitter identity, cell morphology, or intrinsic electrophysiological properties have failed to separate IC neurons into consistent groups. This in turn has made identification of cellular markers to limit investigation to a narrower type of IC cell difficult. The majority of recently developed tools for neuroscience research rely on a unique cell type specific genetic marker for controlling the expression of detector and effector proteins to certain populations of cells. While there has been some limited success in the IC with VIP-positive cells in the IC, the majority of IC cells elude a unique identifier. We tested the effects of noradrenergic modulation in excitatory cells in the IC using the CaMK2a promoter. While we did not observe any changes in intracellular calcium in excitatory cells, this result begs the question of what is occurring in inhibitory cells in the IC with regards to noradrenergic modulation. Further insights into unique markers for groups of neurons in the IC would open up investigations using a variety of tools.

At the cellular level, it is important to understand how norepinephrine alters the electrophysiological properties of IC neurons. Currently, the variety of cells in the IC makes investigating the modulation of electrophysiological properties of IC neurons a daunting task. A marker for cells that are sensitive to norepinephrine would ease the efforts of future researchers to ask the detailed questions the work presented here invites. For example, our *in situ* results suggest that many cells express more than one type of adrenergic receptor. In vitro electrophysiology would allow a researcher to potentially parse apart the actions of multiple receptors within a single cell.

Electrophysiological studies of noradrenergic modulation in the IC could be made in vivo as well. The IC has long been a popular target for in vivo recordings due to its fundamental role in auditory processing and anatomical location on the dorsal surface of the midbrain, allowing for access with recordings electrodes. While many investigations have examined the effects of neuromodulators on tone-evoked responses in IC neurons, to our knowledge none have investigated norepinephrine modulatory effects in this way. This would be a critical step in understanding the role of noradrenergic modulation in auditory processing. In other sensory systems and in other auditory nuclei, norepinephrine has been shown to enhance signal-to-noise and it would be interesting to understand if the same is occurring in the IC.

There are many steps that are needed to understand the role of norepinephrine in the inferior colliculus. The work presented in this dissertation represents the first evidence for noradrenergic modulation in the auditory midbrain and the first step towards

understanding how the noradrenergic system can alter sensory processing in the auditory midbrain.

4.3 References

1. Lohr, C., Grosche, A., Reichenbach, A. & Hirnet, D. Purinergic neuron-glia interactions in sensory systems. *Pflügers Arch. - Eur. J. Physiol.* **466**, 1859–1872 (2014).

VITA

Charles A. Williams was born in Saint Paul, MN, and was raised in Traverse City, MI. He received his Bachelor of Science in Neuroscience at the University of Michigan in 2010. He worked as a technician in the lab of Orie Shafer in the department of Molecular, Cellular, and Developmental Biology at the University of Michigan from 2011 to 2012 before being accepted into the Ph.D. program of the Department of Biology at the University of Washington. He earned his Ph.D. in Biology from the University of Washington in 2019.